



**Universidade do Minho**  
Escola de Engenharia

Daniel Alexandre da Silva Madalena

**Design of a 3D in vitro gastric model with in situ analysis for the assessment of food digestibility and nanomaterials behavior**

**Design of a 3D in vitro gastric model with in situ analysis for the assessment of food digestibility and nanomaterials behavior**

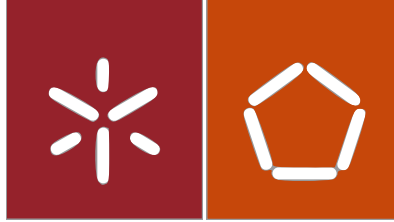
Daniel Alexandre da Silva Madalena

This dissertation was financially supported by a PhD scholarship provided by the Foundation for Science and Technology (SFRH/BD/129127/2017) under the scope of the strategic funding of UIDB/04469/2020 and UIDB/50016/2020 units and the I&D&I project AgriFood XXI with the operation number NORTE-01-0145-FEDER-000041, co-funded by the Fundo Europeu de Desenvolvimento Regional (FEDER) through NORTE 2020 (Programa Operacional Regional do Norte 2014/2020).



UMinho | 2022

April 2022



**Universidade do Minho**  
Escola de Engenharia

Daniel Alexandre da Silva Madalena

**Design of a 3D in vitro gastric model with in situ analysis for the assessment of food digestibility and nanomaterials behaviour**

PhD Thesis  
Biomedical Engineering

Work carried out under the supervision of:

**Ana Cristina Braga Pinheiro, PhD**

**Óscar Leandro Silva Ramos, PhD**

**António Augusto Martins de Oliveira Soares Vicente, PhD**

## **COPYRIGHT AND WORKING CONDITIONS BY THIRD PARTIES**

This is an academic work that may be used by third parties, provided that the international rules and good practices accepted in respect of copyright and related rights are respected.

Thus, the present work can be developed in terms of public availability.

If the user needs to be authorized to use this work in conditions not subject to prior agreement, contact the author through the University of Minho's RepositóriUM.



**Atribuição-NãoComercial-SemDerivações**

**CC BY-NC-ND**

<https://creativecommons.org/licenses/by-nc-nd/4.0/>

## ACKNOWLEDGEMENTS/AGRADECIMENTOS

Não seria possível a realização deste trabalho sem a ajuda e colaboração de muitas pessoas, em especial das que me são mais próximas! Gostaria de em primeiro lugar agradecer ao professor António Vicente pela confiança que depositou em mim desde sempre, sendo o principal responsável pelo caminho que tracei na investigação e por essa razão, entre outras, um muito obrigado! Um obrigado especial à Ana Cristina Pinheiro e Óscar Ramos por todo o seu apoio e paciência em ouvir e esclarecer as minhas dúvidas assim como pela sua amizade.

Não poderia deixar de agradecer todos os meus colegas que ajudaram a criar o ambiente propício à criação deste projeto, nomeadamente, a sua boa disposição. Assim, um muito obrigado ao Pedro Geada, Leandro Madureira, Luís Machado, Luís Loureiro, Miguel Fernandes, Michel Fernandes, Raquel Gonçalves, Maria José Costa, Arlete Marques, Pedro Silva, Joana Martins, Ricardo Pereira, Rui Rodrigues, Luís Abrunhosa, Filipe Maciel, João Araújo, Márcia Marques, Rita Leal, Vitor Sousa e Gonçalo Carvalho. Um muito obrigado!

Gostaria também de agradecer à Zita Avelar pela sua ajuda com a eletroforese tendo contribuído muito significativamente para o avanço deste trabalho. Um muito obrigado à Salomé pela sua preciosa ajuda com o GC e sem ela algumas conclusões que pude retirar deste trabalho não seriam possíveis. Agradeço também o professor Senentxu Lanceros-Mendez pela sua boa disposição e ajuda. Um muito obrigado ao Néilson Pereira e Sérgio Gonçalves pela ajuda que deram com a impressão 3D e troca de ideias.

Claro que também gostaria de agradecer aos meus amigos mais chegados por me ouvirem e partilharem comigo momentos de lazer!

Um muito obrigado especial à Mariana por partilhar comigo uma vida sendo fruto dessa partilha a nossa filha, a Madalena, e por isso lhes dedico este trabalho pois sem elas certamente nada disto seria possível. Um muito obrigado por me ouvirem, terem muita paciência nos momentos menos bons deste trabalho e, com um sorriso e palavra amiga fazerem com que tudo fique melhor.

Finalmente, gostaria de agradecer à minha família por todo o seu apoio e carinho que me deram pois sem eles não seria quem sou hoje e por isso, muito obrigado!

## **STATEMENT OF INTEGRITY**

I hereby declare having conducted this academic work with integrity. I confirm that I have not used plagiarism or any form of undue use of information or falsification of results along the process leading to its elaboration.

I further declare that I have fully acknowledged the Code of Ethical Conduct of the University of Minho.

Design of a 3D *in vitro* gastric model with *in situ* analysis for the assessment of food digestibility and nanomaterials behaviour

## Abstract

The regular consumer is becoming more concern regarding their nutritional habits and, as such, novel healthier food products with additional functional properties must be developed to give response to the increase from the food market demand. However, while developing innovative food products through, for instance, the addition of nanosystems for the controlled delivery of bioactive compounds, it is important to understand their behaviour under digestion conditions by assessing their toxicity (i.e., the release of toxins during the digestion process), hydrolysis kinetics, nutrient absorption, etc. Ideally, *in vivo* trials should be used for this purpose since they represent as more accurately the GI conditions. However, due to all the ethical constrains, cost and complexity associated to their application, *in vitro* digestion models have been widely used as an alternative since they are faster, cheaper and less labour-intensive, with no ethical constrains. This way, several *in vitro* digestion models have been created to try to simulate the conditions of the human GI tract which have been widely used by the scientific community to study the digestion of food products, micro/nanosystems and drug dissolution. However, despite the development of a few anatomical accurate digestion models with dynamic behaviour over the past few years, there is still room for improvement. Therefore, the present study aims at the development of a modular dynamic *in vitro* RGM with *in situ* analysis, using UV-VIS-NIR spectrometry. This model is capable of replicating, as close as possible, the physicochemical conditions along the human stomach regarding its peristaltic contractions, as well as anatomical and physiological characteristics. The present model will allow to monitor in real-time the digestion process of food products, controlled release systems, bioactive compounds and drugs, thus being an important research, development and control tool for the food and pharmaceutical industries.

**Keywords:** Food digestion; *In vitro* digestion models; Milk digestion; Real-time analysis, Machine learning.

Desenvolvimento de um modelo *in vitro* gástrico com análise *in situ* para avaliar a digestão de alimentos e o comportamento de nanomateriais

Resumo

A preocupação por parte do consumidor final com os seus hábitos nutricionais provocou a necessidade de desenvolver novos produtos alimentares mais saudáveis, com novas propriedades funcionais para responder ao aumento da procura por parte do mercado alimentar. No entanto, com o desenvolvimento de produtos alimentícios inovadores através de, por exemplo, a adição de nanossistemas para a libertação controlada de compostos bioativos, tornou-se importante entender o seu comportamento em condições de digestão de modo a avaliar a sua toxicidade (i.e., a libertação de toxinas durante o processo de digestão), cinética de hidrólise, absorção de nutrientes, etc. Idealmente, tais estudos deveriam ser realizados *in vivo*. No entanto, devido a todas as restrições éticas, custo e complexidade associados à sua aplicação, os modelos de digestão *in vitro* têm sido amplamente utilizados como alternativa por serem mais rápidos, baratos e mais simples, não apresentando restrições éticas. Desta forma, vários modelos *in vitro* foram criados para tentar simular as condições do trato GI humano, os quais têm sido amplamente utilizados pela comunidade científica para estudar a digestão de produtos alimentares, micro/nanossistemas e dissolução de fármacos. No entanto, apesar do desenvolvimento de alguns modelos de digestão anatomicamente precisos com comportamento dinâmico ao longo dos últimos anos, ainda há espaço para novos desenvolvimentos. Como tal, o presente estudo visa o desenvolvimento de um RGM modular dinâmico *in vitro* com análise *in situ*, utilizando espectrometria UV-VIS-NIR. Este modelo é capaz de replicar, o mais próximo possível, as condições físico-químicas do estômago humano, mais especificamente no que diz respeito às suas contrações peristálticas, bem como características anatómicas e fisiológicas. O presente modelo permitirá monitorizar em tempo-real o processo de digestão de produtos alimentares, sistemas de libertação controlada, compostos bioativos e fármacos, sendo assim uma importante ferramenta de investigação, desenvolvimento e controlo para as indústrias alimentar e farmacêutica.

**Palavras-chave:** Análise em tempo-real; Digestão de alimentos; Digestão de nanossistemas; Modelos de digestão *in vitro*.

## TABLE OF CONTENTS

CHAPTER 1 - GENERAL INTRODUCTION.....	1
1.1 Research background and motivation .....	2
1.2 Research aims .....	3
1.3 Thesis outline.....	3
1.4 References.....	4
CHAPTER 2 - LITERATURE REVIEW.....	6
2.1 Introduction.....	7
2.2 <i>In vitro</i> digestion models.....	8
2.2.1 Static <i>in vitro</i> digestion models.....	8
2.2.2 Semi-dynamic/ dynamic <i>in vitro</i> digestion models .....	11
2.2.3 <i>In vitro</i> digestion protocol challenges.....	14
2.3 <i>In vitro</i> digestion of food and delivery systems.....	17
2.3.1 Assessment of food under <i>in vitro</i> digestion.....	17
2.3.1.1. Protein-based nanosystems.....	19
2.3.1.2. Lipid-based nanosystems .....	23
2.3.1.3. Polysaccharide-based nanosystems.....	26
2.3.2 Current challenges of <i>in vitro</i> digestion assessment techniques .....	28
2.3.2.1. Particle characterization challenges.....	28
2.3.2.2. Rheological Characterization.....	30
2.3.2.3. Non-conventional <i>in vitro</i> digestion assessment techniques .....	32
2.4 NIR spectroscopy .....	35
2.4.1 Theory and fundamentals .....	35
2.4.2 NIR spectral multivariate calibration .....	39
2.4.2.1. Smoothing: Savitzky–Golay filter .....	39
2.4.2.2. Baseline correction.....	39
2.4.2.3. Variable Selection - PLS.....	40



2.4.2.4.	Regression .....	41
2.4.2.5.	Model assessment .....	41
2.5	Conclusions and future perspectives .....	41
2.6	References .....	43
CHAPTER 3 - DEVELOPMENT OF A REPRODUCIBLE <i>IN VITRO</i> RGM .....		56
3.1	Introduction.....	57
3.2	Materials and methods.....	57
3.2.1	Materials .....	57
3.2.2	Model description .....	58
3.2.3	3D printing process .....	59
3.2.4	PB development using an experimental design .....	59
3.2.4.1.	Design parameters selection .....	60
3.2.4.2.	Finite element analysis of PB contraction.....	61
3.2.5	Silicone casting moulding – A step by step guide.....	63
3.2.5.1.	Gastric compartment's production process.....	63
3.2.5.2.	PBs' production process.....	64
3.2.6	Control system design – An IoT approach .....	65
3.2.6.1.	User interface and user flow .....	65
3.2.6.2.	System control modules .....	67
3.2.6.3.	Stomach emptying control.....	68
3.2.6.4.	Gastric pH control .....	68
3.2.6.5.	Peristaltic pump flow measurement.....	70
3.2.7	Hydrodynamic characterization of the RGM .....	70
3.2.8	Statistical Analysis .....	71
3.3	Results and discussion .....	72
3.3.1	PB modulation using an experimental design .....	72
3.3.1.1.	Variable selection using a Plackett-Burman experimental design.....	72

3.3.2	RGM characterization.....	74
3.3.2.1.	pH kinetics profile .....	74
3.3.2.2.	RTD assessment.....	75
3.4	Conclusions .....	76
3.5	References.....	77
CHAPTER 4 -REAL-TIME ASSESSMENT OF FOOD <i>IN VITRO</i> DIGESTION USING UV-VIS-SWNIR SPECTROSCOPY IN AN RGM .....		
		80
4.1	Introduction.....	81
4.2	Materials and methods.....	81
4.2.1	Materials .....	81
4.2.2	<i>In vitro</i> digestion protocol.....	82
4.2.3	Offline milk <i>in vitro</i> digestion assessment .....	82
4.2.3.1.	OPA Method.....	83
4.2.3.2.	SDS-PAGE.....	83
4.2.3.3.	Free fatty acid analysis using GC .....	84
4.2.3.4.	CSLM .....	85
4.2.4	UV-VIS-SWNIR Spectroscopy.....	85
4.2.4.1.	Description .....	85
4.2.4.2.	Signal processing software .....	85
4.2.4.3.	Sample separation .....	86
4.2.4.4.	Spectrum smoothing.....	86
4.2.4.5.	Baseline correction and resolution enhancement .....	86
4.2.4.6.	Wavelength selection.....	87
4.2.4.7.	Regression .....	87
4.2.5	Statistical Analysis .....	87
4.3	Results and discussion .....	87
4.3.1	<i>Ex situ</i> assessment of milk digestion. ....	87

4.3.1.1.	Protein hydrolysis.....	87
4.3.1.2.	FFA assessment through GC .....	90
4.3.1.3.	Assessing milk protein and lipid digestion – A multivariate analysis. ....	91
4.3.2	Real-time monitoring of milk protein digestion .....	94
4.4	Conclusions .....	97
4.5	References.....	98
CHAPTER 5 - GENERAL CONCLUSIONS AND FUTURE WORK .....		101
5.1	General conclusions .....	102
5.2	Future perspectives .....	103

## LIST OF FIGURES

<b>Figure 1</b> - Comparison between the different standardized <i>in vitro</i> digestion models. ....	10
<b>Figure 2</b> - Illustration of some important protein enzymatic interactions that occur during the gastric and intestinal phases of the digestion process. This figure is based on the work of Mackie & Macierzanka, (2010). *Protein digestion starts typically in the stomach; **Flocculation may occur from mucin interactions with adsorbed proteins; ***Polysaccharides are typically resistant to gastric digestion and their digestion mainly occurs in the gut by the microflora with a few exceptions like starch which digestion process is depicted in this figure. ....	19
<b>Figure 3</b> – Illustration of one photon of electromagnetic radiation traveling through the x-axis and its electric (E <sub>y</sub> ) and magnetic (B <sub>z</sub> ) components – Adapted from (Hollas, 2004). ....	36
Figure 4 – Molecular state transition during the interaction between electromagnetic radiation and molecules or atoms - Image adapted from (Hollas, 2004). ....	37
<b>Figure 5</b> – Illustrative representation of the RGM where: M1a – SGF and enzymes input; M1b – module 1 connection with module 2; M2 – module 2; M3a – acid/base input; M3b – pH electrode support; M4a – module 4; M4b – pylorus; M4c – Fibre optics support; M4d – level sensor; M4e – stomach emptying output; M5 – module 5; M6a - module 6; M6b – electrovalve. ....	58
<b>Figure 6</b> – Illustrative representation of a PB3 (A), the design parameters used in the Plackett-Burman experimental design (B) and the representation of the rotation angle (C) .....	60
<b>Figure 7</b> - Silicone’s stress-strain curve (A) using the ISO 37 dumbbell (B). ....	62
Figure 8 – FEA contacts in the PB. ....	63
<b>Figure 9</b> – Illustrative representation of the gastric compartment production where A and B correspond to the silicone mould inner and outer parts in a connected and divided view, respectively, and C, D, E, F, G and H correspond to the steps required to produce a gastric model. Furthermore, the numbers in the illustration represent: 1 – outer parts of the mould; 2- inner parts of the mould; 3 – top left part of the outer mould; 4 - top right part of the outer mould; 5 - bottom right part of the outer mould; 6 - bottom left part of the outer mould; 7 – top left part of the inner mould; 8 - top right part of the inner mould; 9 - bottom left part of the inner mould; 10 – bottom right part of the inner mould; 11 – liquid silicone; 12 – cured silicone. ....	64

<b>Figure 10</b> – Step-by-step illustration of the PB production process where: 1 – top part of the inflation chambers; 2 – bottom part of the inflation chambers; 3 - strain limiting layer mould; 4 – inflation chambers’ mould filled with liquid silicone; 5 – paper sheet; 6 – half of the strain limiting layer mould filled with liquid silicone; 7 – silicone tube .....	65
<b>Figure 11</b> – System control modules’ schematics. ....	68
<b>Figure 12</b> – pH and pH standard deviation over ten measurements to determine the standard deviation of a stable pH read. ....	70
<b>Figure 13</b> – Gastric pH kinetics control characterization.....	74
<b>Figure 14</b> – Response of the stomach to a tracer injection at different volumetric flow rates. .	75
<b>Figure 15</b> – Average residence time of particles inside the stomach at different flow rates. Note: columns with the same letter are not statistically different from each other ( <i>p-value</i> > 0.05) .....	76
<b>Figure 16</b> – Protein hydrolysis during the <i>in vitro</i> RGM digestion where: A – quantification of free NH <sub>2</sub> per gram of protein; B, C and D correspond to the correlation between the experiment 1, 2 and 3 pH profile and the free NH <sub>2</sub> per gram of protein, respectively. ....	89
<b>Figure 17</b> – Protein digestion assessment using SDS-PAGE where: Molecular weight marker; MC – undigested milk samples; the lanes identified with the numbers 2, 4, 6, 8, 10 and 12 correspond to the respective stomach emptying. ....	90
<b>Figure 18</b> – FFA release profiles during the RGM <i>in vitro</i> digestion. ....	91
<b>Figure 19</b> – CLSM images obtained through the digestion process of three distinct experiments (i.e., Exp1, Exp 2, and Exp 3) at times 0 (milk sample), 29.76 (SE6) and 59.50 (SE12) minutes as well as the 3D projection at time 29.76 minutes. The white bar represents 20 μm.....	93
<b>Figure 20</b> - PCA of milk <i>in vitro</i> digestion in the RGM. Values within parenthesis account for the variability explained by the respective principal component. ....	94
<b>Figure 21</b> – Savitzky-Golay optimization using an FCD.....	95

**Figure 22** – Effect of smoothing and SNV transformation of the serine spectra at different concentrations where: A – raw spectra; B – smoothed spectra; C – SNV. Note that each spectrum is represented as the average of 50 acquired spectra. .... 96

**Figure 23** – Comparison between protein hydrolysis obtained experimentally and estimated.. 97

## LIST OF TABLES

<b>Table 1</b> - Plackett-Burman experimental design with 12 experiments and 1 central point. All independent variable values are expressed in mm. The RA7, RA15, and RA21 correspond to the RA of the PB with 7, 15 and 21 inflation chambers, respectively which are expressed in degrees. ....	61
<b>Table 2</b> – Mooney-Rivlin 5 parameter model coefficients.....	62
<b>Table 3</b> – Project registration fields and their respective description. It is important to refer that these fields can be subject to change in the future. ....	66
<b>Table 4</b> – Peristaltic pumps' pumping rate characterization. ....	70
<b>Table 5</b> – Stomach emptying flow rates used for the hydrodynamic characterization the RGM. The portion and nutritional values are examples of commercially available dairy products and were obtained from the respective producer. The stomach emptying (i.e., volumetric flow rate) were calculated based on the semi-dynamic <i>in vitro</i> digestion standard protocol developed by Mulet-Cabero et al. (2020). ....	71
<b>Table 6</b> – Plackett-Burman experimental design results with a 5% significance level. ....	72
<b>Table 7</b> – CCRD experimental design experiments using the selected independent variables. .	73
<b>Table 8</b> – Summary of the main <i>in vitro</i> digestion conditions.....	82
<b>Table 9</b> – Regression results. ....	97

## LIST OF GENERAL NOMENCLATURE

### **Abbreviations**

AI – Artificial intelligence

AGDS – Artificial gastric digestive system

ANN – Artificial neural networks

APS - Ammonium persulphate

BRR – Bayesian ridge regression

BSA – Bovine serum albumin

CCRD – Central composite rotational design

CN - Casein

CSLM - Confocal scanning laser microscope

CSTR – Continuous stirred reactor

DCM – Dichloromethane

DOE – Design of experiment

ENR – Elastic net regression

FFA – Free-fatty-acids

FID - Flame ionization detector

FCD – Face centered design

FITC - Fluorescein isothiocyanate

GC - Gas chromatography

GI – Gastrointestinal

H – Height

HPLC – High performance liquid chromatography



IoT – Internet of things

IS – Internal standard

L – Length

La – lactalbumin

LCFA - Long chain fatty acids

LF – Lactoferrin

Lg – Lactoglobulin

LASSO – Least absolute shrinkage and selection operator regression

ML – Machine learning

MLR – Multiple linear regression

MSC – Multiple scattering correction

MSE – Mean squared error

OPA - o-phthaldialdehyde

PB – Peristaltic bands

PC – Principal component

PCA – Principal component analysis

PFR – Plug flow reactor

PLS – Partial least squares

PLSR – Partial least squares regression

RA – Rotation angle

RF – Random Forest

RGM – Realistic gastric model

RMSE – Root mean squared error

RR – Ridge regression

RTD – Retention time distribution

SDS - Sodium dodecyl sulphate

SDS-PAGE - Sodium dodecyl sulphate–polyacrylamide gel electrophoresis

SE – Stomach emptying

SGF – Simulated gastric fluid

SIF - Simulated intestinal fluid

SNV – Standard normal variate

SSF - Simulated salivary fluid

SVR – Support vector machine regression

TEMED – Tetramethylethylenediamine

Tris - Tris(hydroxymethyl)aminomethane

UV-VIS-SWNIR – Ultraviolet-visible-short wave near infrared

VIP – Variable importance projections

### **Symbols:**

A – Absorbance

a – Additive effect

b – Multiplicative effect

C – Concentration

$C_{total}$  – Total concentration of food colouring dispersed during the experiment

$c$  - Speed of light in the vacuum ( $2.988 \times 10^8$  m/s)

E – Electric field

E(t) – Retention time distribution as function of time

$h$  – Planck constant ( $6.625 \times 10^{-34}$  J.s)

LT – Lateral thickness of the air chambers

I - Light intensity after sample interaction

$l$  – Optic path length

M – Magnetic field

N – Number of air chambers

n – Number of predictions

P – Loadings of independent data

$\text{pH}_{\text{read}}$  – pH value read

$\text{pH}_{\text{target}}$  – Desired pH value

$pI$  – Isoelectric point

Q – Loadings of the dependent data

$\text{RTD}_{\text{avg}}$  – Average retention time distribution of the food colouring

S - Space between chambers

T – Scores of independent data

TT – Top thickness of the air chambers

U – Scores of dependent data

W – Width of the air chambers

X – Independent data matrix

Y – Dependent data matrix

$\hat{E}$  – Intercept of the independent data

$\hat{F}$  – Intercept of the dependent data

$b_0$  – Linear regression intercept

$I_0$  - Light intensity before sample interaction

$m_k$  – Regression coefficient of the  $k^{\text{th}}$  independent variable

$x_k^*$  - Scaled and centered point at the wavelength k

$x_k$  - Absorbance at wavelength k

$\bar{x}$  - Average of the sample spectrum

$\bar{x}_k$  - Average of the samples spectra at the k wavelength

$y_i$  - Experimental value

$\hat{y}_i$  - Predicted value

$\bar{y}$  - Average of the experimental data

$u_i$  - Predicted score of the  $i^{\text{th}}$  sample point

$r_i$  - Weights of the  $i^{\text{th}}$  sample point

$r^2$  - Coefficient of determination

$SS_{\text{res}}$  - Sum squared of the residuals

$SS_{\text{total}}$  - Total sum of squares

$t_i$  - Score of the independent data point

$\varepsilon$  - Molar absorptivity or extinction coefficient at a given wavelength

$\lambda$  - Wavelength

$\nu$  - Frequency

$\tilde{\nu}$  - Wavenumber

w - Savitzky-Golay filter window

$\sigma$  - Spectrum standard deviation

## PATENT APPLICATIONS

**Madalena, D. A.**, Pinheiro, A. C., Ramos, Ó. L., & Vicente, A. A. (2022). PT116961 - Modelo dinâmico de digestão gástrica e programa de computador.

## LIST OF PUBLICATIONS

**Madalena, D. A.**, Pereira, R. N., Vicente, A. A., & Ramos, Ó. L. (2019). New Insights on Bio-Based Micro- and Nanosystems in Food. In *Encyclopaedia of Food Chemistry* (pp. 708–714). Elsevier. <https://doi.org/10.1016/B978-0-08-100596-5.21859-3>

**Madalena, D. A.**, Fernandes, J.-M., Avelar, Z. S., Gonçalves, R. F., Ramos, Ó. L., Vicente, A. A., & Pinheiro, A. C. Emerging challenges in assessing food grade bio-based nanosystems' behaviour under *in vitro* digestion – A critical view and future perspectives. Submitted to *Food Research International*.

## WORK PARTICIPATIONS

Bourbon, A. I., Martins, J. T., Pinheiro, A. C., **Madalena, D. A.**, Marques, A., Nunes, R., & Vicente, A. A. (2019). Nanoparticles of lactoferrin for encapsulation of food ingredients. *Biopolymer Nanostructures for Food Encapsulation Purposes*, 147–168. <https://doi.org/10.1016/B978-0-12-815663-6.00006-9>

Ramos, O. L., Pereira, R. N., Simões, L. S., **Madalena, D. A.**, Rodrigues, R. M., Teixeira, J. A., & Vicente, A. A. (2019). Nanostructures of whey proteins for encapsulation of food ingredients. *Biopolymer Nanostructures for Food Encapsulation Purposes*, 69–100. <https://doi.org/10.1016/B978-0-12-815663-6.00003-3>

Fernandes, J.-M., **Madalena, D. A.**, Pinheiro, A. C., & Vicente, A. A. (2020). Rice *in vitro* digestion: application of INFOGEST harmonized protocol for glycaemic index determination and starch morphological study. *Journal of Food Science and Technology*, 57(4), 1393–1404. <https://doi.org/10.1007/s13197-019-04174-x>

Fernandes, Jean-Michel, **Madalena, D. A.**, Vicente, A. A., & Pinheiro, A. C. (2021). Influence of the addition of different ingredients on the bioaccessibility of glucose released from rice during dynamic *in vitro* gastrointestinal digestion. *International Journal of Food Sciences and Nutrition*, 72(1), 45–56. <https://doi.org/10.1080/09637486.2020.1763926>

## CONFERENCE PARTICIPATIONS

**Madalena, D. A.**, Pinheiro, A. C., Ramos, Ó. L., & Vicente, A. A. (2022). Development of a reproducible, automated, realistic *in vitro* gastric model. Poster presentation in the international conference “Food Structures, Digestion, & Health 6th International Conference”

CHAPTER 1.  
GENERAL INTRODUCTION

1.1	RESEARCH BACKGROUND AND MOTIVATION .....	2
1.2	RESEARCH AIMS .....	3
1.3	THESIS OUTLINE .....	3
1.4	REFERENCES .....	4

## 1.1 RESEARCH BACKGROUND AND MOTIVATION

The food industry is increasingly focused on preventing nutrition-related diseases and improving consumer wellbeing. The result is a growing trend for healthy foods towards the use of food products enriched with functional compounds produced through the application of innovative and safe technologies. The development of novel controlled delivery systems through the use of nanotechnology has been recently used in the food industry in order to address these challenges (Kagan, 2016). Therefore, understanding their behaviour under digestion conditions, assessing their efficiency and safety is thereby of utmost importance (Cerqueira et al., 2014; Kagan, 2016).

*In vitro* digestion models are crucial to study the digestion of food products and the behaviour of controlled delivery nanosystems since they do not raise ethical issues, they are less time consuming and cheaper processes, when compared with *in vivo* assays (Pineiro et al., 2017). However, the assessment of food products digestion and specially the behaviour of controlled delivery nanosystems under GI conditions is a very difficult process since *in vitro* assays comprise the addition of GI secretions (e.g. enzymes, salts) resulting in high dilution and interferences (e.g. enzymes when tracking a protein-based system). Moreover, the effect of post-experimental interferences inherent to *ex-situ* analyses (e.g., exposure to oxygen, light, and temperature variations, as well as the required enzymatic deactivation step) cannot be neglected (Akbari & Wu, 2016). Furthermore, there are limitations regarding the accuracy of their results since they are affected by the interferences inherent to the addition of GI secretions and to *ex-situ* analyses, which could be circumvented by an *in situ* analytical apparatus.

This dissertation addresses all these gaps by proposing the development of an *in vitro* RGM to evaluate the digestion of foods and the behaviour of controlled delivery nanosystems, under gastric conditions. This model is comprised by a 3D printed stomach, to achieve with anatomical precision the human stomach physiognomy and its inherent motility phenomena.

In terms of the RGM's characterization, a hydrodynamic study was made to understand the mixing and emptying properties of the RGM. Furthermore, samples at the macro (i.e., food product) and nano (i.e., controlled delivery nanosystem) scales were used to characterize the *in vitro* stomach model. These samples were subsequently analysed by conventional techniques and by an *in situ* analytical technique. This was achieved through the use of an UV-VIS-SWNIR spectroscopy apparatus, using fibre optics to track in real time and *in situ* the digestion of food and the behaviour

of controlled delivery nanosystems under GI conditions, since it is a versatile, accurate, inexpensive and simple system (L. I. B. Silva et al., 2009; W. K. Silva et al., 2011).

This project explores novel technologies to provide food industry players with more accurate tools for evaluation, and further development of safer, nutritious, and healthy foods.

## **1.2 RESEARCH AIMS**

This thesis integrates different scientific activities that intend to tackle the previously discussed challenges regarding the *in vitro* assessment of food products' digestion and of controlled delivery nanosystems' behaviour in the GI tract. As such, the main objectives of this dissertation are:

- i. the development of an RGM that simulates, as close as possible, the mechanical and physicochemical properties of the human stomach.
- ii. Development of a real-time analytical tool to assess food and nanosystems' digestion

These objectives can be further addressed through the following specific objectives:

- Design of a RGM prototype (i.e., 3D printing of the stomach);
- Development of the appropriate contraction mechanism for the 3D printed stomach;
- Development of a software to control the *in vitro* gastric model, controlling the frequency, amplitude and force of the peristaltic contractions, gastric emptying, pH and secretions;
- Evaluation of the digestibility of a food product (e.g., milk) in the RMG;
- Evaluation of the behaviour of a previously optimized model nanostructure composed of bio-based materials and of a bioactive entrapped into it [6], throughout the complete *in vitro* digestion model, using an *in situ* UV-VIS-SWNIR spectroscopy with a fibre optic apparatus;
- Development of a software to process the results from the UV-VIS-SWNIR spectroscopy.

## **1.3 THESIS OUTLINE**

To achieve the dissertation objectives, it was organized in 6 chapters. Chapter 2 gives the theoretical framework to chapters 3-5 which represent the experimental work of this dissertation.



Chapter 6 represents the main conclusions of his work. A more detailed description is subsequently provided.

**Chapter 2:** This chapter gives the historical perspective and state of the art regarding the development of *in vitro* digestion models as well as some theoretical background regarding the application of UV-VIS-SWNIR spectroscopy for food analysis. Furthermore, some considerations are made regarding the IOT approach.

**Chapter 3 –** This chapter provides all the necessary steps for the development of a modular RGM in terms of the stomach compartment, PB and all the modules associated with the system. The RGM was further characterized regarding the pH profile and its hydrodynamic behaviour.

**Chapter 4 –** This chapter applies real-time analysis through the application of a UV-VIS-SWNIR fibre optics to assess the *in vitro* digestion of milk. Furthermore, conventional analytical techniques were used to compare with the real-time analysis.

**Chapter 5 –** This chapter provides some final considerations regarding this dissertation as well as some future perspectives.

## **1.4 REFERENCES**

Akbari, A., & Wu, J. (2016). Cruciferin nanoparticles: Preparation, characterization and their potential application in delivery of bioactive compounds. *Food Hydrocolloids*, 54, 107–118. <https://doi.org/10.1016/J.FOODHYD.2015.09.017>

Ariano, P., Accardo, D., Lombardi, M., Bocchini, S., Draghi, L., De Nardo, L., & Fino, P. (2015). Polymeric materials as artificial muscles: an overview. *Journal of Applied Biomaterials & Functional Materials*, 13(1), 0–0. <https://doi.org/10.5301/jabfm.5000184>

Cerqueira, M. A., Pinheiro, A. C., Silva, H. D., Ramos, P. E., Azevedo, M. A., Flores-López, M. L., Rivera, M. C., Bourbon, A., Ramos, Ó. L., & Vicente, A. A. (2014). Design of Bio-nanosystems for Oral Delivery of Functional Compounds. *Food Engineering Reviews*, 6(1–2), 1–19. <https://doi.org/10.1007/s12393-013-9074-3>

Kagan, C. R. (2016). At the Nexus of Food Security and Safety: Opportunities for Nanoscience and Nanotechnology. *ACS Nano*, 10(3), 2985–2986. <https://doi.org/10.1021/acsnano.6b01483>

Pinheiro, A. C., Coimbra, M. A., & Vicente, A. A. (2016). *In vitro* behaviour of curcumin nanoemulsions stabilized by biopolymer emulsifiers - Effect of interfacial composition. *Food Hydrocolloids*, 52, 460–467. <https://doi.org/10.1016/j.foodhyd.2015.07.025>

Pinheiro, A. C., Gonçalves, R. F., Madalena, D. A., & Vicente, A. A. (2017). Towards the understanding of the behavior of bio-based nanostructures during *in vitro* digestion. *Current Opinion in Food Science*, 15, 79–86. <https://doi.org/10.1016/J.COFS.2017.06.005>

Silva, L. I. B., Rocha-Santos, T. A. P., & Duarte, A. C. (2009). Optical fiber analyzer for *in situ* determination of nitrous oxide in workplace environments. *Journal of Environmental Monitoring*, 11(4), 852–857. <https://doi.org/10.1039/b817639f>

Silva, W. K., Chicoma, D. L., & Giudici, R. (2011). In-situ real-time monitoring of particle size, polymer, and monomer contents in emulsion polymerization of methyl methacrylate by near infrared spectroscopy. *Polymer Engineering & Science*, 51(10), 2024–2034. <https://doi.org/https://doi.org/10.1002/pen.22100>

CHAPTER 2.  
LITERATURE REVIEW

2.1	INTRODUCTION .....	7
2.2	<i>IN VITRO</i> DIGESTION MODELS.....	8
2.3	<i>IN VITRO</i> DIGESTION OF FOOD AND DELIVERY SYSTEMS .....	17
2.4	NIR SPECTROSCOPY .....	35
2.5	CONCLUSIONS AND FUTURE PERSPECTIVES.....	41
2.6	REFERENCES .....	43

## 2.1 INTRODUCTION

Food digestion is a very complex process that involves biological, chemical and physical mechanisms to breakdown food into small particles that can be absorbed, mainly, in the small intestine. As such, the digestion of food starts at the mouth where mastication plays a very significant role towards mincing and mixing it with the saliva which is composed by water (ca. 99.5%), proteins/enzymes (e.g., salivary  $\alpha$ -amylase, mucin, globulin) and salts. It is at this stage that the bolus is formed and subsequently swallowed so that it can reach the stomach to continue the digestion process (Ji et al., 2021). The stomach is composed by the fundus, body, antrum and pylorus. It is mainly responsible for digesting protein and, with a lower extent, lipids due to the presence of pepsin and gastric lipase, respectively. It also plays an important role in mixing, through peristalsis (i.e., typically 3-5 contraction/minute), sieving through the pylorus (i.e., only particles that present a diameter between 1-3 mm pass to the duodenum) and storage. The bolus turns into chyme that passes through the pyloric sphincter to the small intestine which is composed by the duodenum, jejunum and ileum. At this step of the digestion, the chyme continues to be broken down into smaller molecules (e.g., amino-acids, FFA and sugars) that can pass through the microvilli of the small intestine via diffusion and transported by the blood stream. Of course that different food products will have different digestion kinetics, different interactions with enzymes, different mixing and retention times in the stomach, among others, depending on their physicochemical properties, e.g., viscosity, nutritional content, etc.

Several studies related to the digestion of food and micro/nanosystems used for the controlled release of bioactive compounds and drugs have been made by the food and pharmaceutical industries to evaluate their performance and optimize their production process. This contributes to the development of more efficient functional foods and drugs (i.e., more precise drug dosage forms which can result in less drug losses during the digestion process) (Mahalakshmi et al., 2020). Ideally, *in vivo* models should be used to assess the impact and toxicity of such systems and infer about their performance under digestion conditions. However, *in vivo* models are expensive, labour intensive, time consuming and present some ethical constraints (Berthelsen et al., 2019). Alternatively, *in vitro* digestion models have been widely used by pharmaceutical and food scientists to:

- i) estimate the release kinetics of bioactive compounds encapsulated into micro/nanosystems (Simões, Abrunhosa, et al., 2020);

- ii) estimate and mathematically modulate the dissolution profiles of drugs (R. F. S. Gonçalves, Martins, Abrunhosa, Vicente, et al., 2021; Sadati Behbahani et al., 2019);
- iii) indirectly quantify the toxicity of metabolites released during the digestion process using epithelial cellular lines (e.g., Caco-2 cells) (Zhongyuan Guo et al., 2020; Wei et al., 2019);
- iv) study physical and biochemical processes that undergo during the digestion of food (e.g., enzymatic digestion process, the peristaltic movements' influence the mechanisms associated to the presence of bile salts and their role in the digestion of proteins, lipids, and carbohydrates, among others).

This way, the following topic will address the development of static, semi-dynamic and dynamic *in vitro* digestion models as well as critically discuss the validation of such models.

## **2.2 IN VITRO DIGESTION MODELS**

### **2.2.1 Static *in vitro* digestion models**

Static *in vitro* digestion models are simpler digestion tools that use standard laboratory equipment which are suitable for biochemical studies regarding the digestion process. This way, they are typically composed by beakers, erlenmeyer flasks or tubes that are kept at 37 °C under stirring through a shaking water bath or magnetic stirring (Ji et al., 2021). They can be composed by a single compartment (i.e., noncompartmental models) or multiple compartments (i.e., multicompartmental). They can also be composed by a single step of the digestion (e.g., gastric digestion) or multiple digestion processes (e.g., oral, gastric and small intestine digestion).

The samples are minced (i.e., if the sample is solid) and mixed with artificial saliva, if the digestion process has an oral phase, which is composed by salivary  $\alpha$ -amylase and electrolyte salts. The oral phase has a typical duration of 2-5 minutes depending on the digestion protocol used, and the samples are kept at 37 °C at pH 7.0. Subsequently, the gastric digestion starts and the pH is lowered to 1.5-3 through the addition of HCl. The samples are then mixed with enzymes (e.g., pepsin, lipase, chymotrypsin, etc) and electrolyte salts with a duration of ca. 90-120 minutes. The small intestine digestion (i.e., represented by a single digestion stage or multiple digestion stages to mimic the duodenum, jejunum and ileum) can then start by incubating the gastric samples for

ca. 120 minutes at pH 7.0-7.5 (by adding NaOH) and mixing them with enzymes (e.g., pancreatic lipase, pancreatic  $\alpha$ -amylase, among others) electrolyte salts and bile salts.

By the previous general description of the *in vitro* static digestion process, it is possible to observe that different conditions are used with different enzymes, salt concentrations, pH, digestion times or even digestion stages. Consequently, comparisons between studies were not possible due to the discrepancy in the digestion protocol. However, a research group took the initiative to develop a standardized static *in vitro* digestion protocol. The COST INFOGEST group introduced a standardized static *in vitro* digestion protocol which is based on *in vivo* physiological data that allows inter-laboratory comparisons between assays (Minekus et al., 2014). This initiative was a significant landmark in the field since, until then, comparing *in vitro* digestion results was limited to studies that used the same *in vitro* digestion conditions/models (e.g., within the same research group) and no inter-laboratory comparisons could be made, unless they used the same digestion protocol. More recently, this standardized protocol was updated by Brodkorb et al. (2019) by introducing the presence of gastric lipase in the gastric phase of the protocol, which was not commercially available until then. In fact, there is a current awareness from the scientific community to develop standard physiologically relevant *in vitro* models, that can be applied by a wide range of research groups is a major concern while developing such protocols (Brodkorb et al., 2019). A comparison of the different standardized *in vitro* digestion models can be seen in Figure X.

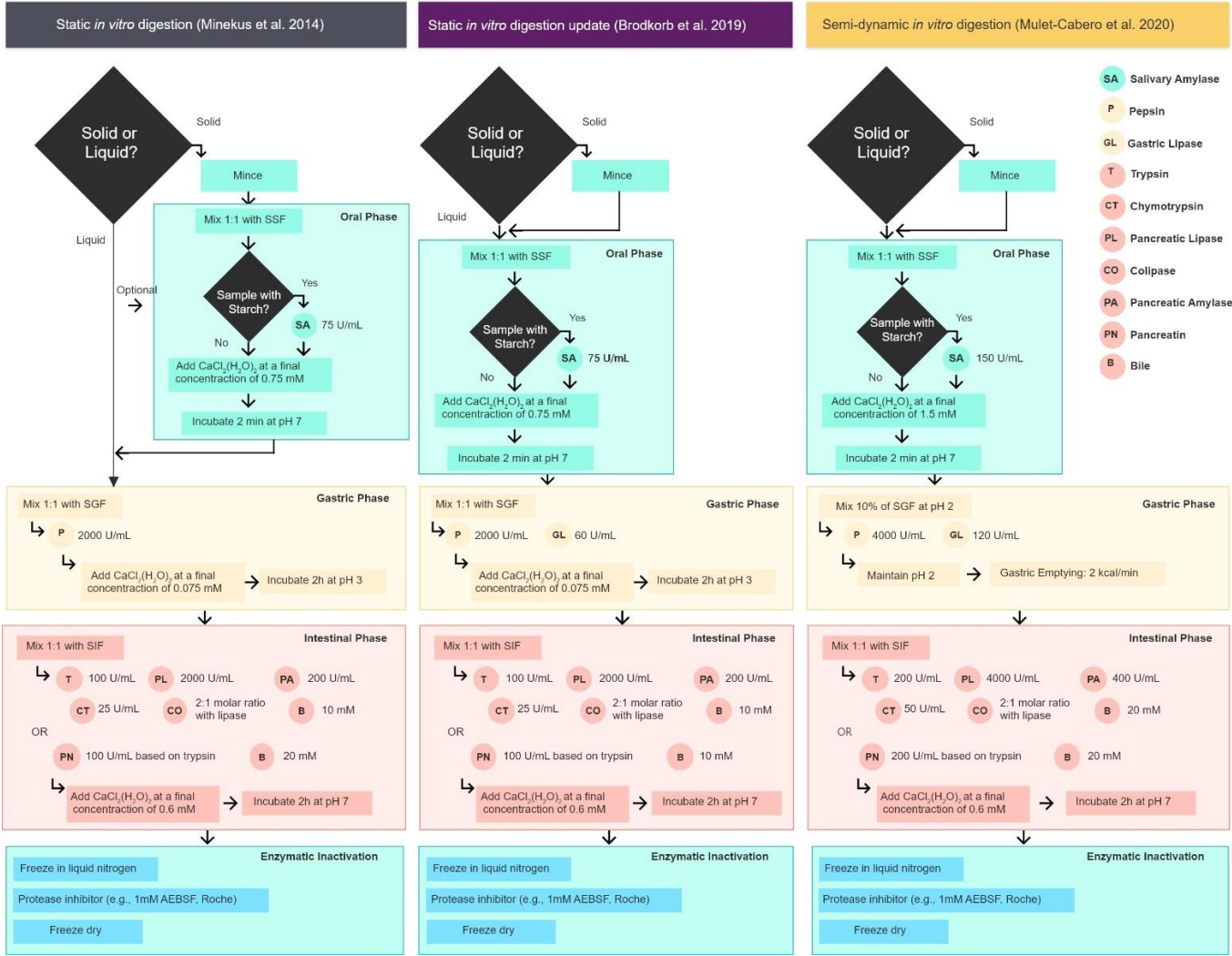


Figure 1 - Comparison between the different standardized *in vitro* digestion models.

The latest embodiment of the standardized *in vitro* digestion model developed by Minekus et al., (2014) and further updated by Brodkorb et al. (2019) encompasses the oral, gastric and intestinal digestions that are kept at 37 °C in a shaking water bath. Primarily, the samples are mixed with SSF in a 1:1 (w/w) ratio and CaCl<sub>2</sub> is added (1.5 mM in SSF). The salivary amylase is added (if the sample contains starch) with an enzymatic activity of 75 U/mL. The samples are then incubated for 2 minutes at a pH 7.0. Note that if the samples are solid, mincing can be done through a manual or electrical mincer. Subsequently, the bolus is mixed with SGF in a 1:1 (w/w) ratio and CaCl<sub>2</sub> is added (0.15 mM in SGF). Pepsin and gastric lipase are added with an enzymatic activity of 2000 and 60 U/mL, respectively and the chyme is incubated for 120 minutes at pH 3.0. The chyme is then mixed with SIF with a 1:1 (w/w) ratio and bile salts (10 mM), CaCl<sub>2</sub> (0.6 mM in SIF) and pancreatin (trypsin activity of 100 U/mL) and incubated for 120 minutes at a pH 7.0 (Brodkorb et al., 2019; Minekus et al., 2014).

Despite of their simplicity, static *in vitro* digestion models have been widely used to study the digestion of food (Gao et al., 2019; Sanchón et al., 2018) and nanosystems in the upper GI tract (Gonçalves, Martins, Abrunhosa, Vicente, et al., 2021; Simões, Martins, et al., 2020; Xu et al., 2021), since they can be used to study the influence of the chemical conditions of the GI tract. However, they are not appropriate to perform kinetic studies since they do not present, e.g., the complex motility of the human GI tract, gradual stomach emptying, etc. For this purpose, semi-dynamic and dynamic *in vitro* digestion models can be used and their description is the subject of the next topic.

### **2.2.2 Semi-dynamic/ dynamic *in vitro* digestion models**

Semi-dynamic (i.e., they present both static and dynamic digestion steps) and dynamic *in vitro* digestion models are *in vitro* digestion tools that take into consideration the physicochemical processes of the digestion, e.g., stomach and intestinal contractions, gradual pH adjustment, gradual stomach emptying, among others, thus closely mimicking the conditions present in the human gastrointestinal tract, allowing kinetic studies of food and micro/nanosystems digestion (Madalena et al., 2019; Mulet-Cabero et al., 2020). It is possible to find in the literature different *in vitro* digestion models and, until the development of a standard *in vitro* digestion model, different models have been used by different research groups, thus hampering accurate comparisons between different studies, as previously mentioned. On this regard, Mulet-Cabero et al. (2020)



recently developed a standardized *in vitro* semi-dynamic model that takes into consideration the gradual pH changes that occur during food digestion.

Briefly, the oral digestion in the standardized semi-dynamic *in vitro* digestion model is similar to the static *in vitro* model, which was previously described, with the exception of the salivary amylase activity which was changed to 150 U/mL. The major differences of this protocol when compared to the standardized static *in vitro* digestion one is the gastric phase. This phase is a dynamic one with a gradual addition of enzymes, salts and stomach emptying. This way, the gastric digestion time will depend on the caloric content of the sample which can be calculated using the Atwater factor (i.e., 4 kcal per gram of protein and carbohydrates and 9 kcal per gram of lipids). This will in turn determine the flow rates of the enzymes, salts and stomach emptying taking into consideration a constant stomach emptying rate of 2 kcal/min. The intestinal phase of the standardized semi-dynamic *in vitro* digestion protocol is identical to the static protocol (Mulet-Cabero et al., 2020).

Despite of the current awareness related to the standardization of *in vitro* digestion models, much work must be done since the current standardized models still do not consider nutrient absorption and intestinal dynamic behaviour. Moreover, some important mechanical grinding phenomena (e.g., retropulsion) and pyloric filtering are not considered and thus, dynamic models are required for such studies. The most recent advances by the scientific community were devoted to the development of novel *in vitro* dynamic digestion models (mostly *in vitro* gastric models), more specifically, to mimic the anatomical, mechanical and physiological behaviour of the human stomach (Y. Li et al., 2019; W. Liu, Fu, et al., 2019; Vrbanac et al., 2020; J. Wang et al., 2019) and small intestine (J. Wang et al., 2019), in addition to simulating the physicochemical conditions of the GI tract. Dynamic *in vitro* digestion models were recently applied to study the digestion of protein (Bourbon et al., 2018), lipid (Machado et al., 2019; Silva et al., 2018) and polysaccharide (Silva et al., 2019) digestion. Furthermore, the most recent dynamic *in vitro* digestion models simulate the anatomical shape and size of the human stomach (i.e., a J-shaped structure), through the application of 3D printing technologies to develop the mould of the stomach and small intestine and by the application of deformable elastic materials. Materials like silicone (Liu et al., 2019) and latex (Li et al., 2019) have been used for this purpose since they are elastic, deformable, non-toxic, chemically resistant and inert materials (Vrbanac et al., 2020; Wang et al., 2019). Moreover, some novel digestion models simulate the inner surface roughness, conferred by the inner surface folds in the human stomach lumen (Li et al., 2019; Wang et al., 2019), aiming at representing a more

realistic dissolution behaviour and grinding forces. Due to the “J” shape of the human stomach and the simulation of the pyloric sphincter, phenomena like retropulsion may take an important role in food grinding and consequent particle sieving, since the pylorus only allows the passage to the duodenum of particles with a diameter below 1-2 mm (Li et al., 2019; Vrbanac et al., 2020).

Simulating the human GI peristalsis has been a concern since it takes a crucial role in food grinding. The simulation of the GI peristaltic movements has been achieved through different approaches. For example, Wang et al. (2019) used a roller system to contract the *in vitro* stomach and small intestine; Li et al. (2019) applied multiple inflated pneumatic syringe systems at different locations to simulate the human stomach contractions; Liu et al. (2019) used a belt system to apply contraction forces to the *in vitro* stomach model; and Vrbanac et al. (2020) simulated the peristaltic contractions through a “worm gear” constriction mechanism. Due to the versatility of *in vitro* digestion models, some can even simulate the GI conditions of population specific groups (e.g., infants and elderly). For instance, infant *in vitro* digestion models are often composed by a gastric and intestinal phase, i.e., the oral phase of digestion is not included mainly due to the lower  $\alpha$ -amylase levels and low swallowing times (i.e., the main source of nutrients comes from milk). These models present higher gastric pH of ca. 5 which lowers pepsin digestion (i.e., optimal pH ranging from 1.6 - 4) but promotes gastric lipase activity (i.e., optimal pH ranging from 3 - 5) which retains its activity throughout the GI tract (i.e., from pH 1.5 - 7), playing an important role during the intestinal lipolysis (Mackie et al., 2020). Similar to the infants, the elderly population also presents higher pH values in the stomach (ca. 4), however, they present higher concentrations of  $\alpha$ -amylase during the oral phase of the digestion (Mackie et al., 2020; Shani-Levi et al., 2017) and lower bile salt concentration in the intestinal phase (Hernández-Olivas et al., 2020; Mackie et al., 2020).

Different approaches have thus been used to simulate the real conditions in the human stomach and small intestine, in terms of anatomy, surface roughness, mechanical behaviour, population specific conditions and sieving capabilities. However, work needs to be done to accommodate the current differences between the existing *in vitro* digestion models and *in vivo* systems. For instance, the presence of mucus in the stomach and gastric selective absorption behaviour could take an important role towards simulating human digestion and this way, obtaining more realistic predictions of food digestion kinetics (C. Li et al., 2020). Moreover, efforts should be done towards standardizing dynamic *in vitro* digestion models so that interlaboratory studies and comparisons

could be made. This way, one should expect that the next step towards the standardization of *in vitro* dynamic models would be the development of easy to replicate dynamic models through the application of, e.g., 3D printing to develop both the digestion compartments and peristaltic mechanisms. To the authors knowledge, there is still a lack of standardized *in vitro* digestion models that simulate the GI conditions of population specific groups (e.g., elderly and infants). However, efforts have been made towards this path with the development of a potential standard *in vitro* infant digestion protocol by Ménard et al., (2018).

### 2.2.3 *In vitro* digestion protocol challenges

Food digestion is a dynamic and very complex process, with several pH transitions, different ionic strengths and several intervenient compounds (i.e., enzymes, salts and bile salts), which interfere with the behaviour of nanosystems under each of these conditions. These interferences should not be ignored, and care must be taken while performing the intended analysis. Therefore, several challenges can be highlighted when evaluating the behaviour of nanosystems throughout the *in vitro* digestion process (C. Li et al., 2020).

During *in vitro* digestion, several samples are usually taken to determine the overall digestion kinetics and the integrity of the nanosystem or the bioactive compounds' release kinetics at the end of each digestion stage. Consequently, the enzymatic digestion must be stopped, or at least attenuated, in order to obtain reliable results at a specific sample time. Commonly, samples are kept at low temperatures (i.e., often through ice baths or liquid nitrogen) to stop further enzymatic reactions. However, the low temperature conditions can influence the overall nanosystem dynamics and its structure, as well as the release kinetics of bioactive compounds (C. Li et al., 2020; Pinheiro et al., 2017). For instance, some proteins present some degree of denaturation at low temperatures which can cause protein unfolding and aggregation, and consequently the release of bioactive compounds (Arsiccio et al., 2020). Other techniques to prevent the enzymatic digestion of the samples may include the addition of sodium hydroxide (NaOH) or sodium bicarbonate (NaHCO<sub>3</sub>) to raise the pH and stop gastric enzymatic digestion and the addition of Pefabloc® SC to block the activity of trypsin and chymotrypsin (Mulet-Cabero et al., 2020). However, raising the pH of digestion samples may induce unwanted phenomena such as particle aggregation due to the isoelectric point of the nanoparticles which can in turn interfere with the digestion results.

Dynamic *in vitro* digestion systems can be used to estimate the bioaccessibility of bioactive compounds, in particular the models that encompass a filtration process in jejunum and ileum

stages such as the TIM-1 model (Dupont et al., 2018). Their dynamic classification is often attributed based on the control of their pH (e.g., gradual pH adjustment in the gastric phase), stomach emptying behaviour, fluid injection over time (i.e., electrolytes, enzymes and bile salts), as well as the presence of peristalsis (Lucas-González et al., 2018). In order to achieve this last feature, plastic bags are often used as containers for the digestion process, which are alternately contracted to simulate GI peristalsis. However, some bioactive compounds present some affinity to plastics and adsorb to their surface (e.g., carotene) (Berni et al., 2019) and this must be taken into account when calculating the release kinetics of bioactive compounds under GI conditions. For instance, Berni et al (2019) reported a change in colour of the plastic bags (i.e., colour changed to a light yellow colour and light red colour for buriti and pitanga emulsions, respectively) due to the affinity of carotene to plastic, especially when in an aqueous medium. This results in an underestimation of bioaccessibility of carotene in the intestinal phase. Moreover, the validation of *in vitro* digestion models is still a major challenge (Ketnawa et al., 2021; Li et al., 2020) and while several papers reviewed the recent developments on digestion models (Gonçalves et al., 2021; Ji et al., 2021; Li et al., 2020), very few discuss the *in vitro* digestion models' validation which is the focus of the next topic.

#### **2.2.4 *In vitro* digestion models' validation**

It is clear from the previously discussed topics that, regarding the development of new dynamic *in vitro* digestion models, different approaches and materials have been used to simulate the digestion conditions of the human GI tract. However, none of the models developed so far are truly validated (Ketnawa et al., 2021; C. Li et al., 2020). In fact, several strategies were used to assess the performance of those models which implies that no standard protocol has not yet been developed to validate such models. It is thus important to discuss what should be considered for their validation, the challenges associated to the validation process as well as some possible solutions.

The validation is perhaps the most complex step in the development of novel *in vitro* digestion models. Therefore, several questions arise while addressing this topic such as: What is a validated model? Which are the current challenges that limit their validation? Which are the possible solutions than can contribute to their validation? Is it possible to have a fully validated model?

One should expect that a fully validated model would be able to predict the bioaccessibility of nutrients and bioactive compounds with lower errors and deviations from *in vivo* data, i.e., with higher accuracy, when compared to unvalidated models. However, the models' validation will

dependent on several factors being one of the most important, their purpose, i.e., an *in vitro* digestion model can be developed for:

- i) the assessment of a specific food product's digestion;
- ii) the simulation of the GI tract of a specific population (e.g., regional, continental, age specific);
- iii) the simulation of the GI tract of specific species (i.e., simulation of the GI tract of mice);
- iv) the assessment of specific GI pathological conditions;
- v) the bioaccessibility assessment of food products and bioactive compounds.

Therefore, a model should only be validated if the *in vivo* validation data used can significantly represent its final application, i.e., if an *in vitro* digestion model is designed to represent the GI tract of a specific population (e.g., population of a given country or region), then the *in vivo* data from the same population should be used for its validation (Shani-Levi et al., 2017). Of course, that obtaining representative *in vivo* digestion data is still a major challenge due to ethical constraints, complexity and cost (Pineiro et al., 2017). In fact, the complexity of the human digestive system poses a major challenge due to high inter and intra-individual variability, e.g., the concentration of enzymes, transit time, gastric emptying rate, among others that vary with the individual's diet, sex or age (Eker et al., 2020; C. Li et al., 2020). Consequently, comparing the statistical difference between *in vitro* and *in vivo* data would not be appropriate. Furthermore, the scarcity of *in vivo* studies, especially regarding the assessment of nanosystems, and the reduced number of test subjects per study (e.g., human or animal test subjects) could pose a challenge towards the representativity of the *in vivo* data in the studied population.

Despite the identified challenges, some strategies could be applied to solve or at least attenuate their consequences. For instance, the development of an open access world-wide database composed, initially, by *in vivo* digestion data of predetermined, standard food products/nanosystems could be a solution towards increasing sample size and consequently, sample representation (Shani-Levi et al., 2017). For such development, it should be investigated which parameters are more appropriate to be considered and measured *in vivo*. Such research would result in the development of a standardized *in vivo* digestion protocol which would be crucial for the comparison of data obtained world-wide, i.e., interlaboratory comparison. With the development of a world-wide database, sophisticated algorithms, e.g., artificial neural networks, random forests, genetic algorithms, support vector machines, cluster analysis, among others, could

be used to identify patterns in the *in vivo* data and consequently estimate the digestion kinetics of the studied product. The same approach could also be used to analyse the data variability among individuals which would result on identifying the patterns related to the *in vivo* data variance. This error pattern identification could be further used to correct the *in vitro* digestion data which would increase the *in vitro*-*in vivo* correlations.

Still, there is a lot of work to be done and world-wide efforts must lean towards the validation of *in vitro* digestion models, either through the development of standard protocols regarding the collection and assessment of *in vivo* data or through the application of technologically advanced analytical techniques to unravel data trends and better correlate *in vitro* and *in vivo* digestion data.

## **2.3 IN VITRO DIGESTION OF FOOD AND DELIVERY SYSTEMS**

### **2.3.1 Assessment of food under *in vitro* digestion**

Many efforts have been driven towards the development of functional foods, i.e., food products that present additional properties beyond their nutritional value (Simões, Martins, et al., 2020). For this purpose, bioactive compounds have been used and incorporated into food products to confer e.g. anticarcinogenic, anti-inflammatory, antifungal, antioxidant, antimicrobial and antiviral properties, among others (Silva et al., 2019). Such compounds may present poor water solubility and susceptibility to the harsh digestion conditions, lowering their bioaccessibility and bioavailability (Mahalakshmi et al., 2020). To overcome this bottleneck, bio-based nanosized delivery systems (i.e., nanosystems) have been used to protect the integrity and functional properties of bioactive compounds (Ramos et al., 2019; Simões, Abrunhosa, et al., 2020). For this purpose, protein (Mahalakshmi et al., 2020), lipid (R. F. S. Gonçalves, Martins, Abrunhosa, Baixinho, et al., 2021) and polysaccharide (Zhongyuan Guo et al., 2020) matrices have been used as vehicles to deliver and protect bioactive compounds since they are generally recognized as safe (GRAS) materials that have the ability to form functional structures (i.e., nanoparticles, nanodroplets, nanofibrils, nanohydrogels and nanoemulsions) that release their content in response to external environmental stimuli (Wei et al., 2019). These materials should fulfil the requirements for the development of controlled delivery systems, namely, ensure the correct and timely release of bioactive compounds.

In fact, controlled delivery nanosystems must be capable of withstanding storage conditions as well as the harsh conditions of the upper GI to be considered reliable delivery nanosystems. This means that they must resist the acidic pH of the stomach and the hydrolytic activity of enzymes (e.g., amylase, pepsin and lipase), to release their content in the appropriate location (Ahmad et al., 2019). If such requirements are met, nanosystems can be widely used to improve food quality and safety, shelf-life stability, cost and nutritional value by the controlled delivery of several bioactive ingredients (e.g., polyphenols, vitamins, minerals, fatty acids, flavours, colours and preservatives) (Das et al., 2020).

This section highlights the behaviour and performance of protein-, lipid- and polysaccharide-based nanosystems under *in vitro* digestion conditions. An overview of the mechanisms that are responsible for the digestion behaviour of proteins, lipids and polysaccharides is depicted in Figure 1, and these subjects are subsequently addressed in the following subsections.

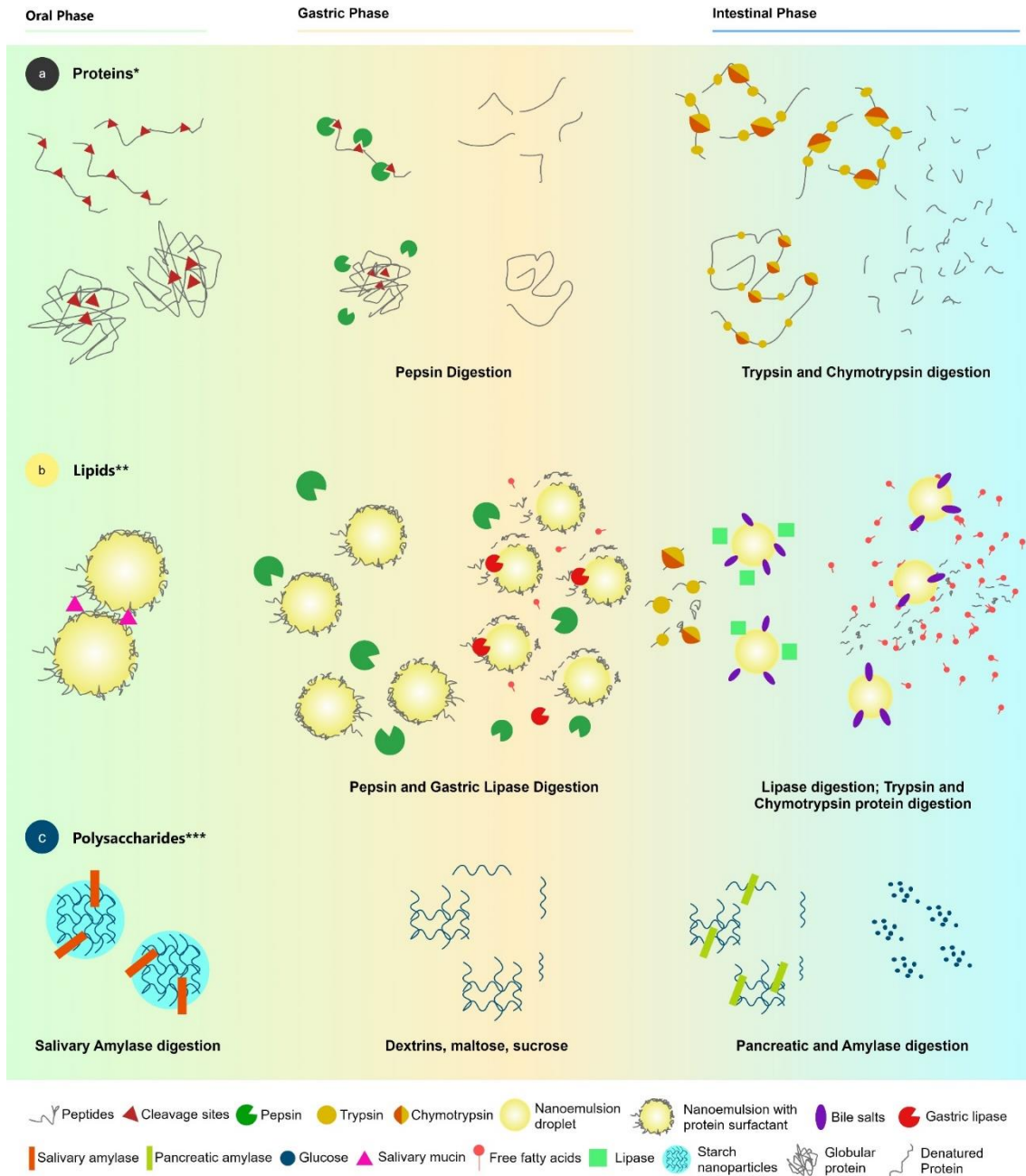


**Figure 2** - Illustration of some important protein enzymatic interactions that occur during the gastric and intestinal phases of the digestion process. This figure is based on the work of Mackie & Macierzanka, (2010). \*Protein digestion starts typically in the stomach; \*\*Flocculation may occur from mucin interactions with adsorbed proteins; \*\*\*Polysaccharides are typically resistant to gastric digestion and their digestion mainly occurs in the gut by the microflora with a few exceptions like starch which digestion process is depicted in this figure.

### 2.3.1.1. Protein-based nanosystems



Proteins are very well known for their relevant functional properties such as emulsification, gelation, foaming and water binding capacity. These properties, together with their biodegradable nature, make them an ideal material for the development of nutraceutical bio-based delivery systems. Their structural versatility allows the production of films, particles, fibres, tubes and hydrogels for the delivery of both hydrophobic and hydrophilic compounds (Simões et al., 2017). Furthermore, proteins have high nutritional value and are GRAS materials (Simões, Martins, et al., 2020). Over the past few years, milk proteins, more specifically whey proteins, have been widely used as effective delivery vehicles for bioactive compounds. For instance,  $\beta$ -lactoglobulin, the major whey protein, is considered a suitable candidate to develop nanosystems due to its gastric stability and capability to bind hydrophobic constituents (Simões, Abrunhosa, et al., 2020; Simões, Martins, et al., 2020). However, the behaviour of protein nanoparticles highly depends on their electrical properties, i.e., their surface charge which in turn depends on the pH of the environment and the exposure of anionic and cationic groups. This way, their surface charge typically changes from negative to positive as the pH decreases and passes through the nanoparticles' isoelectric point where the surface charge is neutral and protein aggregation occurs (McClements, 2018a).

Protein nanohydrogels (or nanogels) have attracted much attention for the encapsulation of bioactive compounds due to their ability to swell in response to chemical (e.g., pH, solvent composition and ionic strength) or physical (e.g., temperature, electric or magnetic field, light and pressure) stimuli. Moreover, they are non-toxic and biodegradable materials that have a small size with a large inner network for multivalent bioconjugation (Araújo et al., 2020). Nanohydrogels consist in a three-dimensional network of hydrophilic polymeric molecules that can associate to each other through covalent or non-covalent (e.g., hydrogen bonds, van der Waals interactions and physical entanglements) interactions (Bourbon et al., 2019). Therefore, due to its stimuli-dependent response, hydrogels can e.g. release the entrapped bioactive compound into the media in the presence of alkaline pH, which makes them important delivery systems of bioactive food ingredients (Simões et al., 2017). For example, under gastric conditions, pH-sensitive hydrogels shrink, but under intestinal conditions they swell which results in the release of the entrapped bioactive compound through the increase of its mobility within the network matrix (Lv et al., 2018; Simões et al., 2017). This indicates that such delivery systems may be used to protect a bioactive compound from the harsh conditions in the human stomach and release its content in the small intestine, improving nutrient solubility, bioaccessibility and consequently their bioavailability. G. Hu et al., (2021) used acylated ovalbumin (AOVA) nanohydrogels as protective carriers of curcumin

under *in vitro* digestion conditions. The authors observed that ca. 23% of curcumin was released during the digestion process which was significantly lower when compared to free curcumin control (ca. 87%). Similar to nanohydrogels, protein nanoparticles can also be used as vehicles for bioactive compounds. As such, recent studies illustrate the potential of protein nanoparticles to be used as controlled delivery systems. For instance, Simões et al. (2020) investigated the *in vitro* digestion performance of  $\beta$ -lactoglobulin micro- and nanoparticles as protective carriers of riboflavin (vitamin B2). The authors showed that  $\beta$ -lactoglobulin nanoparticles with an initial size of 79.4 nm were able to retain  $61.7 \pm 4.1\%$  of riboflavin allowing its release in the small intestine which improved its bioavailability. Moreover, the authors also observed an increase in particle size to ca.  $4017.5 \pm 497.6\text{nm}$  and  $600.8 \pm 44.8\text{nm}$  in the gastric and intestinal phase, as well as an increase in polydispersity to ca.  $0.97 \pm 0.05$  and  $0.66 \pm 0.06$ , respectively, probably due to the low surface charge in the stomach (ca.  $0.9 \pm 0.5\text{mV}$ ) and consequently the absence of repulsive electrostatic forces that prevent particle aggregation. Casein nanoparticles can also be used to produce nanosystems to protect bioactive compounds during digestion. For instance, Du et al., (2022) assessed the performance of casein nanoparticles to encapsulate curcumin and assessed their stability and curcumin release during *in vitro* digestion. The authors observed that the casein nanoparticles remain stable in terms of their size during the gastric phase of the digestion (i.e., size of ca. 107 nm) with a curcumin release of ca. 18.5%. However, in the intestinal phase of the digestion, particle aggregation was observed, with particle sizes ranging from ca. 200 nm to 650 nm and a curcumin release of ca. 76.4% which indicates that casein nanoparticles can significantly increase curcumin bioaccessibility. Alternative sources of protein are also being used for the development of nanosystems.

Soy protein isolate (SPI) nanoparticles were recently used as protective carriers for vitamin D3 during *in vitro* digestion. It has been shown that the incorporation of vitamin D3 in SPI nanoparticles treated with high pressure homogenization improves its release kinetics by ca. 18.8% when compared with isolated vitamin D3. The authors observed that adding carboxymethyl chitosan, forming a protein-polysaccharide conjugate, significantly improved the performance of developed nanosystems by ca. 46.5% and 37.2% when compared with free vitamin D3 and SPI nanoparticles respectively (A. Zhang et al., 2020). In fact, the application of polysaccharides and lipids to improve protein-based nanosystems stability during *in vitro* digestion is common. For example, proteins can be conjugated with k-carrageenan (Lv et al., 2018), propylene glycol alginate (Wei et al., 2018), rhamnolipids (L. Dai et al., 2018), chitosan (W. Dai et al., 2020), among others, to improve

bioactive compounds' stability and, consequently, bioaccessibility, during *in vitro* digestion (Bourbon et al., 2019).

Different protein digestion kinetics can be associated to different structural characteristics of protein nanosystems (depicted in Figure 1a), which in turn are modulated by production processing techniques (e.g., heating, high-pressure, ultra-sound, among others) (Jin et al., 2021; Q. Liang et al., 2021). For instance, protein digestibility can be modulated by thermal treatment since protein denaturation significantly changes its conformational state, making previously inaccessible chemical groups accessible to enzymatic interactions and thus proteolysis occurs (Rahaman et al., 2017). High pressure processing (i.e., pressure between 100 and 800 MPa) of proteins can also determine the fate of protein-based nanosystems within the GI tract. Studies show that high pressure treatments enhance protein digestibility by promoting partial (i.e., for pressures up to 450 MPa) protein denaturation and aggregation or complete (i.e., for pressures higher than 500 MPa) protein denaturation and partial aggregation (Kurpiewska et al., 2019; Xue et al., 2020). Ultrasonic treatments can also take a relevant role in improving protein digestibility. It has been reported that ultrasonic treatments may induce high pressures and shear forces that can promote significant changes to protein secondary and tertiary structures, particle size, charge and SH groups' exposure, which leads to an increase of protein susceptibility to pepsin and trypsin digestion (J. Li et al., 2018; Q. Liang et al., 2021). Proteins can also have a buffering effect during gastric digestion due to their ability to bind H<sup>+</sup> ions, specifically under acidic conditions and, consequently, change enzymatic activation and digestion kinetics. However, such effect is highly dependent on protein structure which in turn can be modulated by the aforementioned pre-processing (Mennah-Govela et al., 2020). Despite of the advances related to the production and optimization of protein-based nanosystems, further work is clearly required to better understand the behaviour of proteins within the GI tract as well as the functional compounds' release mechanisms at the nanoscale. Furthermore, tracking protein secondary structures during *in vitro* digestion is still a challenge. The interference of, e.g., enzymes, bile salts, among others, play a relevant role on the acquisition of circular dichroism spectra and, if properly obtained (i.e., without interferences) this information could lead to a better understanding of protein unfolding, hydrolysis and bioactive compounds' release kinetics during *in vitro* digestion. It is also important to mention that some proteins present some form of allergenicity, and this must be taken into consideration when choosing protein nanosystems for the oral delivery of bioactive compounds. For instance, protein allergenicity is partially associated to the resistance to the proteolytic effect of pepsin by some proteins (Mackie &

Macierzanka, 2010). An example of this behaviour is  $\beta$ -Lg which is the main responsible for milk allergenicity (Kurpiewska et al., 2019). However, such allergenicity may be reduced by the previously discussed processing methods (e.g., thermal and high pressure processing) (Bhat et al., 2021b).

#### 2.3.1.2. Lipid-based nanosystems

Different lipid-based delivery nanosystems have been developed in the past decades to be applied in the oral route to overcome the low bioavailability of bioactive compounds with poor water solubility, chemical instability and low intestinal permeability. Their main benefits, which include high biocompatibility, efficient permeation and enhanced bioavailability, are related to their capacity of stimulating biliary and pancreatic secretions, to increase the residence time in the GI tract and stimulation of lymphatic transport (Berthelsen et al., 2019).

The most common lipid-based nanosystems are nanoemulsions (NE), solid lipid nanoparticles (SLN), nanostructured lipid carriers (NLC) and liposomes. NE are composed by two immiscible liquids (i.e., oil and water) and stabilized with emulsifiers or surfactants (e.g., Tween 20, Tween 80, lecithin and sodium caseinate). SLN are constituted by a solid lipid in the core and stabilized with emulsifiers and surfactants. NLC are the next generation of SLN, where the core is composed by a mixture of a solid lipid and a liquid oil also stabilized with surfactants or emulsifiers. Finally, liposomes are vesicular structures formed with amphiphilic molecules, such as phospholipids (Simões et al., 2017). However, liposomes may present some stability issues which may lead to aggregation and early drug release and degradation during storage or digestion. This way, SLN and NLC are presented as viable alternatives to liposomes. Despite their similarity in terms of manufacture, some differences can be identified between SLN and NLC. For instance, the SLN nanosystems are composed by solid lipids in the core and surfactants in the shell while NLC are composed by a mixture of solid and liquid lipids in the core and surfactants in the shell. NLC are generally developed for high loadings and stability due to their non-ideal crystalline structure in the core (Katopodi & Detsi, 2021; Nasirizadeh & Malaekheh-Nikouei, 2020).

Nevertheless, after ingestion, lipid-based delivery systems are subjected to several physicochemical conditions, such as low pH and high ionic strength in the stomach, that may alter their structural properties (i.e. surface charge and steric coating) and their stability (Wang & Luo, 2019). For instance, triglycerides' digestion starts in the stomach due to the presence of gastric lipase, with a lower extent, but it is in the small intestine where most lipids are hydrolysed into fatty acids. This

process is an interfacial process, since lipase needs to adsorb to the oil-water interface before it starts to convert triacylglycerols (TAG) and diacylglycerols (DAG) into monoglycerides (MAG) and FFA (McClements, 2018b). The extension of lipase's adsorption is related to the physicochemical properties of the oil-water interface, such as interfacial structure, composition and surface area (Ye et al., 2019). Lipid digestion products and endogenous surfactants present in bile secretions (i.e., phospholipids and bile salts) can then interact via electrostatic and hydrophobic interaction and form several structures, such as unilamellar and multilamellar vesicles, and mixed micelles, where the bioactive compounds can be incorporated (Berthelsen et al., 2019; Macierzanka et al., 2019). Furthermore, bile salts have a significant interference in lipolysis, since it has been reported that their physiological function is related to the emulsification of lipids and consequently, their role significantly changes the production of micelles (Macierzanka et al., 2019). These micellar structures can enhance the transport of bioactive compounds across the mucus to the surface of the intestinal membrane and their absorption (Wang & Luo, 2019). In fact, evidence points out that the droplet size and oil type play a significant role during *in vitro* lipolysis (Salvia-Trujillo et al., 2019). In this sense, nanoemulsions composed by medium chain triglycerides (MCT) present a higher and faster free fatty acid release in the small intestine when compared with emulsions composed of long chain triglycerides (LCT). This is due to a higher water dispersibility observed for MCT containing lipids and to the fact that nanoemulsions' *in vitro* digestion results in the formation of smaller micelles that are more prone to lipase hydrolysis. However, in terms of bioactive compound bioaccessibility, e.g. LCT lipids showed a higher eugenol bioaccessibility when compared with MCT lipids, which can be related to the larger lipophilic micelle cores as a result of LCT *in vitro* digestion (Majeed et al., 2016). Moreover, Gonçalves et al. (2021) recently assessed different lipid nanosystems' digestibility (e.g., SLN, NE and NLC). The authors concluded that all nanosystems presented a fast FFA release within the first minutes of digestion with subsequent stabilization. The authors also observed that SLN presented a significantly higher FFA release at the end of the digestion process, when compared with NE and NLC, of ca. 23.8 % and 38.6 %, respectively. These differences were attributed to the nanoparticle instability and agglomeration of NE during the gastric phase (i.e., the increase in particle size promotes a lower surface area for lipase interaction and therefore, lower lipolysis) and the combination of solid lipids and liquid (i.e., in the case of NLC) which results in a higher enzymatic resistance. These nanosystems can also protect the associated tissues of the GI tract by reducing the mucosa irritation caused by continuous contact with some bioactive compounds (Madalena et al., 2019; C. Zhang et al., 2013).

For instance, triptolide (TP) is known to cause several adverse conditions to the human GI tract, namely, GI ulcer, bleeding, vomiting, mucosa irritation, among others. Regarding the irritation of the GI mucosa, it occurs due to the cellular damage caused by oxidative stress. However, the encapsulation of TP in SLN shown to have significant results in terms of mucosa irritation and this nanosystem can then be used to prevent this condition (C. Zhang et al., 2013).

Recent studies also showed that nanoemulsions' digestion is also surfactant dependent. In fact, Verkempinck et al. (2018) observed that nanoemulsions prepared with Tween 80 present a higher lipolysis rate when compared with nanoemulsions prepared with sucrose esters as surfactant. Gasá-Falcon et al. (2019) also investigated the influence of several emulsifiers (i.e., Tween 20, lecithin, sodium caseinate and sucrose palmitate), at different concentrations on the *in vitro* digestion of  $\beta$ -carotene nanoemulsions. The authors concluded that using low mass emulsifiers, such as Tween 20 and lecithin, produced smaller droplets when compared with sodium caseinate and sucrose palmitate, since low mass emulsifiers are capable of adsorbing to the droplets, preventing their aggregation. In fact, Tween 20 and lecithin containing nanoemulsions have shown to be more stable under gastric conditions and lecithin containing nanoemulsions partially resisted to intestinal *in vitro* digestion (i.e., around 73 % of lipid digestion). This resulted in an enhancement of the  $\beta$ -carotene bioaccessibility.

Proteins can also be used as surfactants and Jiang et al. (Jiang et al., 2019) recently studied the performance of pea protein nanoemulsions and nanocomplexes as delivery systems for vitamin D3. The authors showed that pH-shifting and sonication exposed some functional lipophilic amino acids which resulted in a high encapsulation efficiency of ca.  $93.2 \pm 2.1$  %. Moreover, pea protein isolate nanoemulsions showed potential towards protecting vitamin D3 during *in vitro* gastric digestion, presenting a release of  $62.9 \pm 11.1$  % in the small intestine phase of the *in vitro* digestion model.

Nanoemulsions can also interact with several disruptive and destabilizing constituents (Sarkar et al., 2019). From enzymes to pH transitions and shear forces (i.e., due to peristalsis), nanoemulsions can be destabilized by:

- i. highly glycosylated salivary mucin via electrostatic interactions with proteins (i.e., if proteins are used as nanoemulsion emulsifiers);
- ii. acidic gastric conditions that may induce a change in the nanoemulsions' structure (e.g., may cause aggregation);

- iii. the proteolytic activity of pepsin, when proteins are used as emulsifiers (which interacts with protein molecules on the nanoemulsion surface, changing its interfacial properties) or interactions with gastric lipase that can cause aggregation, flocculation and coalescence, depending on the nature of the emulsifier used;
- iv. the interaction with other enzymes present in the small intestine (where most of lipid digestion takes place) such as trypsin and chymotrypsin (i.e., if protein emulsifiers are used), bile salts and pancreatic lipase (i.e., responsible for the release of free fatty acids - FFA), and pancreatic amylase (i.e., if carbohydrates are used as emulsion stabilizers) (Macierzanka et al., 2019; Sarkar et al., 2019).

An example of a lipid digestion process can be seen in Figure 1b. It is essential to study the behaviour of lipid-based delivery systems during *in vitro* digestion processes, once the stability of these systems and the nature of the micellar structures formed is determinant to understand possible mechanisms used in the solubilization and absorption of the bioactive compounds. This knowledge can then be applied to better tailor the production conditions so that these lipophilic nanosystems can meet designated application requirements.

#### 2.3.1.3. Polysaccharide-based nanosystems

There has been an increasing interest in the use of polysaccharides for the formulation of bio-based nanosystems since they:

- i. are natural, abundant and can be obtained from renewable sources (Dave & Gor, 2018);
- ii. have high versatility since they are able to form different nanosystems depending on the applied chemical or physical processes (Dave & Gor, 2018);
- iii. present important inherent biological properties such as antimicrobial, anti-inflammatory and mucoadhesive (Dragan & Dinu, 2019);
- iv. have a hydrophilic character with high biocompatibility (Anda-Flores et al., 2019).

The production of polysaccharide-based nanosystems relies on chemical and biological modifications, allowing them to withstand the normal enzymatic activity and acid conditions of the upper GI tract and to act in response to a specific stimulus (e.g., changes in pH). During digestion, polysaccharides are broken down into disaccharides or monosaccharides which facilitates their

absorption in the small intestine and their easier fermentation by the gut microbiota (Lovegrove et al., 2017). An example of a polysaccharide digestion process can be seen in Figure 1c.

Chitosan is one of the most studied polysaccharides as it presents a great potential for application in the food industry. This biopolymer has antimicrobial and antifungal activities, with particular physicochemical properties responsible for its biocompatibility with human tissues and enhanced permeability (Mohebbi et al., 2019). It can be used as a controlled delivery nanosystem since it presents a slow bioactive compound release profile and high mucoadhesiveness, thus improving the bioaccessibility of bioactive compounds (e.g., polyphenols) (J. Liang et al., 2017). Recently, Guo et al. (2020) evaluated the effect of *in vitro* digestion conditions on chitosan's morphological and cytotoxicity properties. The authors observed that chitosan nanoparticles, when applied to a fasting food model (i.e., pH 7 phosphate buffer), did not dissolve during the *in vitro* digestion process, which resulted in agglomeration in the small intestine phase. In addition, chitosan nanoparticles did not significantly change the transepithelial electrical resistance (TEER) as well as cell viability, at the studied doses, when compared with the control (i.e., fasting food model). Starch and alginate are also extensively explored polysaccharides, obtained from cereals and marine algae, respectively (Ahmad et al., 2019). Studies in the literature show that these polysaccharide nanosystems present a protective effect towards bioactive compounds stability. In fact, Ahmad et al. (2019) studied the encapsulation of catechin using horse chestnut starch nanoparticles and evaluated their performance under *in vitro* digestion. The authors observed that catechin was protected against the *in vitro* gastric conditions. Free catechin presented a significant drop on its pancreatic lipase inhibition of ca. 81%, dipeptidyl peptidase IV (DPP-IV) of ca. 87.7 % and  $\alpha$ -glucosidase of ca. 9.1 %. On the other hand, under encapsulation, catechin was able to significantly retain most of its inhibitory capabilities.

It is important to consider that most polysaccharides (except for starch and starch-based structures) are resistant to the enzymatic digestion in the upper GI track. For instance, marine algae polysaccharides (e.g., alginate, carrageenan, among others) are mainly digested in the colon by the microflora fermentation, i.e., by breaking down glycosidic bonds and consequently releasing reducing sugars that are used as substrate and consumed by the microflora. This indicates that, despite their application in enhancing bioactive compounds bioaccessibility, they can also be used as prebiotic to stimulate the microflora to release beneficial compounds e.g., short-chain fatty acids (Y. Guo et al., 2021; L. X. Zheng et al., 2020) as well as modulate its composition through



increasing the bacterial growth of beneficial bacteria such as *Phascolarctos*, *Bifidobacterium*, *Enterococcus*, among others (Y. Guo et al., 2021). Polysaccharides can also be conjugated with other particles in order to synergistically enhance the overall nanosystem functionality (L. Dai et al., 2018). For instance, a chitosan layer can be added to  $\beta$ -lactoglobulin (Simões, Martins, et al., 2020; Wei et al., 2019) and to improve the mucoadhesive properties of the nanosystem, prolonging its residence time and, consequently, the bioactive compound bioaccessibility (W. Dai et al., 2020). Polysaccharide conjugation can also be achieved with lipidic nanosystems, thus promoting emulsion stability and bioactive compound protection (Silva et al., 2019).

Notwithstanding the increasing interest and developments on polysaccharide nanosystems, their evaluation and characterization lacks in specificity, and they are often used as standalone systems without being added into a food matrix. This means that there is still a need for improvements in the development of analytical methods, which would maximize and simplify the evaluation of polysaccharide hydrolysis.

### **2.3.2 Current challenges of *in vitro* digestion assessment techniques**

Nanosystems subjected to *in vitro* digestion can be characterized in relation to their size (Simões, Martins, et al., 2020), surface charge (He & Ye, 2019), shape (Ahmad et al., 2019), porosity (Wei et al., 2019) and rheological properties (L. Liu & Kong, 2019). Moreover, those systems can be evaluated in relation to their FFA release, if applicable, (Gonçalves, Martins, Abrunhosa, Baixinho, et al., 2021) and bioaccessibility (Bhat et al., 2021a). For this purpose, several characterization techniques have been used to assess nanosystems' behaviour under *in vitro* digestion conditions and detailed information regarding some of these techniques can be found elsewhere (Allen et al., 2019; Erdman et al., 2019; Nellist, 2019; Rahdar et al., 2019; Wiercigroch et al., 2017). This way, this review will focus on the challenges associated to using these techniques to assess nanosystems under *in vitro* digestion.

#### **2.3.2.1. Particle characterization challenges**

Several techniques can be employed to assess particle aggregation (Araújo et al., 2020), flocculation (B. Zheng et al., 2019) and coalescence (R. F. S. Gonçalves, Martins, Abrunhosa, Baixinho, et al., 2021), depending on the nanosystem's nature (i.e., lipidic, protein or polysaccharide). These phenomena are usually attributed to the presence of electrolytic salts, pH variation, enzymatic digestion and interactions with bile salts (Brodkorb et al., 2019; Pabois et al.,

2020). To assess such behaviour during *in vitro* digestion, light scattering techniques are often applied. For this purpose, the dynamic light scattering (DLS) is the most widely used technique and it is used for routine quality control of nanoparticle production and to assess their *in vitro* digestion behaviour since:

- i. it presents rapid analysis and acquisition times at reduced costs (Modena et al., 2019);
- ii. it enables the measurement of a larger number of particles (when compared with microscopy measurements) (Rahdar et al., 2019), which will give a better idea regarding particle size distribution in solution;
- iii. it enables particle characterization in different solvent environments (Modena et al., 2019) which is important since the *in vitro* digestion process has a complex and dynamic environment, with different conditions along the GI tract (i.e., different pH, enzymes, electrolyte concentrations and presence of bile salts).

Despite being a simple and practical technique, DLS presents some requirements and limitations that should be taken into consideration when applied to assess the performance of nanosystems under *in vitro* digestion conditions. For instance, samples must be transparent to obtain feasible particle analysis results (Modena et al., 2019; Rahdar et al., 2019; Simões, Martins, et al., 2020). However, *in vitro* digestion samples, in particular from the small intestine, present high turbidity due to the presence of, e.g., bile salts, typically from porcine bile extract, which present an orange/yellow colour as well as some potential aggregates which makes really challenging the application of DLS to analyse samples in the small intestine since its operation is highly influenced by large aggregates (Stetefeld et al., 2016). Thus, dilutions must be made in order to obtain clear transparent samples (Majeed et al., 2016; Wei et al., 2019), which may alter the overall behaviour of nanosystems. It is also important to consider that this technique is highly dependent on temperature since it will interfere with the solvent viscosity and, consequently, with the light scattering behaviour. As a result, the temperature of analysis must be controlled and constant, and the viscosity of the solvent must be known. Moreover, DLS does not differentiate particles that are close to each other, neither their shape, which makes this technique a low-resolution technique (Modena et al., 2019; Rahdar et al., 2019). Complementary, nanoparticle tracking analysis can also be used to study and assess size (i.e., from ca. 50 nm to 1000 nm), distribution and concentration. This technique combines DLS with dynamic microscopy to track individual particles in solution by analysing the centre of the light scattered when it interacts with the particles and recording each nanoparticle trajectory (Gross-Rother et al., 2020). This way, a real-time

visualization of the nanoparticles' movements is possible and, adjusting the analysis parameters (e.g., refractive index) may lead to the identification of different nanoparticle aggregates which can make this approach more suitable for polydisperse samples (Gross-Rother et al., 2020; van der Pol et al., 2010). On the other hand, since this technique can be dependent on the analysis settings, it can consequently be more subjective since it may depend on the user interpretation. Furthermore, the analysis of protein particles can pose a challenge due to their low refractive index and consequently low scattered light (Gross-Rother et al., 2020).

Nanosystems can also be classified regarding their morphology since their shape is linked to their functionality, environmental response and bioactive compounds' release kinetics (Mourdikoudis et al., 2018). This way, the morphological characterization of nanosystems is one of the most important assessment procedures to evaluate their properties and behaviour. Some of the most used conventional morphology characterization techniques are transmission electronic microscopy (TEM), scanning electronic microscopy (SEM), atomic force microscopy (AFM), fluorescence microscopy and confocal laser scanning microscopy (CLSM) where SEM and TEM are the most used techniques to assess the size and shape of nanosystems and, as such, are often used in combination with scattering techniques (e.g., DLS) (Modena et al., 2019) and fluorescent and CLSM microscopy can be used to assess nanoemulsion and detect droplet coalescence through the digestion process (R. F. S. Gonçalves, Martins, Abrunhosa, Vicente, et al., 2021). Studying the morphological changes that occur during the *in vitro* digestion process provide a more realistic idea regarding particle aggregation, size and shape, when compared with standalone analytical techniques such as scattering techniques (e.g., DLS) (Falsafi et al., 2020). However, in the context of *in vitro* digestion, some challenges can be identified regarding this assessment. For instance, sample manipulation is often needed to perform such analysis (e.g., sample dilutions, surface coatings, among others) (Vladár & Hodoroba, 2020) which can interfere with the performance of nanosystems under *in vitro* digestion conditions. Furthermore, it is important to take into consideration that microscopic techniques are destructive assessment techniques that only represent a portion of the analysed sample.

#### 2.3.2.2. Rheological Characterization

Rheology is a well-established science of the deformation and flow of matter. Rheological properties are obtained by relating the stress applied on a material and the subsequent deformation as a function of time. Nowadays, with the advances in instrumentation, food rheology not only plays a

crucial role in measuring apparent viscosity, but also provides in-depth information on microstructure and fluidity of a food matrix, allowing the assessment of the network structure integrity (Mandala & Apostolidis, 2020).

Nanosystems' rheological properties play a crucial role in modifying the texture of foods and in their performance during *in vitro* digestion. Few studies have been conducted regarding the assessment of apparent viscosity of nanosystems during the different digestion phases aiming at a better understand of their behaviour in the GI tract and their effects on food digestion and nutrient absorption (Liu & Kong, 2019). This information can be used to tailor the production of functional food products. For instance, studying the changes in viscosity during gastric digestion can lead to the conclusion that the application of high viscosity materials can promote stomach emptying retardation and consequently, an increasing perception of satiety (Espert et al., 2019). In fact, Espert et al., (2019) observed that higher amounts of xanthan gum and consequently, higher apparent viscosity, promoted a significant decrease on the amount of oleic acid released from cream digestion. Rheological studies can also be used to indirectly assess the integrity of intermolecular bonds between nanoparticles during the *in vitro* digestion process and their resistance to the hydrolytic effect (Pabois et al., 2020). Recently, Liu & Kong, (2019) studied the influence of different types of nanocellulose (NC) on whey protein isolate digestion. For this purpose, the authors used cellulose nanofibrils (CNF), TEMPO-oxidized CNF and cellulose nanocrystals (CNC) and observed that the digesta viscosity was positively correlated to the concentration of CNF and CNC which resulted in lower whey protein isolate hydrolysis through lowering the initial free amino nitrogen diffusion rates by ca. 31.4 % and 68.4 % in the case of CNF and CNC respectively.

There are some limitations that can be identified regarding the application of rheological studies as a tool for assessing nanosystems during *in vitro* digestion. For instance, the complex environment of an *in vitro* digestion poses a major challenge towards data interpretation since several interfacial phenomena occurs during digestion (Zornjak et al., 2020) and isolating such phenomena is quite challenging. Furthermore, the rheological assessment can be a time consuming and destructive process (i.e., since it is a contact technique) that is very difficult to apply as an *in situ* analytical tool since it will interfere with the digestion process and micro-rheology can be used for this purpose.. Micro-rheology is a rheological technique that uses particle tracers as probes and advanced imaging and processing techniques to study complex structures (e.g., gel like structures), particles' interfaces, among others. As such, the mean square displacement of the

tracer is measured over time which will give important information regarding the viscoelastic properties of the sample (Xia et al., 2018). Different particle probes (e.g., fluorescent, magnetic) can be used for this purpose and more detailed information regarding this subject can be found in the work of Xia et al., (2018). The application of micro-rheology to the digestion process can give important insights regarding, e.g., the interfacial properties of nanoemulsion during the digestion process (Yang et al., 2021), the trajectory of nanoparticles using fluorescent tracers (Xia et al., 2018), among others. When compared with traditional rheology, micro-rheology presents a higher sensitivity which makes it a potential technique to identify the effects and phenomena that occur during the *in vitro* digestion of nanosystems. Despite its potential, the application of micro-rheology to assess nanosystems during the digestion process is still very limited and very few studies are found in the literature regarding this subject.

#### 2.3.2.3. Non-conventional *in vitro* digestion assessment techniques

The assessment of nanosystems under *in vitro* digestion can also be achieved by non-conventional techniques to further unravel the structural changes that occur in such systems and understand the phenomena associated to the digestion process. Methods such as small-angle X-ray scattering (SAXS), Raman spectroscopy, fluorescence resonance energy transfer (FRET) and nuclear magnetic resonance spectroscopy (NMR) can be applied for this purpose.

SAXS is a technique that can be used to perform structural analysis (e.g., particle size, shape, dispersity, morphology) of polymeric molecules in solution. This way, an X-ray beam is transmitted and passes through the sample. The elastically scattered electrons are then collected, at a small angle, by a two-dimensional detector to form a SAXS image which is then processed. Subsequently, each pixel of the image is converted into the scattering angle. Thus, different scattering angle patterns can determine the structural characteristics of a given sample (Brotherton et al., 2019; Lv et al., 2018). For instance, Lv et al., (2018) applied this technique, *in situ*, to understand the structural changes of lipidic microemulsions during *in vitro* digestion as well as the influence of the mucus on lipolysis. The authors observed the formation of liquid crystalline phases during lipolysis which were subsequently damaged in the presence of the mucus, which is attributed to the hydrophobic interactions between the crystalline structures and the mucus. This technique can be further improved by coupling it with a synchrotron, improving the scattering intensity of the radiation (Franke & Svergun, 2020; Khan et al., 2016). This method can be used to assess the development of colloidal structures during lipolysis in real-time. In fact, this assessment was conducted by Khan

et al., (2016), which evaluated the precipitation and the solid-state form of lipidic nanoemulsions (i.e., composed by fenofibrate). The authors concluded that fenofibrate precipitates in its thermodynamically stable crystalline form during lipolysis. Therefore, SAXS techniques can be used to study the structural changes that occur during the *in vitro* digestion of nanosystems, allowing a better understanding regarding their fate and digestion kinetics (e.g., bioactive compounds' release rates, enzymatic activity, among others) in the GI tract. Furthermore, smaller scattering angles can be used, i.e., ultra-small angle x-ray scattering (USAXS), to perform a wider colloidal analysis since it enables the detection of particles from 300 nm to ca. 2000 nm, when compared to SAXS (up to 100 nm) (Sakurai, 2017). This way, this technique has the potential to be used in *in vitro* digestion studies to assess, for instance, nanoparticle interactions during the digestion process (e.g., particle aggregation, coalescence, among others) since it can analyse a wider range of particle sizes. However, SAXS techniques are not widely available (i.e., especially synchrotron SAXS), since they require expensive equipment, maintenance and highly specialized knowledge regarding signal processing and data interpretation (Franke & Svergun, 2020; J. Li et al., 2018).

Raman spectroscopy is a vibrational spectroscopic technique that uses monochromatic light to extract information regarding the molecular vibrational modes (i.e., it correlates with the inelastic scattering of photons) and transitions which will in turn allow inferring about intermolecular interactions (Deidda et al., 2019; Salim et al., 2020). This methodology is a fast, non-destructive and eco-friendly technique that requires little to no sample preparation prior to analysis and it can be used for qualitative determinations such as to assess food quality (W. Zhang et al., 2020), deterioration (R. Hu et al., 2019) and fraud detection (Berghian-Grosan & Magdas, 2020), as well as for quantitative studies such as fermentation monitoring (A. Zhang et al., 2020) or compound quantification (Chen et al., 2019). Under *in vitro* digestion conditions, Raman spectroscopy can be applied to analyse, in real-time, bioactive compounds' solubilization (Salim et al., 2020) and crystallization (Stillhart et al., 2013). However, this approach needs to be coupled with powerful analytical techniques for spectra interpretation and thus, chemometric approaches (e.g., Partial Least Squares Regression, Principal Component Regression) (Zhiming Guo et al., 2019; W. Zhang et al., 2020) and machine learning (artificial neural networks, support vector machines, among others) (Berghian-Grosan & Magdas, 2020; Z. Zhang, 2020) have been used for this purpose.

Despite the advancements in the application of Raman spectroscopy for the assessment of nanosystems' performance under *in vitro* digestion conditions, these studies are still very scarce and information on dynamic *in vitro* digestion models is still very limited, perhaps due to their

dynamic nature which will interfere and lower the signal to noise ratio of Raman spectra (Deidda et al., 2019). Furthermore, care must be taken when applying this technique for *in vitro* digestion assessment since inconsistent results were frequently observed regarding e.g., compounds' solubilization when compared to other techniques (e.g., SAXS) (Salim et al., 2020).

FRET is a physical phenomenon that occurs when the energy of an excited fluorophore donor is transferred to an acceptor fluorophore through dipole-dipole interactions. Thus, this technique requires that the two fluorophores must be near to each other (i.e., at a distance between ca. 1 to 10 nm) (Zhiming Guo et al., 2019). This principle can be used to study the interfacial properties of emulsions (Pan & Nitin, 2016) and their interactions with other constituents (e.g., mucus) under *in vitro* digestion conditions (Lv et al., 2018). Pan & Nitin (2016) assessed, in real-time, the dynamics of a lecithin emulsion (with and without chitosan coating) interface under *in vitro* intestinal digestion conditions. The authors observed that the phospholipids in the emulsion interface were immediately disrupted by the addition of bile salts. This disruption was significantly prevented by the addition of a chitosan layer which implies a lower rate of FFA release. Lv et al. (2018) also used FRET to investigate the fate of a self-microemulsifying drug delivery system under *in vitro* digestion conditions. As previously mentioned, the authors used SAXS and observed that the initial liquid crystalline phases disappeared. However, FRET measurements enabled the authors to conclude that the interaction between the emulsion and the mucus formed micelles from the liquid crystalline phases. Therefore, FRET can be used as a standalone or combined technique to investigate the structural changes that may occur to bioactive compounds' delivery systems under *in vitro* digestion conditions.

NMR spectroscopy can also be a potential technique to assess nanosystems during the digestion process. Briefly, this technique uses a magnetic field that takes advantage of the magnetic properties of molecular nuclei (typically  $^1\text{H}$ ,  $^{13}\text{C}$  and  $^{31}\text{P}$  – proton NMR) which are then subjected to radiation in the radiofrequency (RF) region of the electromagnetic spectrum (Hatzakis, 2019). This technique can then give important qualitative (i.e., the position of the spectrum peaks determines the molecular structure of the samples) and quantitative (i.e., the area under the peaks is proportional to the number of nuclei responsible for that peak) information regarding the chemical composition of samples and, consequently, it can be applied to monitor nanosystems' digestion by analysing the release of metabolites during the digestion process (Smeets et al., 2021). It can be used to assess the lipolysis of nanoemulsions (Nieva-Echevarría et al., 2016, 2017), protein hydrolysis (Deng et al., 2022) and conformational changes (Jain & Sekhar, 2022),

among others. However, some challenges can be identified which include low sensitivity and high cost, it requires in-depth NMR knowledge regarding theoretical and spectra interpretation. Moreover, a standard protocol addressing sample preparation is still required for this technique to be generalized along with the publication of NMR spectra databases so that comparisons and statistical analysis can be made in complex samples (Hatzakis, 2019).

## **2.4 NIR SPECTROSCOPY**

### **2.4.1 Theory and fundamentals**

According to Hollas, J. M. (2004), spectroscopy can be defined as the empirical subject that focuses on the study of absorption, emission and/or scattering of electromagnetic radiation by molecules and/or atoms. In other words, spectroscopy is the study of the interaction of matter with electromagnetic radiation (Csuros & Csuros, 2010; Hammes, 2005). This subject, at least nowadays, uses the principles of theoretical quantum mechanics to output readable data that can be interpreted. Despite the wide use of this technique in modern scientific studies, its application goes back to the 17th century, with the famous experiment of Newton, in 1665, regarding white light dispersion when it passes through a triangular prism. However, it was only in 1860 that the first spectroscopic prism was developed, by Bunsen and Kirchhoff, that was intended to be used as an analytical tool. It was then possible to observe some emission spectra of various samples under a flame (i.e., light source). In 1885 Balmer was able to fit the resulting series of black lines (from the emission spectra of a flame) with a mathematical model. Until the 20th century, spectroscopic theory as based on Newtonian laws, and thus could not explain some phenomena observed in experimental assays. More precise theoretical predictions became possible with the development of quantum mechanics by Schrödinger in 1926. Still, experimental data most often contradicted the theoretical predictions of more complex molecules due to the number of approximations made to facilitate the calculations. Since 1960, with the development of computer science, accurate predictions regarding the spectroscopic properties of small molecules became possible (Hollas, 2004). This way it was possible to assess the interactions between electromagnetic radiation and matter and correlate theoretical predictions with experimental data. Electromagnetic radiation is a form of radiation that is comprised by an electric and magnetic component that propagate in perpendicular planes. If one photon of such radiation would travel in



space, along the x-axis, the electric and magnetic component of the radiation would propagate in an oscillating wave like form and would be represented by an electric and magnetic field with magnitude E and B, respectively, as it is illustrated in Figure 1 (Hollas, 2004).

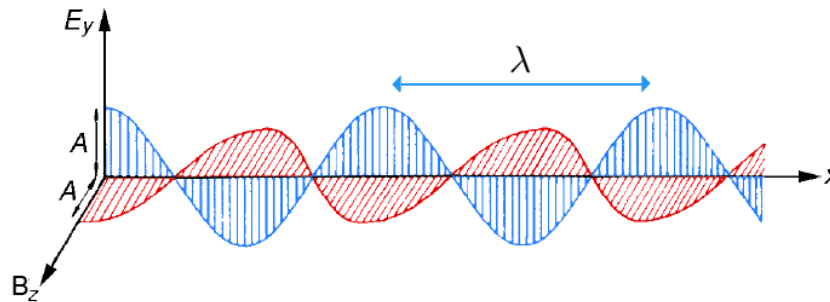


**Figure 3** – Illustration of one photon of electromagnetic radiation traveling through the x-axis and its electric ( $E_y$ ) and magnetic ( $B_z$ ) components – Adapted from (Hollas, 2004).

It is possible to observe in Figure 1 that the photon has an oscillatory, sinusoidal trajectory for both its electric and magnetic component, that can have different wavelengths ( $\lambda$  - nm) or wavenumber ( $\tilde{\nu}$  -  $\text{cm}^{-1}$ ) and, therefore, can be associated to different energy levels that are described by the Planck relationship (Csuros & Csuros, 2010; Hammes, 2005):

$$E = h\nu = hc/\lambda \quad (1)$$

This implies that different wavelengths describe different types of radiation which can be schematically represented by the electromagnetic spectrum - Figure 2 (Csuros & Csuros, 2010; Hammes, 2005; Hollas, 2004).

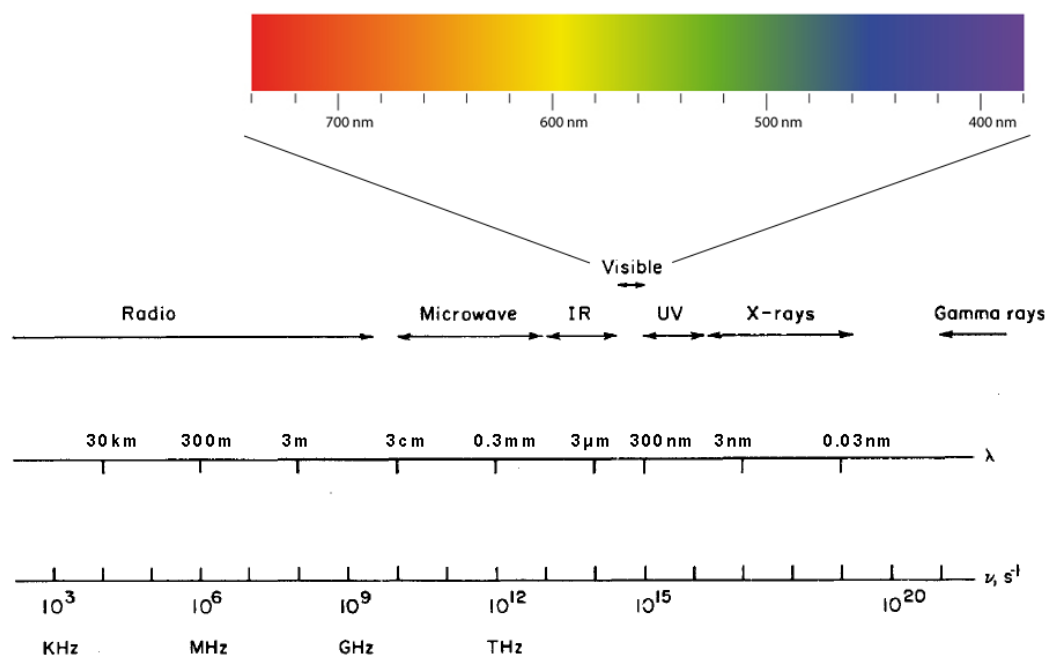


**Figure 4** – Molecular state transition during the interaction between electromagnetic radiation and molecules or atoms - Image adapted from (Hollas, 2004).

This way, three types of processes can occur: induced absorption, spontaneous emission and induced emission. Induced absorption occurs when a molecule or atom absorbs a quantum of electromagnetic radiation and gets into an excited state, which is represented by the transition from  $m$  to  $n$ . Spontaneous emission corresponds to the spontaneous release of radiation from an atom or molecule, without stimuli. Induced emission corresponds to the release of radiation when an atom or molecule is stimulated by radiation (Csuros & Csuros, 2010; Hollas, 2004).

Typically, spectroscopy studies are carried out by making a continuous light beam pass through a sample and measurements of its intensity are made. This way, it is possible to quantify the amount of light that is absorbed, transmitted, reflected or scattered by the sample, depending on the equipment apparatus (Hammes, 2005). This work will focus on absorption spectroscopy since it is a fast analysis that most often does not require the addition of reagents or sample incubation (Nilapwar et al., 2011).

Light absorption, at different wavelengths, is a phenomenon that can be observed everywhere since it is responsible for a given colour of an object. For instance, objects with a blue colour absorb light in the yellow wavelength range (i.e., 576–580 nm) of the electromagnetic spectrum and, therefore, transmit blue light with a wavelength range between 465 and 482 nm. This way, absorption

spectroscopy is commonly applied to obtain the absorption spectrum of atoms and molecules for qualitative and quantitative applications. The materials absorption properties and light absorption are described by the Beer-Lambert law which can be expressed by (Hammes, 2005; Nilapwar et al., 2011):

$$A = \log\left(\frac{I_0}{I}\right) = \epsilon Cl \quad (2)$$

It is possible to conclude that the equipment apparatus can influence significantly the measure of sample absorption, since it depends on the light path length, and thus, equipment calibration is of utmost importance (Nilapwar et al., 2011).

A region of the electromagnetic spectra that has been receiving much attention from the food industry is the NIR region. NIR spectroscopy is a fast, non-destructive, low cost and simple technique to measure biological (Qi et al., 2022; Di Wu et al., 2008) and synthetic polymer (Holze, 2004) materials, among other. Infrared absorption is a process restricted to molecules that present changes, during molecular vibration, in their electric dipole moment when they are submitted to radiation (e.g., contractions and expansion of molecular bonds). This way, infrared spectra is typically obtained by submitting a sample to infrared radiation and analyse the absorbed radiation at a corresponding energy (Stuart & Preface, 2004). Particularly, NIR absorption spectroscopy studies the absorption of incident radiation at a wavelength range between 780 and 1050 nm (Di Wu et al., 2008). NIR signals are more reliable, fast and the typical infrared absorption behaviour of water is mitigated (Kaavya et al., 2020). It is a suitable technique to analyse molecules containing C-H, N-H, S-H or O-H bonds and it is widely applied in biological (e.g., lipid, protein, nucleic acids and disease analysis, etc) and industrial (e.g., pharmaceutical, food, agriculture and paint industries, etc) applications, among others (Kaavya et al., 2020; Stuart & Preface, 2004). In fact, D. Wu et al., (2008) used SWNIR spectroscopy to identify different brands of milk powder. Encina-Zelada et al., (2017) assessed the accuracy of the physicochemical characterization of quinoa using NIR spectroscopy. The authors concluded that this technique, in conjunction with some multivariate correction algorithms, was able to predict the dietary composition of quinoa grains and thus, demonstrating its potential for routine analysis in an industrial environment. Weng et al., (2020) applied NIR spectroscopy to assess minced beef adulteration with a coefficient of prediction of 0.973 which indicates that NIR spectroscopy can in fact be used for beef adulteration detection, Despite the great potential of this technique, advanced mathematical models must be used to process, extract information and interpret the NIR spectra. This can be achieved, essentially,

through two distinct approaches: using chemometrics or artificial intelligence, more specifically, machine learning.

### **2.4.2 NIR spectral multivariate calibration**

Due to its complexity, NIR spectra interpretation must be done by resorting to advanced algorithms that can extract the relevant information and correlate them with a specific application. Chemometrics is then used for this purpose since it is a collection of computer science, mathematical and statistical tools that aim at extracting important chemical information from a large and complex data collection (Granato et al., 2018; Qi et al., 2022). An important field in chemometrics is multivariate calibration which is done to detect trends and relationships between the obtained spectra and a conventional analytical procedure. For instance, this approach is commonly used for spectra smoothing (e.g., Savitzky–Golay filter), baseline correction (e.g., first and second derivatives, SNV), MSC, variable selection (e.g., PLS), modelling (e.g., MLR, RR), assessment metrics (e.g., coefficient of determination, MSE), among others (Qi et al., 2022; H.-P. Wang et al., 2022) which will be discussed in the following topics.

#### **2.4.2.1. Smoothing: Savitzky–Golay filter**

The smoothing of spectra is one of the most used spectra pre-processing techniques since it removes noise from the spectra and improve the signal-to-noise ration. The Savitzky-Golay filter is one of the most applied techniques for spectra smoothing. Briefly, it fits a polynomial curve to a predetermined set of points of the spectra (i.e., window). This way, two choices must be made regarding the application of this filter, the window size and polynomial order. These parameters are often determined via trial and error. It is of course important to mention that smoothing techniques must retain the original spectra shape (H.-P. Wang et al., 2022; Zahir et al., 2022).

#### **2.4.2.2. Baseline correction**

The correction of the baseline is another pre-processing technique that is often applied to NIR spectra. The main objective of this approach is to eliminate the influence of particle size, i.e., light scattering which is responsible for the vertical displacement of the spectra. Therefore, the application of this pre-processing step only makes sense if the particle size is not important. Several techniques can be used to correct the baseline of the spectra, namely the SNV and MSC. The SNV transformation applies scaling and centres the spectra by subtracting the average of the sample spectrum to a specific point of the spectrum (i.e., reading at a specific wavelength) and dividing it

by the spectrum standard deviation. This can be represented by the following equation (Naes et al., 2004):

$$x_k^* = (x_k - \bar{x})/\sigma \quad (3)$$

This technique not only enhances the spectra resolution, but it corrects scattering effects of the samples by correcting the baseline. Another popular technique for this purpose is the MSC. This technique compares an individual spectrum to the average of the samples' spectra and corrects the additive and multiplicative effects caused by scattering. This way, it can be represented by the following equation (Naes et al., 2004; Zahir et al., 2022):

$$x_k^* = a + b\bar{x}_k \quad (4)$$

#### 2.4.2.3. Variable Selection - PLS

Variable (i.e., wavelength) selection methods are often used to choose, among all the spectrum wavelengths, the ones that contribute the most to explain the variance in the dependent variable of the study. As such, these methods make the calibration process much simpler. PLS has been widely used for this purpose, more specifically, the VIP scores of PLS. PLS is a multivariate, data dimension reduction technique, very similar to PCA in a way that it uses PCA to calculate the loadings (i.e., slope of the respective principal component) and scores (i.e., the distance between the point and its projection on the principal component) of both dependent and independent variables. This way, principal components, also denominated as latent variables (i.e., orthogonal linear correlations), are determined for both X and Y matrices and this is the major difference between PLS and PCA. PLS then uses the scores of the independent variables to predict the scores of the dependent variables and, as such, it can be used for regression. The fundamental calculations are represented in the following equations:

$$X = TP + \dot{E} \quad (5)$$

$$Y = UQ + \dot{F} \quad (6)$$

$$u_i = r_i t_i \quad (7)$$

Each principal component will essentially explain the variance between the variables. As such, VIP can be calculated since it corresponds to the sum of the Y variance explained by each variable divided by the total explained Y variance. This parameter will indicate which variables are important for a given application. Typically, variables with a VIP higher than 1 or lower than -1 are considered important and thus are selected for further analysis.

#### 2.4.2.4. Regression

To estimate experimental values, e.g., protein, lipid or carbohydrate content of food samples using NIR spectroscopy, regression models are used. As previously mentioned, PLS can be used to predict the dependent variables (PLSR) which makes this a linear regression model. Other linear regression models can be used to predict data e.g., MLR, RR, LASSO, ENR, BRR, among others. MLR is one of the most used linear regression techniques that uses multiple regression coefficients to estimate the response variable and it is represented by the following equation:

$$y = b_0 + \sum_{k=1}^k m_k x_k \quad (8)$$

#### 2.4.2.5. Model assessment

It is very common to use multiple regression models to estimate a dependent variable given the values of the independent variables. Some model assessment metrics can be used to assess which model has the better performance, i.e., the models that best fits the data. Among several metrics that are used to evaluate and compare regression models, the  $r^2$  and RMSE are widely used for this purpose and can be calculated according to the following equations:

$$r^2 = \frac{SS_{res}}{SS_{total}} \quad (9)$$

$$SS_{res} = \sum_i (y_i - \hat{y}_i)^2 \quad (10)$$

$$SS_{total} = \sum_i (y_i - \bar{y})^2 \quad (11)$$

$$RMSE = \sqrt{\frac{1}{n} SS_{res}} \quad (12)$$

## 2.5 CONCLUSIONS AND FUTURE PERSPECTIVES

The assessment of food and nanosystems as controlled delivery systems of bioactive compounds under *in vitro* digestion conditions is of utmost importance to understand their fate in the GI tract and unravel knowledge regarding the phenomena that occur during this process. The knowledge of their behaviour under simulated *in vitro* conditions allows the optimization of nanosystems' design and production taking into consideration their performance under *in vitro* digestion, so that

material dosage and processing can be adjusted. Protein, polysaccharide and lipid-based nanosystems have been used as bio-based protective vehicles of bioactive compounds, showing promising results regarding their protective performance under harsh digestion conditions. However, efforts must be made to further enhance nanosystems' performance in terms of expanding their functional properties and protective ability, as well as understanding their digestion mechanisms and bioactive compounds' release kinetics. It is also important to take into consideration that, despite all the advantages of delivery systems at the nano scale, some concerns remain unanswered regarding the safety and, consequently, the application of nanosystems to food products and their consumption. This way, regulatory agents must address this issue to overcome this bottleneck. To assess the performance of nanosystems under digestion conditions, it is crucial to develop reliable analytical methods for particle size, dispersibility and surface charge determination, as well as for morphological, rheological, electrophoretic, free fatty acid, bioaccessibility (and consequently, bioavailability) and cytotoxicity assessment. Despite their routine application, care must be taken while performing such analysis since the digestion process involves the presence of several factors that can interfere with the assessment of nanosystems' behaviour (e.g., presence or absence of peristalsis, stomach emptying, gastric pyloric sieving, among others). Therefore, advances in the development of reliable and realistic *in vitro* digestion models are crucial so that better correlations with *in vivo* data can be obtained.

There is a current effort by the scientific community to standardize *in vitro* digestion protocols, so that interlaboratory comparisons can be established, as well as to develop anatomical accurate dynamic *in vitro* digestion models with realistic peristaltic contractions, inner surface rugosity, pyloric sieving and stomach emptying. This way, it is expected that more robust, generalized and complex *in vitro* digestion systems will be developed to obtain accurate results regarding nanosystems' digestion behaviour. However, the validation of *in vitro* digestion models is still a challenge due to the complexity of *in vivo* studies.

The fast-paced increase of research regarding the *in vitro* digestion field can lead to the development of more sophisticated real-time analytical tools, so that many of the challenges discussed in this review can be overcome. Furthermore, with the development of novel, accurate and sophisticated analytical tools and *in vitro* digestion models, more opportunities in the field of *in silico* analysis could arise so that resources could be spared. The development of an open access word-wide database containing data related to *in vivo* studies could catalyse the creation of a standardized *in vivo* digestion protocol and consequently the creation of an *in vitro* digestion model

validation assessment through the application of advanced analytical techniques (e.g., artificial intelligence).

Therefore, a lot of work must be done towards improving *in vitro*-*in vivo* correlations by taking into consideration e.g., the presence of a stomach mucus layer and gastric absorption, as well as by including cellular models within *in vitro* digestion systems, so that bioactive compounds' absorption can be assessed *in situ* and, therefore, avoiding sample manipulation.

NIR spectroscopy is currently being used in the food industry and both chemometric and machine learning (or a combination of both) have been used to extract information from the spectra. However, despite the historical success of chemometrics, ML algorithms are currently becoming a trend, perhaps due to the technological evolution of computer science which promotes fast calculations to complex mathematical problems (i.e., ML algorithms).

## 2.6 REFERENCES

Ahmad, M., Mudgil, P., Gani, A., Hamed, F., Masoodi, F. A., & Maqsood, S. (2019). Nano-encapsulation of catechin in starch nanoparticles: Characterization, release behavior and bioactivity retention during simulated *in-vitro* digestion. *Food Chemistry*, 270, 95–104. <https://doi.org/10.1016/J.FOODCHEM.2018.07.024>

Allen, R. C., Saravis, C. A., & Maurer, H. R. (2019). Gel Electrophoresis and Isoelectric Focusing of Proteins: Selected Techniques. De Gruyter. <https://doi.org/doi:10.1515/9783110863635>

Anda-Flores, Y. De, Rascón-Chu, A., Campa-Mada, A. C., Lizardi-Mendoza, J., Tanori-Cordova, J., & Carvajal-Millan, E. (2019). Polysaccharides nanoparticles as oral drug delivery systems. In *Natural Polysaccharides in Drug Delivery and Biomedical Applications* (pp. 399–417). Elsevier. <https://doi.org/10.1016/B978-0-12-817055-7.00017-0>

Araújo, J. F., Bourbon, A., Simões, L., Vicente, A. A., Coutinho, P. J. G., & Ramos, Ó. L. (2020). Physicochemical characterisation and release behaviour of curcumin-loaded lactoferrin nanohydrogels into food simulants. *Food & Function*, 11(1), 305–317. <https://doi.org/10.1039/C9F001963D>

Arsiccio, A., McCarty, J., Pisano, R., & Shea, J.-E. (2020). Heightened Cold-Denaturation of Proteins at the Ice–Water Interface. *Journal of the American Chemical Society*, 142(12), 5722–5730. <https://doi.org/10.1021/jacs.9b13454>

Barbon, S., Costa Barbon, A. P. A. da, Mantovani, R. G., & Barbin, D. F. (2018). Machine Learning Applied to Near-Infrared Spectra for Chicken Meat Classification. *Journal of Spectroscopy*, 2018, 1–12. <https://doi.org/10.1155/2018/8949741>



Berghian-Grosan, C., & Magdas, D. A. (2020). Raman spectroscopy and machine-learning for edible oils evaluation. *Talanta*, 218, 121176. <https://doi.org/10.1016/j.talanta.2020.121176>

Berni, P., Pinheiro, A. C., Bourbon, A., Guimarães, M., Canniatti-Brazaca, S. G., & Vicente, A. A. (2019). Characterization of the behavior of carotenoids from pitanga (*Eugenia uniflora*) and buriti (*Mauritia flexuosa*) during micr oemulsion production and in a dynamic gastrointestinal system. *Journal of Food Science and Technology*. <https://doi.org/10.1007/s13197-019-04097-7>

Berthelsen, R., Klitgaard, M., Rades, T., & Müllertz, A. (2019). *In vitro* digestion models to evaluate lipid based drug delivery systems; present status and current trends. In *Advanced Drug Delivery Reviews*. <https://doi.org/10.1016/j.addr.2019.06.010>

Bhat, Z. F., Morton, J. D., Bekhit, A. E.-D. A., Kumar, S., & Bhat, H. F. (2021a). Emerging processing technologies for improved digestibility of muscle proteins. *Trends in Food Science & Technology*, 110, 226–239. <https://doi.org/10.1016/j.tifs.2021.02.010>

Bhat, Z. F., Morton, J. D., Bekhit, A. E.-D. A., Kumar, S., & Bhat, H. F. (2021b). Thermal processing implications on the digestibility of meat, fish and seafood proteins. *Comprehensive Reviews in Food Science and Food Safety*, 1541-4337.12802. <https://doi.org/10.1111/1541-4337.12802>

Bourbon, A., Pereira, R. N., Pastrana, L. M., Vicente, A. A., & Cerqueira, M. A. (2019). Protein-Based Nanostructures for Food Applications. *Gels* (Basel, Switzerland), 5(1), 9. <https://doi.org/10.3390/gels5010009>

Bourbon, A., Pinheiro, A. C., Cerqueira, M. A., & Vicente, A. A. (2018). *In vitro* digestion of lactoferrin-glycomacropeptide nanohydrogels incorporating bioactive compounds: Effect of a chitosan coating. *Food Hydrocolloids*, 84(May), 267–275. <https://doi.org/10.1016/j.foodhyd.2018.06.015>

Brodkorb, A., Egger, L., Alminger, M., Alvito, P., Assunção, R., Ballance, S., Bohn, T., Bourlieu-Lacanal, C., Boutrou, R., Carrière, F., Clemente, A., Corredig, M., Dupont, D., Dufour, C., Edwards, C., Golding, M., Karakaya, S., Kirkhus, B., Le Feunteun, S., ... Recio, I. (2019). INFOGEST static *in vitro* simulation of gastrointestinal food digestion. *Nature Protocols*, 14(4), 991–1014. <https://doi.org/10.1038/s41596-018-0119-1>

Brotherton, E. E., Hatton, F. L., Cockram, A. A., Derry, M. J., Czajka, A., Cornel, E. J., Topham, P. D., Mykhaylyk, O. O., & Armes, S. P. (2019). *In situ* Small-Angle X-ray Scattering Studies During Reversible Addition–Fragmentation Chain Transfer Aqueous Emulsion Polymerization. *Journal of the American Chemical Society*, 141(34), 13664–13675. <https://doi.org/10.1021/jacs.9b06788>

Chen, X., Lin, M., Sun, L., Xu, T., Lai, K., Huang, M., & Lin, H. (2019). Detection and quantification of carbendazim in Oolong tea by surface-enhanced Raman spectroscopy and gold nanoparticle substrates. *Food Chemistry*, 293, 271–277. <https://doi.org/10.1016/j.foodchem.2019.04.085>

Csuros, C., & Csuros, M. (2010). Fundamentals of Spectroscopy. *Environmental Sampling and Analysis for Metals*, 79–88. <https://doi.org/10.1201/9781420032345.ch5>

Dai, L., Li, R., Wei, Y., Sun, C., Mao, L., & Gao, Y. (2018). Fabrication of zein and rhamnolipid complex nanoparticles to enhance the stability and *in vitro* release of curcumin. *Food Hydrocolloids*, 77, 617–628. <https://doi.org/10.1016/J.FOODHYD.2017.11.003>

Dai, W., Ruan, C., Sun, Y., Gao, X., & Liang, J. (2020). Controlled release and antioxidant activity of chitosan and  $\beta$ -lactoglobulin complex nanoparticles loaded with epigallocatechin gallate. *Colloids and Surfaces B: Biointerfaces*, 188, 110802. <https://doi.org/https://doi.org/10.1016/j.colsurfb.2020.110802>

Das, A. K., Nanda, P. K., Bandyopadhyay, S., Banerjee, R., Biswas, S., & McClements, D. J. (2020). Application of nanoemulsion-based approaches for improving the quality and safety of muscle foods: A comprehensive review. *Comprehensive Reviews in Food Science and Food Safety*, 19(5), 2677–2700. <https://doi.org/https://doi.org/10.1111/1541-4337.12604>

Dave, P. N., & Gor, A. (2018). Natural Polysaccharide-Based Hydrogels and Nanomaterials. In *Handbook of Nanomaterials for Industrial Applications* (pp. 36–66). Elsevier. <https://doi.org/10.1016/B978-0-12-813351-4.00003-1>

Deidda, R., Sacre, P. Y., Clavaud, M., Coïc, L., Avohou, H., Hubert, P., & Ziemons, E. (2019). Vibrational spectroscopy in analysis of pharmaceuticals: Critical review of innovative portable and handheld NIR and Raman spectrophotometers. *TrAC - Trends in Analytical Chemistry*, 114, 251–259. <https://doi.org/10.1016/j.trac.2019.02.035>

Deng, R., Seimys, A., Mars, M., Janssen, A. E. M., & Smeets, P. A. M. (2022). Monitoring pH and whey protein digestion by TD-NMR and MRI in a novel semi-dynamic *in vitro* gastric simulator (MR-GAS). *Food Hydrocolloids*, 125, 107393. <https://doi.org/10.1016/J.FOODHYD.2021.107393>

Dragan, E. S., & Dinu, M. V. (2019). Polysaccharides constructed hydrogels as vehicles for proteins and peptides. A review. *Carbohydrate Polymers*, 225(May), 115210. <https://doi.org/10.1016/j.carbpol.2019.115210>

Du, X., Jing, H., Wang, L., Huang, X., Mo, L., Bai, X., & Wang, H. (2022). pH-shifting formation of goat milk casein nanoparticles from insoluble peptide aggregates and encapsulation of curcumin for enhanced dispersibility and bioactivity. *LWT*, 154, 112753. <https://doi.org/10.1016/J.LWT.2021.112753>

Dupont, D., Alric, M., Blanquet-Diot, S., Bornhorst, G., Cueva, C., Deglaire, A., Denis, S., Ferrua, M., Havenaar, R., Lelieveld, J., Mackie, A. R., Marzorati, M., Menard, O., Minekus, M., Miralles, B., Recio, I., Van den Abbeele, P., & den Abbeele, P. Van. (2018). Can dynamic *in vitro* digestion systems mimic the physiological reality? *Critical Reviews in Food Science and Nutrition*, 59(10), 1–17. <https://doi.org/10.1080/10408398.2017.1421900>

Eker, M. E., Aaby, K., Budic-Leto, I., Brnčić, S. R., El, S. N., Karakaya, S., Simsek, S., Manach, C., Wiczowski, W., & Pascual-Teresa, S. de. (2020). A Review of Factors Affecting Anthocyanin Bioavailability: Possible Implications for the Inter-Individual Variability. *Foods*, 9(1), 2. <https://doi.org/10.3390/FOODS9010002>

Encina-Zelada, C., Cadavez, V., Pereda, J., Gómez-Pando, L., Salvá-Ruiz, B., Teixeira, J. A., Ibañez, M., Liland, K. H., & Gonzales-Barron, U. (2017). Estimation of composition of quinoa

(Chenopodium quinoa Willd.) grains by Near-Infrared Transmission spectroscopy. *LWT - Food Science and Technology*, 79, 126–134. <https://doi.org/10.1016/j.lwt.2017.01.026>

Erdman, N., Bell, D. C., & Reichelt, R. (2019). Scanning Electron Microscopy BT - Springer Handbook of Microscopy (P. W. Hawkes & J. C. H. Spence (eds.); pp. 229–318). Springer International Publishing. [https://doi.org/10.1007/978-3-030-00069-1\\_5](https://doi.org/10.1007/978-3-030-00069-1_5)

Espert, M., Constantinescu, L., Sanz, T., & Salvador, A. (2019). Effect of xanthan gum on palm oil *in vitro* digestion. Application in starch-based filling creams. *Food Hydrocolloids*, 86, 87–94. <https://doi.org/10.1016/j.foodhyd.2018.02.017>

Falsafi, S. R., Rostamabadi, H., Assadpour, E., & Jafari, S. M. (2020). Morphology and microstructural analysis of bioactive-loaded micro/nanocarriers via microscopy techniques; CLSM/SEM/TEM/AFM. *Advances in Colloid and Interface Science*, 280, 102166. <https://doi.org/10.1016/J.CIS.2020.102166>

Franke, D., & Svergun, D. I. (2020). Synchrotron Small-Angle X-Ray Scattering on Biological Macromolecules in Solution BT - Synchrotron Light Sources and Free-Electron Lasers: Accelerator Physics, Instrumentation and Science Applications (E. J. Jaeschke, S. Khan, J. R. Schneider, & J. B. Hastings (eds.); pp. 1645–1672). Springer International Publishing. [https://doi.org/10.1007/978-3-030-23201-6\\_34](https://doi.org/10.1007/978-3-030-23201-6_34)

Gao, J., Lin, S., Jin, X., Wang, Y., Ying, J., Dong, Z., & Zhou, W. (2019). *In vitro* digestion of bread: How is it influenced by the bolus characteristics? *Journal of Texture Studies*, 50(3), 257–268. <https://doi.org/10.1111/JTXS.12391>

Gasa-Falcon, A., Odriozola-Serrano, I., Oms-Oliu, G., & Martín-Belloso, O. (2019). Impact of emulsifier nature and concentration on the stability of  $\beta$ -carotene enriched nanoemulsions during *in vitro* digestion. *Food & Function*, 10(2), 713–722. <https://doi.org/10.1039/C8FO02069H>

Gonçalves, A., Estevinho, B. N., & Rocha, F. (2021). Methodologies for simulation of gastrointestinal digestion of different controlled delivery systems and further uptake of encapsulated bioactive compounds. *Trends in Food Science & Technology*, 114, 510–520. <https://doi.org/10.1016/J.TIFS.2021.06.007>

Gonçalves, R. F. S., Martins, J. T., Abrunhosa, L., Baixinho, J., Matias, A. A., Vicente, A. A., & Pinheiro, A. C. (2021). Lipid-based nanostructures as a strategy to enhance curcumin bioaccessibility: Behavior under digestion and cytotoxicity assessment. *Food Research International*, 143, 110278. <https://doi.org/10.1016/j.foodres.2021.110278>

Gonçalves, R. F. S., Martins, J. T., Abrunhosa, L., Vicente, A. A., & Pinheiro, A. C. (2021). Nanoemulsions for Enhancement of Curcumin Bioavailability and Their Safety Evaluation: Effect of Emulsifier Type. In *Nanomaterials* (Vol. 11, Issue 3). <https://doi.org/10.3390/nano11030815>

Granato, D., Putnik, P., Kovačević, D. B., Santos, J. S., Calado, V., Rocha, R. S., Cruz, A. G. Da, Jarvis, B., Rodionova, O. Y., & Pomerantsev, A. (2018). Trends in Chemometrics: Food Authentication, Microbiology, and Effects of Processing. *Comprehensive Reviews in Food Science and Food Safety*, 17(3), 663–677. <https://doi.org/https://doi.org/10.1111/1541-4337.12341>

- Gross-Rother, J., Blech, M., Preis, E., Bakowsky, U., & Garidel, P. (2020). Particle Detection and Characterization for Biopharmaceutical Applications: Current Principles of Established and Alternative Techniques. In *Pharmaceutics* (Vol. 12, Issue 11). <https://doi.org/10.3390/pharmaceutics12111112>
- Guo, Y., Chen, X., Gong, P., Chen, F., Cui, D., & Wang, M. (2021). Advances in the *in vitro* digestion and fermentation of polysaccharides. *International Journal of Food Science & Technology*, 56(10), 4970–4982. <https://doi.org/https://doi.org/10.1111/ijfs.15308>
- Guo, Zhiming, Wang, M., Wu, J., Tao, F., Chen, Q., Wang, Q., Ouyang, Q., Shi, J., & Zou, X. (2019). Quantitative assessment of zearalenone in maize using multivariate algorithms coupled to Raman spectroscopy. *Food Chemistry*, 286, 282–288. <https://doi.org/https://doi.org/10.1016/j.foodchem.2019.02.020>
- Guo, Zhongyuan, Cao, X., DeLoid, G. M., Sampathkumar, K., Ng, K. W., Loo, S. C. J., & Demokritou, P. (2020). Physicochemical and Morphological Transformations of Chitosan Nanoparticles across the Gastrointestinal Tract and Cellular Toxicity in an *In vitro* Model of the Small Intestinal Epithelium. *Journal of Agricultural and Food Chemistry*, 68(1), 358–368. <https://doi.org/10.1021/acs.jafc.9b05506>
- Hammes, G. G. (2005). Fundamentals of Spectroscopy. In *Spectroscopy for the Biological Sciences* (pp. 1–15). <https://doi.org/https://doi.org/10.1002/0471733555.ch1>
- Hatzakis, E. (2019). Nuclear Magnetic Resonance (NMR) Spectroscopy in Food Science: A Comprehensive Review. *Comprehensive Reviews in Food Science and Food Safety*, 18(1), 189–220. <https://doi.org/10.1111/1541-4337.12408>
- He, S., & Ye, A. (2019). Formation and gastrointestinal digestion of  $\beta$ -carotene emulsion stabilized by milk fat globule membrane. *Journal of Food Process Engineering*, October, 1–8. <https://doi.org/10.1111/jfpe.13301>
- Hernández-Olivas, E., Muñoz-Pina, S., Andrés, A., & Heredia, A. (2020). Impact of elderly gastrointestinal alterations on *in vitro* digestion of salmon, sardine, sea bass and hake: Proteolysis, lipolysis and bioaccessibility of calcium and vitamins. *Food Chemistry*, 326, 127024. <https://doi.org/10.1016/J.FOODCHEM.2020.127024>
- Hollas, J. M. (2004). *Modern Spectroscopy* (4th Editio). John Wiley and Sons Inc.
- Holze, R. (2004). Fundamentals and applications of near infrared spectroscopy in spectroelectrochemistry. *Journal of Solid State Electrochemistry*, 8(12), 982–997. <https://doi.org/10.1007/s10008-004-0524-y>
- Hu, G., Batool, Z., Cai, Z., Liu, Y., Ma, M., Sheng, L., & Jin, Y. (2021). Production of self-assembling acylated ovalbumin nanogels as stable delivery vehicles for curcumin. *Food Chemistry*, 355, 129635. <https://doi.org/10.1016/J.FOODCHEM.2021.129635>
- Hu, R., He, T., Zhang, Z., Yang, Y., & Liu, M. (2019). Safety analysis of edible oil products via Raman spectroscopy. In *Talanta* (Vol. 191, pp. 324–332). Elsevier B.V. <https://doi.org/10.1016/j.talanta.2018.08.074>

Jain, S., & Sekhar, A. (2022). Elucidating the mechanisms underlying protein conformational switching using NMR spectroscopy. *Journal of Magnetic Resonance Open*, 10–11, 100034. <https://doi.org/10.1016/J.JMRO.2022.100034>

Ji, H., Hu, J., Zuo, S., Zhang, S., Li, M., & Nie, S. (2021). *In vitro* gastrointestinal digestion and fermentation models and their applications in food carbohydrates. *Critical Reviews in Food Science and Nutrition*, 1–23. <https://doi.org/10.1080/10408398.2021.1884841>

Jiang, S., Yildiz, G., Ding, J., Andrade, J., Rababah, T. M., Almajwal, A., Abulmeatyc, M. M., & Feng, H. (2019). Pea Protein Nanoemulsion and Nanocomplex as Carriers for Protection of Cholecalciferol (Vitamin D3). *Food and Bioprocess Technology*, 12(6), 1031–1040. <https://doi.org/10.1007/s11947-019-02276-0>

Jin, J., Okagu, O. D., Yagoub, A. E. G. A., & Udenigwe, C. C. (2021). Effects of sonication on the *in vitro* digestibility and structural properties of buckwheat protein isolates. *Ultrasonics Sonochemistry*, 70, 105348. <https://doi.org/10.1016/j.ultsonch.2020.105348>

Kaavya, R., Pandiselvam, R., Mohammed, M., Dakshayani, R., Kothakota, A., Ramesh, S. V., Cozzolino, D., & Ashokkumar, C. (2020). Application of infrared spectroscopy techniques for the assessment of quality and safety in spices: a review. *Applied Spectroscopy Reviews*, 1–19. <https://doi.org/10.1080/05704928.2020.1713801>

Katopodi, A., & Detsi, A. (2021). Solid Lipid Nanoparticles and Nanostructured Lipid Carriers of natural products as promising systems for their bioactivity enhancement: The case of essential oils and flavonoids. *Colloids and Surfaces A: Physicochemical and Engineering Aspects*, 630, 127529. <https://doi.org/10.1016/J.COLSURFA.2021.127529>

Ketnawa, S., Reginio, F. C., Thuengtung, S., & Ogawa, Y. (2021). Changes in bioactive compounds and antioxidant activity of plant-based foods by gastrointestinal digestion: a review. *Critical Reviews in Food Science and Nutrition*, 1–22. <https://doi.org/10.1080/10408398.2021.1878100>

Khan, J., Hawley, A., Rades, T., & Boyd, B. J. (2016). *In situ* Lipolysis and Synchrotron Small-Angle X-ray Scattering for the Direct Determination of the Precipitation and Solid-State Form of a Poorly Water-Soluble Drug During Digestion of a Lipid-Based Formulation. *Journal of Pharmaceutical Sciences*, 105(9), 2631–2639. <https://doi.org/10.1002/jps.24634>

Kurpiewska, K., Biela, A., Loch, J. I., Lipowska, J., Siuda, M., & Lewiński, K. (2019). Towards understanding the effect of high pressure on food protein allergenicity:  $\beta$ -lactoglobulin structural studies. *Food Chemistry*, 270, 315–321. <https://doi.org/10.1016/j.foodchem.2018.07.104>

Li, C., Yu, W., Wu, P., & Chen, X. D. (2020). Current *in vitro* digestion systems for understanding food digestion in human upper gastrointestinal tract. In *Trends in Food Science and Technology* (Vol. 96, pp. 114–126). Elsevier Ltd. <https://doi.org/10.1016/j.tifs.2019.12.015>

Li, J., Jiao, A., Chen, S., Wu, Z., Xu, E., & Jin, Z. (2018). Application of the small-angle X-ray scattering technique for structural analysis studies: A review. In *Journal of Molecular Structure* (Vol. 1165, pp. 391–400). Elsevier B.V. <https://doi.org/10.1016/j.molstruc.2017.12.031>

- Li, Y., Fortner, L., & Kong, F. (2019). Development of a Gastric Simulation Model (GSM) incorporating gastric geometry and peristalsis for food digestion study. *Food Research International*, 125(March), 108598. <https://doi.org/10.1016/j.foodres.2019.108598>
- Li, Z., Zhu, L., Zhang, W., Zhan, X., & Gao, M. (2019). New dynamic digestion model reactor that mimics gastrointestinal function. *Biochemical Engineering Journal*, 107431. <https://doi.org/10.1016/j.bej.2019.107431>
- Liang, J., Yan, H., Puligundla, P., Gao, X., Zhou, Y., & Wan, X. (2017). Applications of chitosan nanoparticles to enhance absorption and bioavailability of tea polyphenols: A review. *Food Hydrocolloids*, 69, 286–292. <https://doi.org/https://doi.org/10.1016/j.foodhyd.2017.01.041>
- Liang, Q., Ren, X., Qu, W., Zhang, X., Cheng, Y., & Ma, H. (2021). The impact of ultrasound duration on the structure of  $\beta$ -lactoglobulin. *Journal of Food Engineering*, 292, 110365. <https://doi.org/10.1016/j.jfoodeng.2020.110365>
- Liu, L., & Kong, F. (2019). Influence of nanocellulose on *in vitro* digestion of whey protein isolate. *Carbohydrate Polymers*, 210, 399–411. <https://doi.org/10.1016/J.CARBPOL.2019.01.071>
- Liu, W., Fu, D., Zhang, X., Chai, J., Tian, S., & Han, J. (2019). Development and validation of a new artificial gastric digestive system. *Food Research International*, 122. <https://doi.org/10.1016/j.foodres.2019.04.015>
- Liu, W., Liu, J., Salt, L. J., Ridout, M. J., Han, J., & Wilde, P. J. (2019). Structural stability of liposome-stabilized oil-in-water pickering emulsions and their fate during *in vitro* digestion. *Food Funct.*, 10(11), 7262–7274. <https://doi.org/10.1039/C9FO00967A>
- Lovegrove, A., Edwards, C. H., De Noni, I., Patel, H., El, S. N., Grassby, T., Zielke, C., Ulmius, M., Nilsson, L., Butterworth, P. J., Ellis, P. R., & Shewry, P. R. (2017). Role of polysaccharides in food, digestion, and health. *Critical Reviews in Food Science and Nutrition*, 57(2), 237–253. <https://doi.org/10.1080/10408398.2014.939263>
- Lucas-González, R., Viuda-Martos, M., Pérez-Alvarez, J. A., & Fernández-López, J. (2018). *In vitro* digestion models suitable for foods: Opportunities for new fields of application and challenges. *Food Research International*, 107, 423–436. <https://doi.org/10.1016/J.FOODRES.2018.02.055>
- Lv, X., Zhang, S., Ma, H., Dong, P., Ma, X., Xu, M., Tian, Y., Tang, Z., Peng, J., Chen, H., & Zhang, J. (2018). *In situ* monitoring of the structural change of microemulsions in simulated gastrointestinal conditions by SAXS and FRET. *Acta Pharmaceutica Sinica B*, 8(4), 655–665. <https://doi.org/10.1016/j.apsb.2018.05.008>
- Machado, A. R., Pinheiro, A. C., Vicente, A. A., Souza-Soares, L. A., & Cerqueira, M. A. (2019). Liposomes loaded with phenolic extracts of Spirulina LEB-18: Physicochemical characterization and behavior under simulated gastrointestinal conditions. *Food Research International*, 120, 656–667. <https://www.sciencedirect.com/science/article/pii/S0963996918309086>
- Macierzanka, A., Torcello-Gómez, A., Jungnickel, C., & Maldonado-Valderrama, J. (2019). Bile salts in digestion and transport of lipids. *Advances in Colloid and Interface Science*, 274, 102045. <https://doi.org/10.1016/j.cis.2019.102045>

Mackie, A., & Macierzanka, A. (2010). Colloidal aspects of protein digestion. In *Current Opinion in Colloid and Interface Science* (Vol. 15, Issues 1–2, pp. 102–108). Elsevier. <https://doi.org/10.1016/j.cocis.2009.11.005>

Mackie, A., Mulet-Cabero, A.-I., & Torcello-Gómez, A. (2020). Simulating human digestion: developing our knowledge to create healthier and more sustainable foods. *Food & Function*, 11(11), 9397–9431. <https://doi.org/10.1039/D0FO01981J>

Madalena, D. A., Pereira, R. N., Vicente, A. A., & Ramos, Ó. L. (2019). New Insights on Bio-Based Micro- and Nanosystems in Food. In *Encyclopedia of Food Chemistry* (pp. 708–714). Elsevier. <https://doi.org/10.1016/B978-0-08-100596-5.21859-3>

Mahalakshmi, L., Leena, M. M., Moses, J. A., & Anandharamakrishnan, C. (2020). Micro- and nano-encapsulation of  $\beta$ -carotene in zein protein: size-dependent release and absorption behavior. *Food & Function*, 11(2), 1647–1660. <https://doi.org/10.1039/C9FO02088H>

Majeed, H., Antoniou, J., Hategekimana, J., Sharif, H. R., Haider, J., Liu, F., Ali, B., Rong, L., Ma, J., & Zhong, F. (2016). Influence of carrier oil type, particle size on invitro lipid digestion and eugenol release in emulsion and nanoemulsions. *Food Hydrocolloids*. <https://doi.org/10.1016/j.foodhyd.2015.07.009>

McClements, D. J. (2018a). Encapsulation, protection, and delivery of bioactive proteins and peptides using nanoparticle and microparticle systems: A review. *Advances in Colloid and Interface Science*, 253, 1–22. <https://doi.org/10.1016/J.CIS.2018.02.002>

McClements, D. J. (2018b). Enhanced delivery of lipophilic bioactives using emulsions: A review of major factors affecting vitamin, nutraceutical, and lipid bioaccessibility. *Food and Function*, 9(1), 22–41. <https://doi.org/10.1039/c7fo01515a>

Ménard, O., Bourlieu, C., De Oliveira, S. C., Dellarosa, N., Laghi, L., Carrière, F., Capozzi, F., Dupont, D., & Deglaire, A. (2018). A first step towards a consensus static *in vitro* model for simulating full-term infant digestion. *Food Chemistry*, 240(March 2017), 338–345. <https://doi.org/10.1016/j.foodchem.2017.07.145>

Mennah-Govela, Y., Cai, H., Chu, J., Kim, K., Maborang, M.-K., Sun, W., & Bornhorst, G. M. (2020). Buffering Capacity of Commercially Available Foods is Influenced by Composition and Initial Properties in the Context of Gastric Digestion. *Food Funct.* <https://doi.org/10.1039/C9FO03033F>

Minekus, M., Alming, M., Alvito, P., Ballance, S., Bohn, T., Bourlieu, C., Carrière, F., Boutrou, R., Corredig, M., Dupont, D., Dufour, C., Egger, L., Golding, M., Karakaya, S., Kirkhus, B., Le Feunteun, S., Lesmes, U., Macierzanka, A., Mackie, A., ... Brodkorb, A. (2014). A standardised static *in vitro* digestion method suitable for food – an international consensus. *Food Funct.*, 5(6), 1113–1124. <https://doi.org/10.1039/C3FO60702J>

Modena, M. M., Rühle, B., Burg, T. P., & Wuttke, S. (2019). Nanoparticle Characterization: What to Measure? *Advanced Materials*, 31(32), 26. <https://doi.org/10.1002/adma.201901556>

Mohebbi, S., Nezhad, M. N., Zarrintaj, P., Jafari, S. H., Gholizadeh, S. S., Saeb, M. R., & Mozafari, M. (2019). Chitosan in biomedical engineering: A critical review. *Current Stem Cell Research and Therapy*, 14(2), 93–116. <https://doi.org/10.2174/1574888X13666180912142028>

- Mourdikoudis, S., Pallares, R. M., & Thanh, N. T. K. (2018). Characterization techniques for nanoparticles: comparison and complementarity upon studying nanoparticle properties. *Nanoscale*, 10(27), 12871–12934. <https://doi.org/10.1039/C8NR02278J>
- Mulet-Cabero, A.-I., Egger, L., Portmann, R., Ménard, O., Marze, S., Minekus, M., Le Feunteun, S., Sarkar, A., Grundy, M. M.-L., Carrière, F., Golding, M., Dupont, D., Recio, I., Brodkorb, A., & Mackie, A. (2020). A standardised semi-dynamic *in vitro* digestion method suitable for food – an international consensus. *Food Funct.* <https://doi.org/10.1039/C9FO01293A>
- Naes, T., Isaksson, T., Fearn, T., & Davies, T. (2004). A user-friendly guide to multivariate calibration and classification. *Journal of Chemometrics*, 17(10), 571–572. <https://doi.org/10.1002/cem.815>
- Nasirizadeh, S., & Malaekheh-Nikouei, B. (2020). Solid lipid nanoparticles and nanostructured lipid carriers in oral cancer drug delivery. *Journal of Drug Delivery Science and Technology*, 55, 101458. <https://doi.org/10.1016/J.JDDST.2019.101458>
- Nellist, P. D. (2019). Scanning Transmission Electron Microscopy BT - Springer Handbook of Microscopy (P. W. Hawkes & J. C. H. Spence (eds.); pp. 49–99). Springer International Publishing. [https://doi.org/10.1007/978-3-030-00069-1\\_2](https://doi.org/10.1007/978-3-030-00069-1_2)
- Nieva-Echevarría, B., Goicoechea, E., Manzanos, M. J., & Guillén, M. D. (2016). A study by <sup>1</sup>H NMR on the influence of some factors affecting lipid *in vitro* digestion. *Food Chemistry*, 211, 17–26. <https://doi.org/10.1016/J.FOODCHEM.2016.05.021>
- Nieva-Echevarría, B., Goicoechea, E., Manzanos, M. J., & Guillén, M. D. (2017). <sup>1</sup>H NMR and SPME-GC/MS study of hydrolysis, oxidation and other reactions occurring during *in vitro* digestion of non-oxidized and oxidized sunflower oil. Formation of hydroxy-octadecadienoates. *Food Research International*, 91, 171–182. <https://doi.org/10.1016/J.FOODRES.2016.11.027>
- Nilapwar, S. M., Nardelli, M., Westerhoff, H. V., & Verma, M. (2011). Absorption Spectroscopy. *Methods in Enzymology*, 500, 59–75. <https://doi.org/10.1016/B978-0-12-385118-5.00004-9>
- Pabois, O., Antoine-Michard, A., Zhao, X., Omar, J., Ahmed, F., Alexis, F., Harvey, R. D., Grillo, I., Gerelli, Y., Grundy, M. M.-L., Bajka, B., Wilde, P. J., & Dreiss, C. A. (2020). Interactions of bile salts with a dietary fibre, methylcellulose, and impact on lipolysis. *Carbohydrate Polymers*, 231(September 2019), 115741. <https://doi.org/10.1016/j.carbpol.2019.115741>
- Pan, Y., & Nitin, N. (2016). Real-time measurements to characterize dynamics of emulsion interface during simulated intestinal digestion. *Colloids and Surfaces B: Biointerfaces*, 141, 233–241. <https://doi.org/10.1016/j.colsurfb.2016.01.053>
- Pinheiro, A. C., Gonçalves, R. F., Madalena, D. A., & Vicente, A. A. (2017). Towards the understanding of the behavior of bio-based nanostructures during *in vitro* digestion. *Current Opinion in Food Science*, 15, 79–86. <https://doi.org/10.1016/J.COFS.2017.06.005>
- Qi, W., Tian, Y., Lu, D., & Chen, B. (2022). Research Progress of Applying Infrared Spectroscopy Technology for Detection of Toxic and Harmful Substances in Food. In *Foods* (Vol. 11, Issue 7). <https://doi.org/10.3390/foods11070930>



Rahaman, T., Vasiljevic, T., & Ramchandran, L. (2017). Digestibility and antigenicity of  $\beta$ -lactoglobulin as affected by heat, pH and applied shear. *Food Chemistry*, 217, 517–523. <https://doi.org/10.1016/j.foodchem.2016.08.129>

Rahdar, A., Amini, N., Askari, F., & Susan, M. A. B. H. (2019). Dynamic light scattering: A useful technique to characterize nanoparticles. *Journal of Nanoanalysis*, 6(2), 80–89. <https://doi.org/10.22034/jna.2019.667079>

Ramos, Ó. L., Teixeira, J. A., & Vicente, A. A. (2019). Nanotechnology in Food. In *Advances in Processing Technologies for Bio-based Nanosystems in Food* (pp. 3–12). CRC Press. <https://doi.org/10.1201/9781315177328-1>

Sadati Behbahani, E., Ghaedi, M., Abbaspour, M., Rostamizadeh, K., & Dashtian, K. (2019). Curcumin loaded nanostructured lipid carriers: *In vitro* digestion and release studies. *Polyhedron*, 164, 113–122. <https://doi.org/10.1016/j.poly.2019.02.002>

Salim, M., Fraser-Miller, S. J., Berziņš, K., Sutton, J. J., Ramirez, G., Clulow, A. J., Hawley, A., Beilles, S., Gordon, K. C., & Boyd, B. J. (2020). Low-Frequency Raman Scattering Spectroscopy as an Accessible Approach to Understand Drug Solubilization in Milk-Based Formulations during Digestion. *Molecular Pharmaceutics*, 17(3), 885–899. <https://doi.org/10.1021/acs.molpharmaceut.9b01149>

Salvia-Trujillo, L., Verkempinck, S., Rijal, S. K., Van Loey, A., Grauwet, T., & Hendrickx, M. (2019). Lipid nanoparticles with fats or oils containing  $\beta$ -carotene: Storage stability and *in vitro* digestibility kinetics. *Food Chemistry*. <https://doi.org/10.1016/j.foodchem.2018.11.039>

Sanchón, J., Fernández-Tomé, S., Miralles, B., Hernández-Ledesma, B., Tomé, D., Gaudichon, C., & Recio, I. (2018). Protein degradation and peptide release from milk proteins in human jejunum. Comparison with *in vitro* gastrointestinal simulation. *Food Chemistry*, 239. <https://doi.org/10.1016/j.foodchem.2017.06.134>

Sarkar, A., Zhang, S., Holmes, M., & Ettelaie, R. (2019). Colloidal aspects of digestion of Pickering emulsions: Experiments and theoretical models of lipid digestion kinetics. In *Advances in Colloid and Interface Science*. <https://doi.org/10.1016/j.cis.2018.10.002>

Shani-Levi, C., Alvito, P., Andrés, A., Assunção, R., Barberá, R., Blanquet-Diot, S., Bourlieu, C., Brodkorb, A., Cilla, A., Deglaire, A., Denis, S., Dupont, D., Heredia, A., Karakaya, S., Giosafatto, C. V. L., Mariniello, L., Martins, C., Ménard, O., El, S. N., ... Lesmes, U. (2017). Extending *in vitro* digestion models to specific human populations: Perspectives, practical tools and bio-relevant information. In *Trends in Food Science and Technology* (Vol. 60). <https://doi.org/10.1016/j.tifs.2016.10.017>

Silva, H. D., Beldíková, E., Poejo, J., Abrunhosa, L., Serra, A. T., Duarte, C. M. M., Brányik, T., Cerqueira, M. A., Pinheiro, A. C., & Vicente, A. A. (2019). Evaluating the effect of chitosan layer on bioaccessibility and cellular uptake of curcumin nanoemulsions. *Journal of Food Engineering*, 243, 89–100. <https://doi.org/10.1016/J.JFOODENG.2018.09.007>

Silva, H. D., Poejo, J., Pinheiro, A. C., Donsi, F., Serra, A. T., Duarte, C. M. M., Ferrari, G., Cerqueira, M. A., & Vicente, A. A. (2018). Evaluating the behaviour of curcumin nanoemulsions

and multilayer nanoemulsions during dynamic *in vitro* digestion. *Journal of Functional Foods*. <https://doi.org/10.1016/j.jff.2018.08.002>

Simões, L., Abrunhosa, L., Vicente, A. A., & Ramos, Ó. L. (2020). Suitability of  $\beta$ -lactoglobulin micro- and nanostructures for loading and release of bioactive compounds. *Food Hydrocolloids*, 101, 105492. <https://doi.org/https://doi.org/10.1016/j.foodhyd.2019.105492>

Simões, L., Madalena, D. A., Pinheiro, A. C., Teixeira, J. A., Vicente, A. A., & Ramos, Ó. L. (2017). Micro- and nano bio-based delivery systems for food applications: *In vitro* behavior. *Advances in Colloid and Interface Science*, 243, 23–45. <https://doi.org/10.1016/J.CIS.2017.02.010>

Simões, L., Martins, J. T., Pinheiro, A. C., Vicente, A. A., & Ramos, Ó. L. (2020).  $\beta$ -lactoglobulin micro- and nanostructures as bioactive compounds vehicle: *In vitro* studies. *Food Research International*. <https://doi.org/10.1016/j.foodres.2020.108979>

Smeets, P. A. M., Deng, R., van Eijnatten, E. J. M., & Mayar, M. (2021). Monitoring food digestion with magnetic resonance techniques. *Proceedings of the Nutrition Society*, 80(2), 148–158. <https://doi.org/DOI: 10.1017/S0029665120007867>

Stetefeld, J., McKenna, S. A., & Patel, T. R. (2016). Dynamic light scattering: a practical guide and applications in biomedical sciences. *Biophysical Reviews*, 8(4), 409–427. <https://doi.org/10.1007/s12551-016-0218-6>

Stillhart, C., Imanidis, G., & Kuentz, M. (2013). Insights into Drug Precipitation Kinetics during *In vitro* Digestion of a Lipid-Based Drug Delivery System Using In-Line Raman Spectroscopy and Mathematical Modeling. *Pharmaceutical Research*, 30(12), 3114–3130. <https://doi.org/10.1007/s11095-013-0999-2>

Stuart, B. H., & Preface, S. (2004). *Infrared Spectroscopy: Fundamentals and Applications*. In *Infrared Spectroscopy: Fundamentals and Applications* (First Edit, Vol. 8). John Wiley & Sons. <https://doi.org/10.1002/0470011149>

van der Pol, E., Hoekstra, A. G., Sturk, A., Otto, C., van Leeuwen, T. G., & Nieuwland, R. (2010). Optical and non-optical methods for detection and characterization of microparticles and exosomes. *Journal of Thrombosis and Haemostasis*, 8(12), 2596–2607. <https://doi.org/https://doi.org/10.1111/j.1538-7836.2010.04074.x>

Verkempinck, S. H. E., Salvia-Trujillo, L., Moens, L. G., Charleer, L., Van Loey, A. M., Hendrickx, M. E., & Grauwet, T. (2018). Emulsion stability during gastrointestinal conditions effects lipid digestion kinetics. *Food Chemistry*. <https://doi.org/10.1016/j.foodchem.2017.11.001>

Vladár, A. E., & Hodoroaba, V.-D. (2020). Chapter 2.1.1 - Characterization of nanoparticles by scanning electron microscopy. In V.-D. Hodoroaba, W. E. S. Unger, & A. G. B. T.-C. of N. Shard (Eds.), *Micro and Nano Technologies* (pp. 7–27). Elsevier. <https://doi.org/https://doi.org/10.1016/B978-0-12-814182-3.00002-X>

Vrbanac, H., Trontelj, J., Berglez, S., Petek, B., Opara, J., Jereb, R., Krajcar, D., & Legen, I. (2020). The biorelevant simulation of gastric emptying and its impact on model drug dissolution and absorption kinetics. *European Journal of Pharmaceutics and Biopharmaceutics*, 149, 113–120. <https://doi.org/10.1016/J.EJPB.2020.02.002>

Wang, H.-P., Chen, P., Dai, J.-W., Liu, D., Li, J.-Y., Xu, Y.-P., & Chu, X.-L. (2022). Recent advances of chemometric calibration methods in modern spectroscopy: Algorithms, strategy, and related issues. *TrAC Trends in Analytical Chemistry*, 153, 116648. <https://doi.org/10.1016/J.TRAC.2022.116648>

Wang, J., Wu, P., Liu, M., Liao, Z., Wang, Y., Dong, Z., & Chen, X. D. (2019). An advanced near real dynamic *in vitro* human stomach system to study gastric digestion and emptying of beef stew and cooked rice. *Food & Function*, 10(5), 2914–2925. <https://doi.org/10.1039/C8FO02586J>

Wang, T., & Luo, Y. (2019). Biological fate of ingested lipid-based nanoparticles: Current understanding and future directions. *Nanoscale*, 11(23), 11048–11063. <https://doi.org/10.1039/c9nr03025e>

Wei, Y., Sun, C., Dai, L., Zhan, X., & Gao, Y. (2018). Structure, physicochemical stability and *in vitro* simulated gastrointestinal digestion properties of  $\beta$ -carotene loaded zein-propylene glycol alginate composite nanoparticles fabricated by emulsification-evaporation method. *Food Hydrocolloids*, 81, 149–158. <https://doi.org/10.1016/J.FOODHYD.2018.02.042>

Wei, Y., Zhang, L., Yu, Z., Lin, K., Yang, S., Dai, L., Liu, J., Mao, L., Yuan, F., & Gao, Y. (2019). Enhanced stability, structural characterization and simulated gastrointestinal digestion of coenzyme Q10 loaded ternary nanoparticles. *Food Hydrocolloids*. <https://doi.org/10.1016/j.foodhyd.2019.03.024>

Weng, S., Guo, B., Tang, P., Yin, X., Pan, F., Zhao, J., Huang, L., & Zhang, D. (2020). Rapid detection of adulteration of minced beef using Vis/NIR reflectance spectroscopy with multivariate methods. *Spectrochimica Acta Part A: Molecular and Biomolecular Spectroscopy*, 230, 118005. <https://doi.org/https://doi.org/10.1016/j.saa.2019.118005>

Wiercigroch, E., Szafranec, E., Czamara, K., Pacia, M. Z., Majzner, K., Kochan, K., Kaczor, A., Baranska, M., & Malek, K. (2017). Raman and infrared spectroscopy of carbohydrates: A review. In *Spectrochimica Acta - Part A: Molecular and Biomolecular Spectroscopy* (Vol. 185, pp. 317–335). Elsevier B.V. <https://doi.org/10.1016/j.saa.2017.05.045>

Wu, D., Feng, S., & He, Y. (2008). Short-Wave Near-Infrared Spectroscopy of Milk Powder for Brand Identification and Component Analysis. *Journal of Dairy Science*, 91(3), 939–949. <https://doi.org/10.3168/jds.2007-0640>

Wu, Di, He, Y., & Feng, S. (2008). Short-wave near-infrared spectroscopy analysis of major compounds in milk powder and wavelength assignment. *Analytica Chimica Acta*, 610(2), 232–242. <https://doi.org/10.1016/j.aca.2008.01.056>

Xu, X., Zhao, W., Ye, Y., Cui, W., Dong, L., Yao, Y., Li, K., Han, J., & Liu, W. (2021). Novel Nanoliposome Codelivered DHA and Anthocyanidin: Characterization, *In vitro* Infant Digestibility, and Improved Cell Uptake. *Journal of Agricultural and Food Chemistry*, 69(32), 9395–9406. <https://doi.org/10.1021/acs.jafc.1c02817>

Xue, S., Wang, C., Kim, Y. H. B., Bian, G., Han, M., Xu, X., & Zhou, G. (2020). Application of high-pressure treatment improves the *in vitro* protein digestibility of gel-based meat product. *Food Chemistry*, 306, 125602. <https://doi.org/10.1016/j.foodchem.2019.125602>

- Ye, Z., Cao, C., Li, R., Cao, P., Li, Q., & Liu, Y. (2019). Lipid composition modulates the intestine digestion rate and serum lipid status of different edible oils: a combination of *in vitro* and *in vivo* studies. *Food Funct.*, 10(3), 1490–1503. <https://doi.org/10.1039/C8FO01290C>
- Zahir, S. A. D. M., Omar, A. F., Jamlos, M. F., Azmi, M. A. M., & Muncan, J. (2022). A review of visible and near-infrared (Vis-NIR) spectroscopy application in plant stress detection. *Sensors and Actuators A: Physical*, 338, 113468. <https://doi.org/10.1016/J.SNA.2022.113468>
- Zhang, A., Chen, S., Wang, Y., Wang, X., Xu, N., & Jiang, L. (2020). Stability and *in vitro* digestion simulation of soy protein isolate-vitamin D3 nanocomposites. *LWT*, 117, 108647. <https://doi.org/10.1016/J.LWT.2019.108647>
- Zhang, C., Gu, C., Peng, F., Liu, W., Wan, J., Xu, H., Lam, C. W., & Yang, X. (2013). Preparation and Optimization of Triptolide-Loaded Solid Lipid Nanoparticles for Oral Delivery with Reduced Gastric Irritation. In *Molecules* (Vol. 18, Issue 11). <https://doi.org/10.3390/molecules181113340>
- Zhang, W., Ma, J., & Sun, D.-W. (2020). Raman spectroscopic techniques for detecting structure and quality of frozen foods: principles and applications. *Critical Reviews in Food Science and Nutrition*, 1–17. <https://doi.org/10.1080/10408398.2020.1828814>
- Zhang, Z. (2020). Rapid Discrimination of Cheese Products Based on Probabilistic Neural Network and Raman Spectroscopy. *Journal of Spectroscopy*, 2020, 8896535. <https://doi.org/10.1155/2020/8896535>
- Zheng, B., Zhang, X., Peng, S., & Julian McClements, D. (2019). Impact of curcumin delivery system format on bioaccessibility: nanocrystals, nanoemulsion droplets, and natural oil bodies. *Food Funct.*, 10(7), 4339–4349. <https://doi.org/10.1039/C8FO02510J>
- Zheng, L. X., Chen, X. Q., & Cheong, K. L. (2020). Current trends in marine algae polysaccharides: The digestive tract, microbial catabolism, and prebiotic potential. *International Journal of Biological Macromolecules*, 151, 344–354. <https://doi.org/10.1016/J.IJBIOMAC.2020.02.168>
- Zornjak, J., Liu, J., Esker, A., Lin, T., & Fernández-Fraguas, C. (2020). Bulk and interfacial interactions between hydroxypropyl-cellulose and bile salts: Impact on the digestion of emulsified lipids. *Food Hydrocolloids*, 106, 105867. <https://doi.org/10.1016/J.FOODHYD.2020.105867>

DEVELOPMENT OF A REPRODUCIBLE *IN VITRO* RGM

3.1	INTRODUCTION .....	57
3.2	MATERIALS AND METHODS.....	57
3.3	RESULTS AND DISCUSSION .....	72
3.4	CONCLUSIONS .....	76
3.5	REFERENCES .....	77

### 3.1 INTRODUCTION

*In vitro* digestion models have been widely used in the fields of food and pharmaceutical sciences to: i) study the release kinetics of bioactive compounds entrapped in micro/nanostructures (Simões et al., 2020); ii) mathematically modulate the dissolution kinetics of drugs (Sadati Behbahani et al., 2019); iii) study the cytotoxicity of metabolites (Guo et al., 2020); and to iv) study the physicochemical phenomena that occur under *in vitro* digestion (e.g., enzymatic digestion, pH transitions, influence of peristalsis, presence of bile salts, among others). These models are faster, less expensive, less labour intensive and do not present any ethical constraints when compared with *in vivo* trials (Madalena et al., 2019). In fact, there is a current effort towards standardizing the *in vitro* digestion process (Brodkorb et al., 2019; Minekus et al., 2014; Mulet-Cabero et al., 2020), as well as developing realistic dynamic *in vitro* digestion models that replicate the anatomical and physical characteristics of the human gastrointestinal (GI) tract (Dang et al., 2020; Li et al., 2019; Liu et al., 2019; Wang et al., 2019). Such efforts unlock the possibility of comparing inter-laboratory studies as well as developing more realistic *in vitro* digestion models that comprise the same anatomy of the human GI tract (e.g., “J” shape of the stomach) which will consequently allow the study of other important phenomena that occur during the digestion process (i.e., retroperistalsis) (Pinheiro et al., 2017). Furthermore, such advancements will consequently produce more reliable *in vitro* digestion data that present better *in vitro/in vivo* correlations. However, none of the current standard *in vitro* digestion models encompass a realistic gastric compartment and the recently developed anatomical accurate digestion models are not easily reproduced in the laboratory (i.e., both gastric compartment and PB) which implies that developing a standardized dynamic system is still a major challenge. This way, the present study proposes the development of a reproducible and realistic *in vitro* gastric model (RGM) through the application of 3D printing technology. An experimental design was made to develop the PB and mathematically modulate their contraction using a finite element analysis (FEA) to assess their behaviour. This model was then characterized in terms of pH control profile and hydrodynamic behaviour by measuring the average residence time at different stomach emptying flow rates.

### 3.2 MATERIALS AND METHODS

#### 3.2.1 Materials

The simulated gastric fluid was prepared based on the protocol reported by Mulet-Cabero et al., (2020). Briefly, the electrolyte gastric solution was made using stock salt solutions of KCl (6.9 mmol L<sup>-1</sup>), KH<sub>2</sub>PO<sub>4</sub> (0.9 mmol L<sup>-1</sup>), NaHCO<sub>3</sub> (25 mmol L<sup>-1</sup>), NaCl (47.2 mmol L<sup>-1</sup>), MgCl<sub>2</sub>(H<sub>2</sub>O)<sub>6</sub> (0.12 mmol L<sup>-1</sup>), (NH<sub>4</sub>)<sub>2</sub>CO<sub>3</sub> (0.5 mmol L<sup>-1</sup>) – values within parentheses correspond to the final salt concentration in the simulated gastric fluid (SGF). The 1.75 mm polylactic acid (PLA) filament, the raspberry pi, the 6V air pump, the ads1115, the temperature sensor, the relay modules, the electrovalves, the pH circuit board and electrode, the level sensor and the peristaltic pumps were purchase from Amazon Inc. (Spain). The silicone (ZN20 with Shore 21 hardness) was purchased from Castro composites (Pontevedra, Spain). The food colouring was purchased in the local supermarket. RGM modules and development process

### 3.2.2 Model description

The RGM was designed on the premise of being easily reproducible so that it could be a potential standard dynamic *in vitro* gastric model. It is composed by six modules which are depicted in Figure 5.

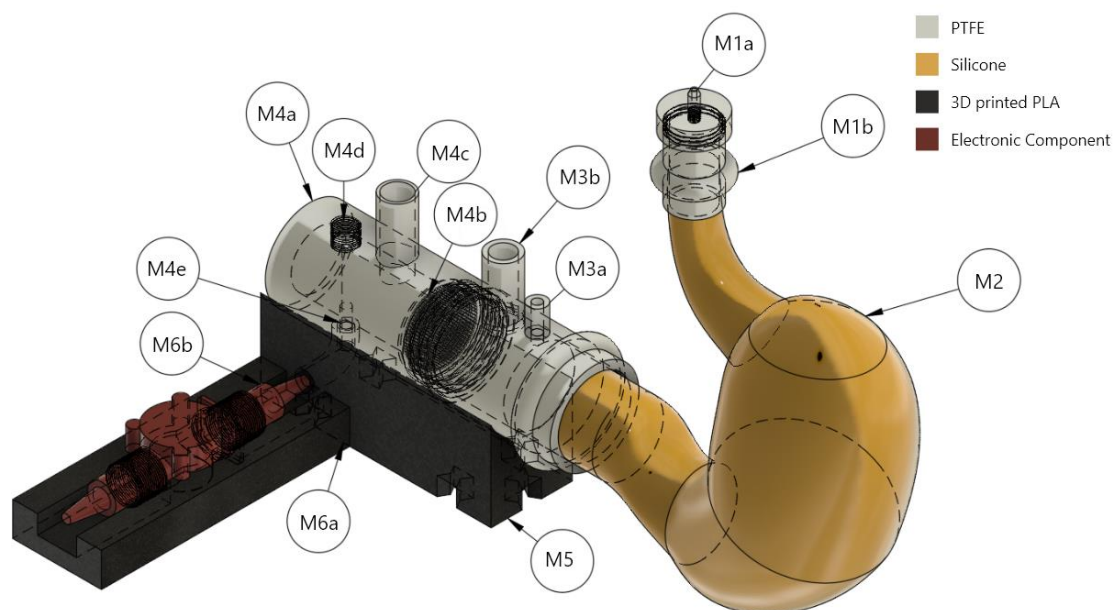


**Figure 5** – Illustrative representation of the RGM where: M1a – SGF and enzymes input; M1b – module 1 connection with module 2; M2 – module 2; M3a – acid/base input; M3b – pH electrode support; M4a – module 4; M4b – pylorus; M4c – Fibre optics support; M4d – level sensor; M4e – stomach emptying output; M5 – module 5; M6a - module 6; M6b – electrovalve.

Briefly, the module 1 corresponds to the sample, SGF and enzymes' input; the module 2 corresponds to the silicone gastric compartment; the module 3 corresponds to the pH electrode support; the module 4 corresponds to the pylorus and level sensor support; the module 5 corresponds to the modules 3 and 4 holder and the module 6 corresponds to the electrovalve support. The modules 1, 3 and 4 are made of polytetrafluoroethylene (PTFE) using an electric lathe; the module 2 is made of silicone since it is an elastic, deformable and inert material with high chemical resistance (Rahimi & Mashak, 2013) and its fabrication process is described in the topic 2.4; modules 5 and 6 are 3D printed components made of PLA using the conditions described in the topic 2.2.2. Furthermore, to perform the peristaltic contractions in the gastric compartment, 3 PBs were placed in the stomach in physiologically relevant locations reported by Ferrua & Singh (2012), with a contraction of 30, 40 and 80%, for PB1, PB2, and PB3, respectively, and their design and fabrication is described in the topic 2.3. The digestion temperature is kept at 37°C using a standard laboratory oven.

### 3.2.3 3D printing process

A Flashforge Dreamer 3D printer (Zhejiang Flashforge 3D Technology Co., Ltd, China) was used with a PLA filament as printing material. All computer-aid designs (CAD) were developed in Fusion360 (Education li-cence, Autodesk Inc., USA) and subsequently exported to a 3D printing compatible file format (.stl or .3mf). The Flashprint (version 4, Zhejiang Flashforge 3D Technology Co., Ltd, China) slicer was used to set the 3D printing conditions for PLA. This way, all PLA parts were 3D printed using the following conditions:

- Extruder printing temperature: 200 °C;
- Bed temperature: 50 °C;
- First layer height: 0.3 mm;
- Layer height: 0.3 mm;
- Base print speed: 80 mm/s;
- Travel speed: 100 mm/s;
- Shell count: 2;
- Fill density: 10%;
- Fill pattern: hexagon;
- Support type (when needed): linear.

### 3.2.4 PB development using an experimental design



Soft robotic actuators were used to simulate the peristaltic contractions of the human stomach and, for this purpose, pneumatic actuators developed by Mosadegh et al., (2013) were used and an example of a PB can be seen in Figure 2A. As such, several design decisions had to be made regarding the dimensions of the PBs, namely, regarding the lateral thickness (LT) of the walls, the top thickness (TT) of the air chambers, the chambers' width (W), height (H) and length (L), the space between chambers (S) and the number of chambers to be used (Figure 2B). Since the number of chambers to be used would be dependent on the total length of the PB at a given location on the gastric compartment, it was determined that the PB1, PB2 and PB3 would be composed by 21, 15 and 7 chambers between the PB extremities, respectively and an experimental design was made for each PB.

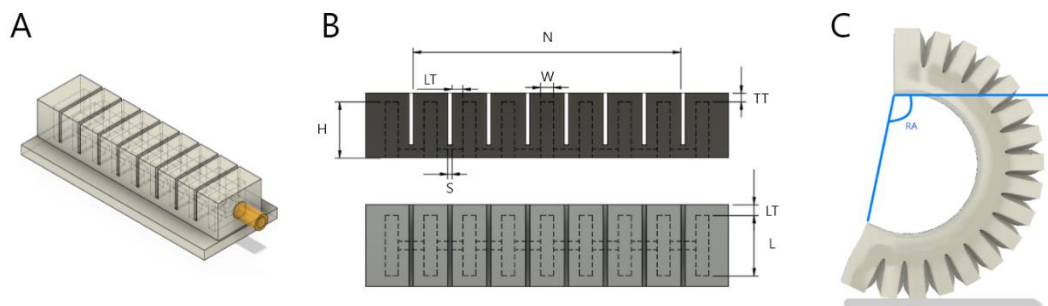


**Figure 6** – Illustrative representation of a PB3 (A), the design parameters used in the Plackett-Burman experimental design (B) and the representation of the rotation angle (C)

#### 3.2.4.1. Design parameters selection

A Plackett-Burman experimental design (Table 1), with 12 experiments and 1 central point, was used to select the most important design parameters using the PB rotation angle (RA) as dependent variable – Figure 6C. The selected parameters were further used in a central composite rotational design (CCRD) to obtain the optimization curve. The RA was obtained *in silico* through a FEA which is described below.

**Table 1** - Plackett-Burman experimental design with 12 experiments and 1 central point. All independent variable values are expressed in mm. The RA7, RA15, and RA21 correspond to the RA of the PB with 7, 15 and 21 inflation chambers, respectively which are expressed in degrees.

Experiment	LT	TT	L	W	H	S	RA7	RA15	RA21
1	4.00	1.00	16.00	2.00	10.00	0.50	11.25	21.93	12.20
2	4.00	3.00	12.00	4.00	10.00	0.50	11.02	40.95	14.20
3	1.00	3.00	16.00	2.00	16.00	0.50	27.79	116.69	63.70
4	4.00	1.00	16.00	4.00	10.00	1.50	24.05	16.74	14.90
5	4.00	3.00	12.00	4.00	16.00	0.50	10.60	18.49	9.70
6	4.00	3.00	16.00	2.00	16.00	1.50	11.10	71.81	26.70
7	1.00	3.00	16.00	4.00	10.00	1.50	53.90	122.65	72.50
8	1.00	1.00	16.00	4.00	16.00	0.50	51.50	180.00	151.10
9	1.00	1.00	12.00	4.00	16.00	1.50	72.70	84.27	46.20
10	4.00	1.00	12.00	2.00	16.00	1.50	15.30	31.00	17.30
11	1.00	3.00	12.00	2.00	10.00	1.50	32.60	83.76	47.40
12	1.00	1.00	12.00	2.00	10.00	0.50	28.50	95.97	88.80
13	2.50	2.00	14.00	3.00	13.00	1.00	20.50	61.74	35.10

#### 3.2.4.2. Finite element analysis of PB contraction

The FEA was made on ANSYS Workbench (2021 R2 version, Education licence, ANSYS Inc., USA) using a “Static structural analysis”. This way, several parameters were determined to simulate the contraction of the PB which includes the material modelling, meshing, defining the connections, boundaries, pressure, and solution which were determined according to Xavier et al., (2020) and Tawk & Alici, (2020), with some modifications.

##### 3.2.4.2.1. Material model

To obtain a realist behaviour of the PB in the *in silico* analysis, a stress-strain assay, based on ISO 37, was made to the silicone rubber using a double axis texture analyser from Stable Microsystems (Surrey, UK), with a load cell of 5 kg and a two grip setup (Stable Microsystems, Surrey, UK). Briefly, ten 3D printed moulds of the dumbbell geometry (Figure 7A) were made and filled with silicone.

The samples were then placed on the grips and stretched until rupture to obtain the correspondent stress-strain curve (Figure 7B).

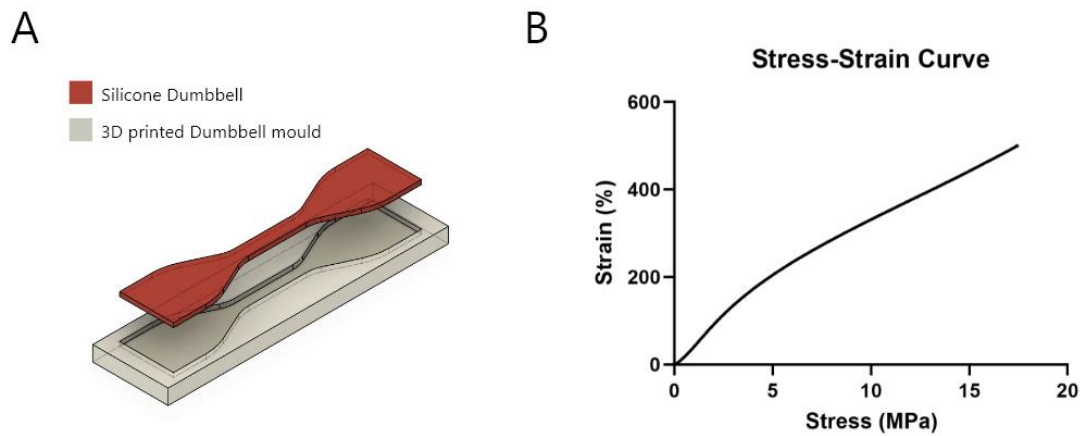


**Figure 7** - Silicone’s stress-strain curve (A) using the ISO 37 dumbbell (B).

At least six samples were prepared for the stress-strain curve and a boxplot (with a whisker coefficient of 0.5) was made to eliminate outlier samples. The average of the outlier free stress-strain curve was then loaded into Ansys Workbench and the Mooney-Rivlin 5 parameter model was used as material model since it presented the lowest calculated residuals (data not shown) when compared with other material models (i.e., Mooney-Rivlin 2, 3 and 9 Parameters, the Yeoh first, second, and third order models, and the Ogden first, second and third order models). The selected model coefficients can be seen in Table 2.

**Table 2** – Mooney-Rivlin 5 parameter model coefficients.

Material Model	Coefficients	Values
Mooney-Rivlin 5 parameter model	C10	-0.081 MPa
	C01	0.151 MPa
	C20	1.748E <sup>-07</sup> MPa
	C11	-2.344E <sup>-05</sup> MPa
	C02	0.024 MPa
	Incompressibility Parameter D1	0 MPa <sup>-1</sup>

#### 3.2.4.2.1.1. Mesh

To obtain convergence, a 3.5 mm “Mesh Size” was used since it is not recommended to use a very fine mesh for large deformations (Tawk & Alici, 2020; Xavier et al., 2020), with a “Nonlinear Mechanical Physics” preference and a “Quadratic Element Order”. Furthermore, a 3.5 mesh size showed to be appropriate for all designs since it was compatible with the Ansys education licence’s limit of 32000 nodes.

#### 3.2.4.2.1.2. Contacts

To detect the contact between two faces upon deflation, several frictional contact pairs were defined (Figure 8) with a “Symmetric” behaviour, to minimize penetration, and an “Augmented Lagrange” formulation (Tawk & Alici, 2020).

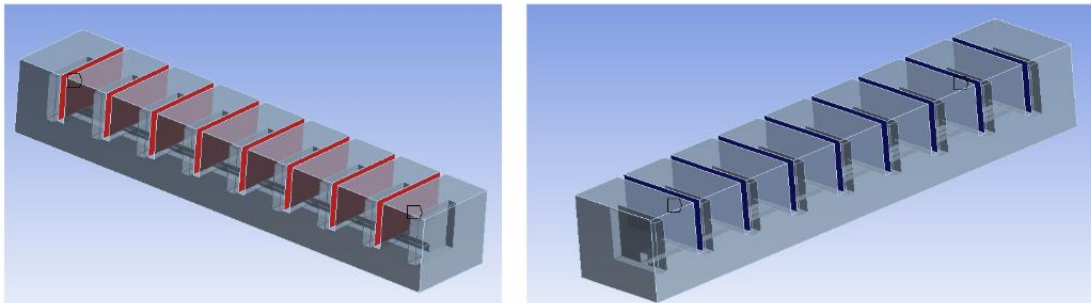


Figure 8 – FEA contacts in the PB.

#### 3.2.4.2.1.3. Analysis Settings

The “Large Deflection” option is turned on and a fixed number of “Substeps” was set to 20 so that the pressure could be gradually applied; with “Auto Time Stepping” on, an “Initial Time Step” of 0.001 s, a “Minimum Time Step” of 0.001 seconds and a “Maximum Time Step” of 0.05 seconds. Additionally, a “Fixed Support” boundary was added to one of the extremities of the PB and a “Pressure” of 5 kPa (i.e., at the 20th substep) was applied to the inner chambers of the PB.

### 3.2.5 Silicone casting moulding – A step by step guide

#### 3.2.5.1. Gastric compartment’s production process

The moulds were 3D printed using the equipment and configurations described on topic 3.2.3. The outer part (Figure 9A-1) and the inner part of the mould (Figure 9A-2) were divided into four different pieces represented by Figure 9A-3, Figure 9A-4, Figure 9A-5, Figure 9A-6 and Figure 9A-7, Figure 9A-8, Figure 9A-9, Figure 9A-10, respectively, due to the dimensions of the 3D printing platform. This way, after 3D printing the pieces, the left pieces (Figure 9A-3 and Figure 9A-6) and

the right pieces (Figure 9A-4 and Figure 9A-5) of the outer part of the mould were glued together. The same procedure was made to the inner part of the mould (left: Figure 9A-7 and Figure 9A-9; right: Figure 9A-8 and Figure 9A-10). Liquid silicone (Figure 9B-11) was then prepared according to the supplier (100:5 ratio between the liquid silicone and the polymerizing agent) and poured in the outer part of the mould. The liquid silicone was then spread using the inner part of the mould (Figure 9C) and dried at 50 °C for 4h, which resulted in a polymerized silicone rubber represented by Figure 9D-12. The same procedure was repeated for the other half of the stomach. Both silicone stomach halves were then connected using more liquid silicone (Figure 9E) and assembled into the module 1 and 3 of the RGM (Figure 9G).

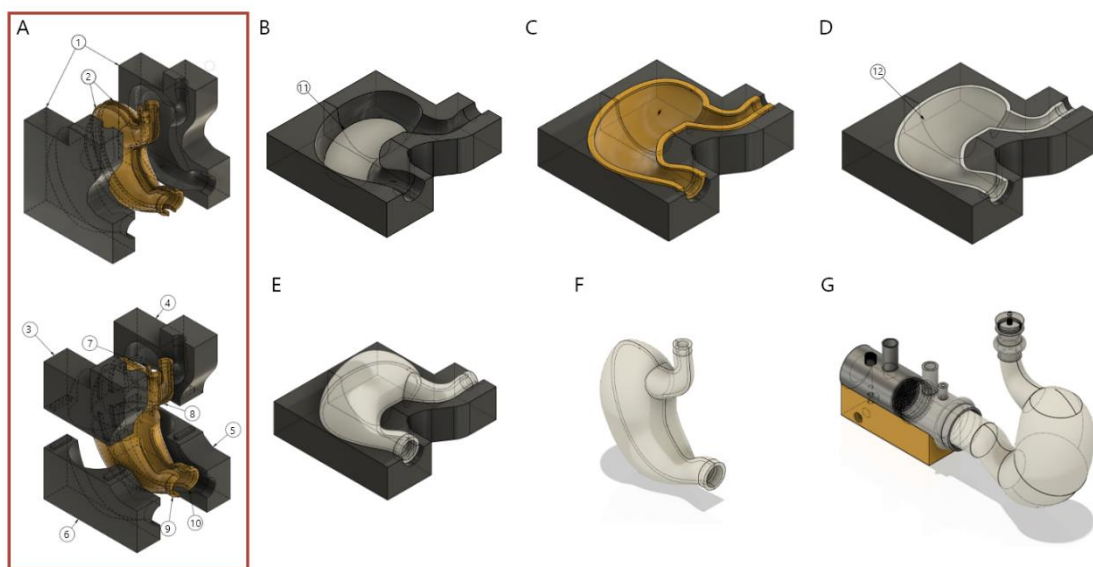


**Figure 9** – Illustrative representation of the gastric compartment production where A and B correspond to the silicone mould inner and outer parts in a connected and divided view, respectively, and C, D, E, F, G and H correspond to the steps required to produce a gastric model. Furthermore, the numbers in the illustration represent: 1 – outer parts of the mould; 2- inner parts of the mould; 3 – top left part of the outer mould; 4 - top right part of the outer mould; 5 - bottom right part of the outer mould; 6 - bottom left part of the outer mould; 7 – top left part of the inner mould; 8 - top right part of the inner mould; 9 - bottom left part of the inner mould; 10 – bottom right part of the inner mould; 11 – liquid silicone; 12 – cured silicone.

#### 3.2.5.2.PBs' production process

The design of the PBs was based on the pneumatic actuators developed by Mosadegh et al., (2013) and a step-by-step guide can be found on the “SoftRoboticsToolKit” website developed by the

“Harvard Biodesign Lab” group. Briefly, three PBs were produced with an N of 7, 15, and 21. The moulds (Figure 10A) were designed according to the specifications obtained in the ED and subsequently 3D printed using the conditions specified in the topic 3.2.3. The inflation chambers’ mould is assembled by connecting the top (Figure 10A-1) and bottom (Figure 10A-2) part and subsequently filled with liquid silicone (Figure 10B-4). Half of the strain limiting layer mould is also filled with liquid silicone and a piece of paper is placed on top of the liquid silicone; the parts are then dried at 50 °C for 4h. The top part of the inflation chambers’ mould is then removed, and the rest of the liquid silicone is poured on the strain limiting layer mould (Figure 10C). The inflation chambers are then carefully placed, so that the chambers’ air channels are not obstructed, on top of the liquid silicone (Figure 10D). The PB is demoulded (Figure 10E), a 5 mm hole is made on one of the extremities of the PB and a silicone tube is placed and fixed with more liquid silicone (Figure 10F).

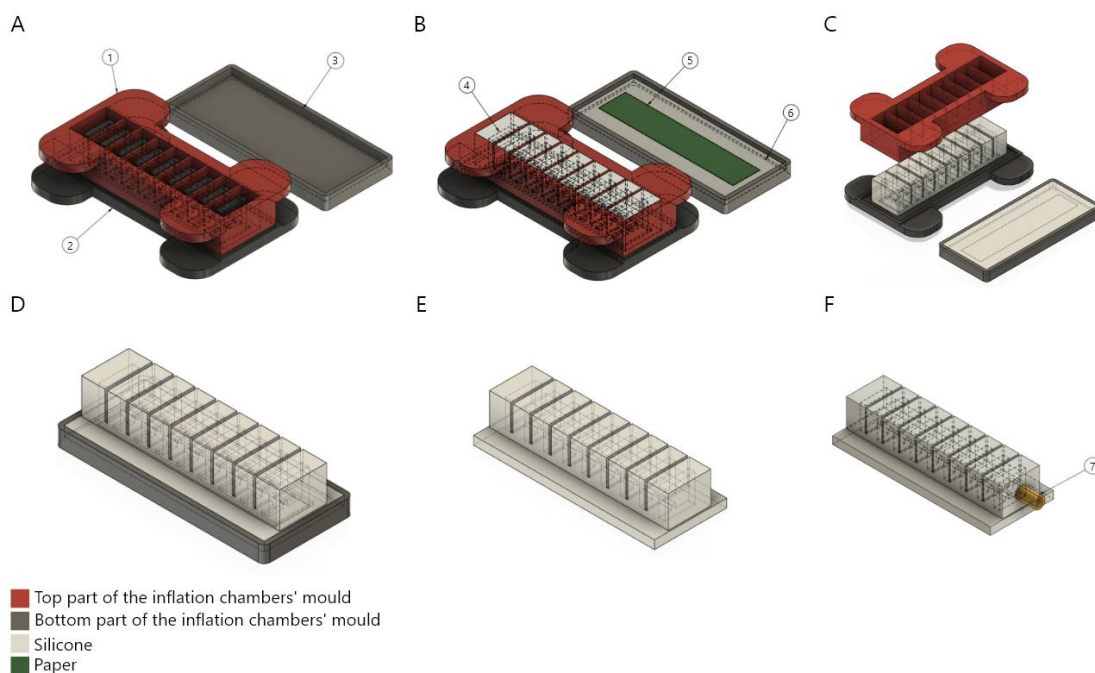


**Figure 10** – Step-by-step illustration of the PB production process where: 1 – top part of the inflation chambers; 2 – bottom part of the inflation chambers; 3 - strain limiting layer mould; 4 – inflation chambers’ mould filled with liquid silicone; 5 – paper sheet; 6 – half of the strain limiting layer mould filled with liquid silicone; 7 – silicone tube

### 3.2.6 Control system design – An IoT approach

#### 3.2.6.1. User interface and user flow

To control the gastric peristalsis, stomach emptying, electrolyte and enzyme solution pumping rates and gastric pH, a web application was created to provide a user interface since it is compatible with all operating systems (OS) without the need to develop OS specific software. The web application communicates with a backend server which serves as a common application programming interface (API) to establish a connection between all sensor data, obtained through sensors connected to a raspberry pi, and the user – an internet of things approach.

**Table 3** – Project registration fields and their respective description. It is important to refer that these fields can be subject to change in the future.

Field	Description
<b>Project Metadata</b>	
Project Type	Possible values: International Standardized Protocol; Automatic; Manual
Title	The project title that will be displayed in the respective project page.
Sample	The sample that will be digested
Sample Type	Possible values: Other system; Controlled Release System; Food Product
Public Project	Choose whether you make your projects' data public or private
<b>Protocol Settings</b>	
Digestion Time <sup>a</sup>	Default: 120 min.
Dry Weight	The sample dry weight (%)
Peristaltic Frequency	Choose the number of contractions per minute: between 3 and 5 contraction per minute.
Food Volume <sup>a</sup>	The amount of sample (mL) that is used in the digestion protocol
Lipid Content <sup>a</sup>	The lipidic content of the sample
Protein Content <sup>a</sup>	The protein content of the sample
Carbohydrate Content <sup>a</sup>	The carbohydrate content of the sample
SGF Rate <sup>a,b</sup>	The electrolyte solution flow (mL/min)
<b>Stomach Emptying Settings</b>	
Stomach Emptying Mode	Possible values: Automatic; Temporized; Manual
Stomach Emptying Time Steps	Number of gastric emptying procedures to be done during the digestion (this option is disabled if the "Gastric Emptying Mode" is "Manual")
Stomach Emptying Volume	The amount (mL) of digesta to be emptied from the stomach
<b>Enzymes' Settings</b>	
Enzymes' Rate <sup>a</sup>	The enzyme solution flow (mL/min)
Lot Number	The respective enzyme lot number
Activity	The respective enzyme activity
Enzyme Solution in Water	The respective enzyme volume (mL)
Ci	The amylase stock solution concentration (mg/mL). This option is only enabled for amylase
<b>pH Settings</b>	
Initial pH	The initial sample pH. Default: 7
pH Delay	The delay time (s) for the microcontroller to start monitoring the pH changes

Pumping Time	The time (s) for the peristaltic pump to be on to control the gastric pH
pH Curve	A pH curve that can be adjusted manually. Based on the pH curve reported by Mans Minekus et al., (1995)

<sup>s</sup> - This parameter will be requested or automatically calculated if the project type is "International Standardized Protocol", <sup>^</sup>- This parameter will be automatically calculated if the project type is "Automatic".

This information described in Table 3 is requested to determine certain digestion parameters (e.g., digestion time, peristaltic pumps flow, etc) as well as some control settings (e.g., pH curve delay and pumping time to adjust the pH). The user can then perform a new experiment where it is possible to manually control all the peristaltic pumps (i.e., to fill the silicone tubing with the respective fluids), calibrate the pH sensor and monitor the pH and temperature during the digestion process as well as control the digestion timer. All data regarding the experiment (i.e., temperature and pH over time) is saved in an external database at the end of the digestion process, which may be consulted and exported on the project's page.

### 3.2.6.2. System control modules

The RGM control system is composed by four distinct modules (Figure 11): the raspberry pi module; the relay module; the peristaltic contraction module; the pH module. The raspberry pi module is the main component as it is responsible for sensor data acquisition and controlling the peristaltic pumps. This way, it is composed by a raspberry pi and an analogue to digital convertor (ADS1115). The relay module is responsible for controlling the stomach emptying, enzymes and electrolytes' peristaltic pumps and stomach emptying electrovalve. As the name implies, it is composed by a four-channel relay module that controls three 12V peristaltic pumps and a 12V electrovalve. The peristaltic contractions' module is responsible for controlling the inflation and emptying of the PB air chambers. For this purpose, it is composed by a 2-channel relay module that controls a 6V air pump and a 5V electrovalve. This module also encompasses an MPX4250 pressure sensor so that the inner pressure of the PB air chambers can be measured and used to control their behaviour. The pH module is responsible for controlling the pH throughout the gastric digestion process. It is composed by a BNC connector module (Figure 11 pH Meter), two peristaltic pumps to inject HCl or NaOH into the gastric compartment and a 2-channel relay module to control the pumps. All modules are connected to the raspberry pi module which communicates with a backend server via WebSocket so that a two-way communication can be established between the raspberry pi and the backend server. This type of communication allows the raspberry pi to send sensor data or notifications without the need of receiving a request from the client (i.e., user).



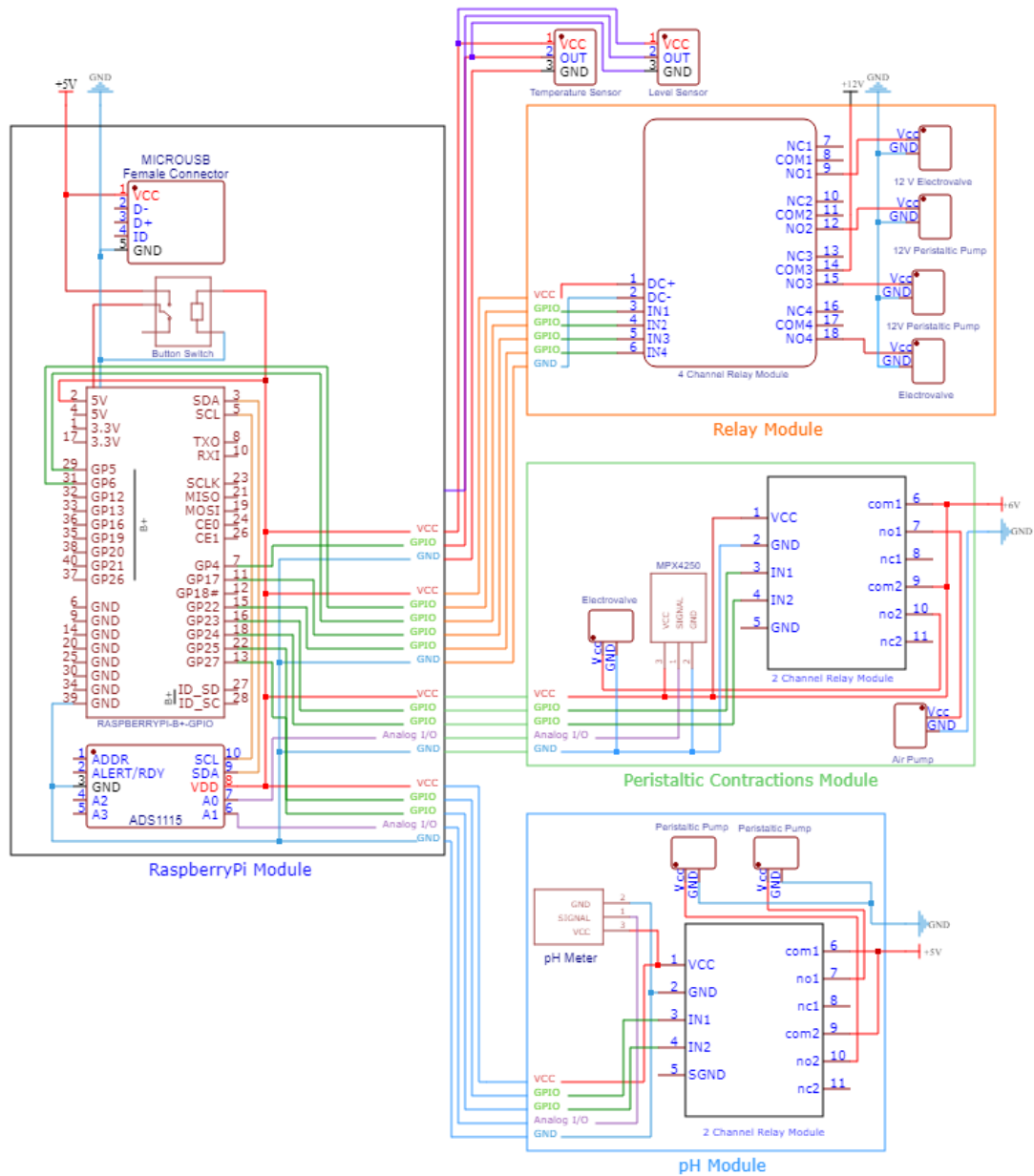


**Figure 11** – System control modules' schematics.

### 3.2.6.3. Stomach emptying control

The stomach emptying can be controlled using three different methods: an automatic method where the stomach emptying will occur when the gastric digesta reaches the level sensor; a temporized method where the stomach emptying will occur periodically based on the “Stomach Emptying Time Steps” calculated (if the project type is the “International Standardized Protocol”) or provided by the user; a manual method where the user decides when to perform a stomach emptying.

### 3.2.6.4. Gastric pH control

During the digestion process, the pH control algorithm is responsible for: checking the desired pH value based on the pH curve and updating the desired pH value depending on the digestion time; adjusting the pH value according to the desired pH; verifying if the pH read is stable. This way, the gastric pH is controlled by injecting 1M HCl or 1M NaOH into the gastric compartment depending on the target pH at a given time. The volume of HCl or NaOH will depend on the “Pumping Time” specified by the user, under the pH settings of the project registration form, and the difference between the target pH value and the actual pH read. This way, the pumping time is determined by the following equation:

$$Pumping\ time\ (s) = \frac{pH_{target} - pH_{read}}{MaxDiff} * Max\ Pumping\ Time \quad (13)$$

The MaxDiff corresponds to the maximum difference between the target and actual pH read which was set to 2, and the Max Pumping Time corresponds to the “Pumping Time” specified by the user. The pH read is obtained by converting the analog signal received from the BNC module into a pH value (i.e., calibration). For this purpose, 20 measurements are taken, and the average analog read is used for conversion. To convert the analog values into pH, the pH meter is calibrated using a standard 4.03 and 7.09 pH solution. The respective analog values are saved into a configuration file and a linear regression is made to determine all pH values. This way, it is important to obtain a stable read prior to saving the corresponding analog values. The algorithm determines the stability of the measurement by analysing the standard deviation of the 20 analog reads. To determine the threshold value of the standard deviation of a stable read, ten measurements were taken (i.e., ten measurements of 20 analog reads) after inducing a pH change (Figure 12).

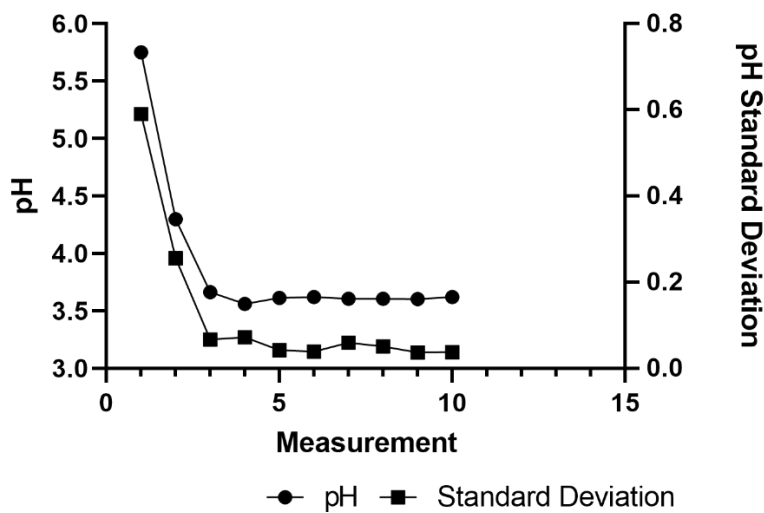


**Figure 12** – pH and pH standard deviation over ten measurements to determine the standard deviation of a stable pH read.

It is possible to observe, from the analysis of Figure 12, that a stable read is obtained from the third measurement which corresponds to a standard deviation of ca. 0.07 (from measurement 3 through 10). This way, a standard deviation of 0.07 was considered an appropriate threshold for a stable pH read and this value was further used in future reads.

#### 3.2.6.5. Peristaltic pump flow measurement

All peristaltic pumps used in the RGM were characterized in terms of their pumping rate. For this purpose, 100 mL of water were emptied using the peristaltic pump and the emptying time was recorded to calculate the emptying rate of the peristaltic pump. The experiment was performed ten times for each pump and the average pumping rate was used to convert liquid volume into pumping time which is represented in Table 4.

**Table 4** – Peristaltic pumps' pumping rate characterization.

	PP1	PP2	PP3
<b>Pumping rate (mL/min)</b>	108.33 ± 1.15	234.97 ± 2.77	293.80 ± 5.74

#### 3.2.7 Hydrodynamic characterization of the RGM

A hydrodynamic characterization of the RGM was made to unravel the gastric geometry influence on the mixing behaviour and particle transportation of the stomach and, consequently, its influence on the digestion of food. For this purpose, 500 mL of distilled water were placed inside the RGM and maintained at 37 °C to mimic the physiological temperature of the Human gastrointestinal tract. Furthermore, 1 mL of food colouring (i.e., tracer, purchased at the local supermarket) was injected into the RGM input module, and a peristaltic pump (120U/DV 200rpm pump, Watson-Marlow Pumps, Falmouth, Cornwall United Kingdom) was used to perform the gastric emptying at a fixed flow rate. The predetermined volumetric flow rates were calculated according to 4 different types of dairy products which are represented in Table 5.

**Table 5** – Stomach emptying flow rates used for the hydrodynamic characterization the RGM. The portion and nutritional values are examples of commercially available dairy products and were obtained from the respective producer. The stomach emptying (i.e., volumetric flow rate) were calculated based on the semi-dynamic *in vitro* digestion standard protocol developed by Mulet-Cabero et al. (2020).

	<b>Yogurt</b>	<b>Milk</b>	<b>Fermented milk</b>	<b>Cheese</b>
Portion (g)	125	250	160	50
Proteins (%)	2.70	3.60	2.30	22.50
Lipids (%)	1.80	1.60	1.60	24.50
Carbohydrates (%)	3.40	4.90	11.00	2.10
<b>Volumetric flow rate (mL/min)</b>	<b>10.64</b>	<b>9.27</b>	<b>6.80</b>	<b>1.88</b>

The concentration of food colouring was determined, in real-time, by a fibre optics (T300-RT-VIS/NIR, Oceanoptics, Orlando, USA) UV-VIS-SWNIR spectrophotometer (AvaSpec-2048-DT-4, 2048-pixel, 200-1100 nm) coupled with a halogen light source (AvaLight-Hal LS-0308016, 360-2500nm, Avantes, Apeldoorn, the Netherlands). All spectra were acquired every 30 seconds for 30 minutes using the AvaSoft 7.5.3 software by averaging 30 spectra on each acquisition. At least six experiments were made for each volumetric flow rate and the average residence time distribution (RTD) was determined using the following equations:

$$C_{total} = \int_0^{\infty} c(t) \cdot \Delta t \quad (14)$$

$$E(t) = \frac{C(t)}{C_{total}} \quad (15)$$

$$RTD_{avg} = \int_0^t E(t) \cdot \Delta t \quad (16)$$

It is important to notice some important factors such as viscosity were not considered during this assay and must be considered in future assessments. The food products listed in Table 5 were merely used to obtain different emptying rates according to the standardized semi-dynamic *in vitro* digestion model (Mulet-Cabero et al., 2020).

### 3.2.8 Statistical Analysis

All statistical analyses applied to experimental data were performed using Origin (2018, OriginLab Corporation, Massachusetts, USA). The statistical significance (at  $p \leq 0.05$ ) was determined using one-way ANOVA followed by post hoc. Tukey's tests with at least triplicate samples, unless it is mentioned on the respective section otherwise. The Plackett-Burman and CCRD experimental design tables and results were obtained in Protimiza Experiment Design Software (<http://experimental-design.protimiza.com.br>)

### 3.3 RESULTS AND DISCUSSION

#### 3.3.1 PB modulation using an experimental design

##### 3.3.1.1. Variable selection using a Plackett-Burman experimental design

A Plackett-Burman experimental design was performed to identify the most significant independent variables in terms of their impact on the RA of the PB and the results are shown in Table 6.

**Table 6** – Plackett-Burman experimental design results with a 5% significance level.

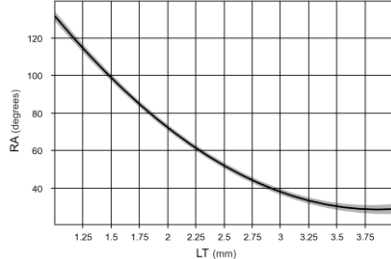
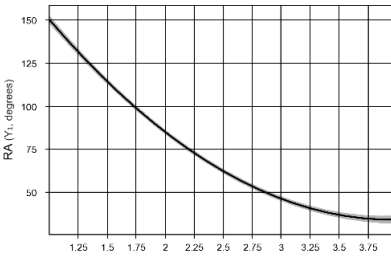
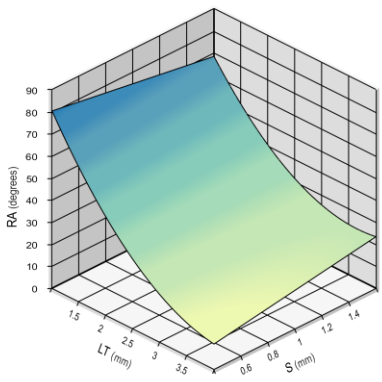
Independent Variable	<i>p</i> -value of PB7	<i>p</i> -value of PB15	<i>p</i> -value of PB21
LT	<b>0.0005</b>	<b>0.0054</b>	<b>0.0137</b>
TT	0.0618	0.8218	0.3825
W	0.7207	0.1496	0.2956
L	<b>0.0090</b>	0.7009	0.6241
H	0.2916	0.2959	0.5485
S	<b>0.0323</b>	0.5630	0.3060

**Note:** Variables with a *p*-value  $\leq 0.05$  are significantly important and are highlighted in bold.

It is possible to observe from the analysis of Table 6 that, depending on the number of inflation chambers (N), different parameters were identified as being significantly important regarding their impact on the RA. For instance, for the PB3, the LT, L and S significantly impact the RA of the PB ( $p$ -value  $\leq 0.05$ ); for the PB2 and PB1, the LT significantly impacts the RA of the PB ( $p$ -value  $\leq 0.05$ ). This indicates that PBs with a higher number of inflation chambers are only affected by the LT of the chambers since N tends to nullify the effects of other variables. Nevertheless, the selected variables were subsequently used in a CCRD experimental design with a significance level of 5%, to mathematically modulate the RA of the PB with the selected variables and the experimental design conditions are shown in Table 7 with the respective equations. The equation's coefficients

that were not statistically significant ( $p\text{-value} > 0.05$ ) were removed from the equations and the obtained curves are shown in Table 7 with their respective models and correlation coefficients.

**Table 7** – CCRD experimental design experiments using the selected independent variables.

Experiment	LT	W	S	L	H	TT	RA	Modulation
<b>PB1</b>								
1	1.24	3.00	1.00	14.00	13.00	2.00	<b>113.70</b>	 $RA_{PB1} = 51.72 - 43.07 LT + 19.92 LT^2$ $(r^2 = 0.9994)$
2	3.76	3.00	1.00	14.00	13.00	2.00	<b>30.00</b>	
3	1.00	3.00	1.00	14.00	13.00	2.00	<b>132.00</b>	
4	4.00	3.00	1.00	14.00	13.00	2.00	<b>27.50</b>	
5	2.50	3.00	1.00	14.00	13.00	2.00	<b>51.60</b>	
<b>PB2</b>								
1	1.24	3.00	1.00	14.00	13.00	2.00	<b>131.20</b>	 $RA_{PB2} = 62.02 - 48.58 LT + 21.05 LT^2$ $(r^2 = 0.9996)$
2	3.76	3.00	1.00	14.00	13.00	2.00	<b>36.00</b>	
3	1.00	3.00	1.00	14.00	13.00	2.00	<b>150.00</b>	
4	4.00	3.00	1.00	14.00	13.00	2.00	<b>32.80</b>	
5	2.50	3.00	1.00	14.00	13.00	2.00	<b>61.70</b>	
<b>PB3</b>								
1	1.61	2.40	0.70	14.00	13.00	2.00	<b>54.30</b>	 $RA_{PB3} = 31.29 - 16.92 LT + 5.14 LT^2 + 1.77 LT S$ $(r^2 = 0.9929)$
2	3.39	2.40	0.70	14.00	13.00	2.00	<b>16.20</b>	
3	1.61	3.60	0.70	14.00	13.00	2.00	<b>55.20</b>	
4	3.39	3.60	0.70	14.00	13.00	2.00	<b>20.50</b>	
5	1.61	2.40	1.30	14.00	13.00	2.00	<b>50.30</b>	
6	3.39	2.40	1.30	14.00	13.00	2.00	<b>21.40</b>	
7	1.61	3.60	1.30	14.00	13.00	2.00	<b>50.70</b>	
8	3.39	3.60	1.30	14.00	13.00	2.00	<b>21.00</b>	
9	1.00	3.00	1.00	14.00	13.00	2.00	<b>75.80</b>	
10	4.00	3.00	1.00	14.00	13.00	2.00	<b>16.50</b>	
11	2.50	1.99	1.00	14.00	13.00	2.00	<b>30.30</b>	
12	2.50	4.01	1.00	14.00	13.00	2.00	<b>30.40</b>	
13	2.50	3.00	0.50	14.00	13.00	2.00	<b>34.80</b>	
14	2.50	3.00	1.50	14.00	13.00	2.00	<b>31.10</b>	
15	2.50	3.00	1.00	14.00	13.00	2.00	<b>31.00</b>	

It is possible to observe, from the results obtained in the experimental design, that the mathematical models for the PB1, PB2 and PB3 have a correlation coefficient of ca. 0.9994, 0.9939, 0.9929, respectively, which makes these models appropriate to predict the RA of a PB given its design parameters. However, the equations can also be used to determine the design parameters of the PB given a desired RA and this was the approach used in this study since the different PBs have different contraction amplitudes due to their location in the gastric compartment. This way, an LT of 3.61, 3.29 and 0.86 mm must be used for a RA of 30, 40 and 80% for the PB1, PB2 and PB3, respectively, considering that the PB3 “s” parameter was set to 0 (i.e., an “s” of 1 mm).

### 3.3.2 RGM characterization

#### 3.3.2.1. pH kinetics profile

A pH kinetics profile assessment was made to characterize the RGM in terms of pH control. For this purpose, the gastric pH was monitored and accordingly adjusted to the correspondent pH at a given time, taking into consideration the pH curve reported by Mans Minekus et al., (1995). The results are depicted in Figure 13.

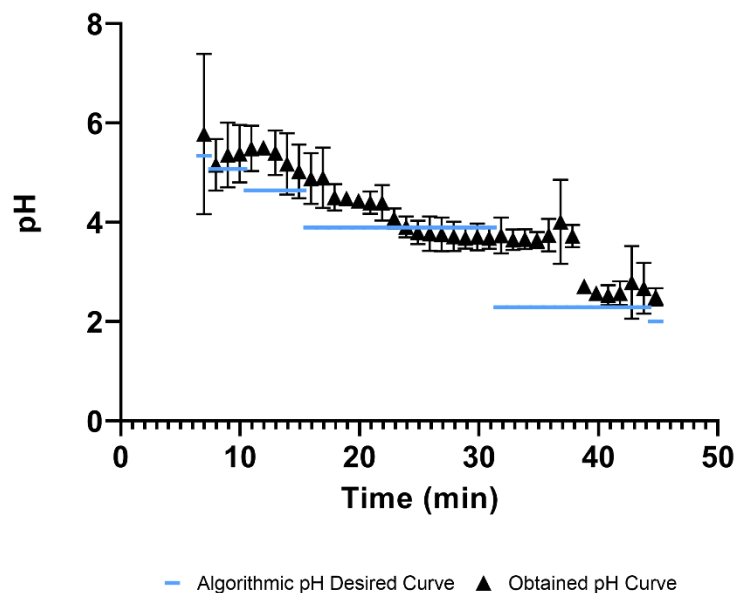


**Figure 13** – Gastric pH kinetics control characterization.

It is possible to observe from Figure 13 that the pH curve obtained experimentally follows the same trend and behavior of the intended algorithmic pH curve. Furthermore, the correlation between both curves is ca. 0.73 which indicates a relatively high correlation. It is important to notice that

the slow mixing of the gastric compartment can significantly influence the homogenization of the pH inside the *in vitro* RGM which explains the relatively high standard deviation among experiments. To further investigate the mixing properties of the RGM, a hydrodynamic characterization was made.

### 3.3.2.2. RTD assessment

The RTD of the particles inside the *in vitro* RGM was evaluated to understand the hydrodynamic characteristics of the stomach. The experiments were made without peristalsis to only characterize the geometry of the stomach and understand its impact on the mixing and transportation of particles. For instance, by using this approach it is possible to identify the presence of dead zones inside the stomach as well as by passing (i.e., particles with very low residence time). Therefore, this approach was used using different volumetric flow rates (i.e., stomach emptying rates) and results are depicted in Figure 14.

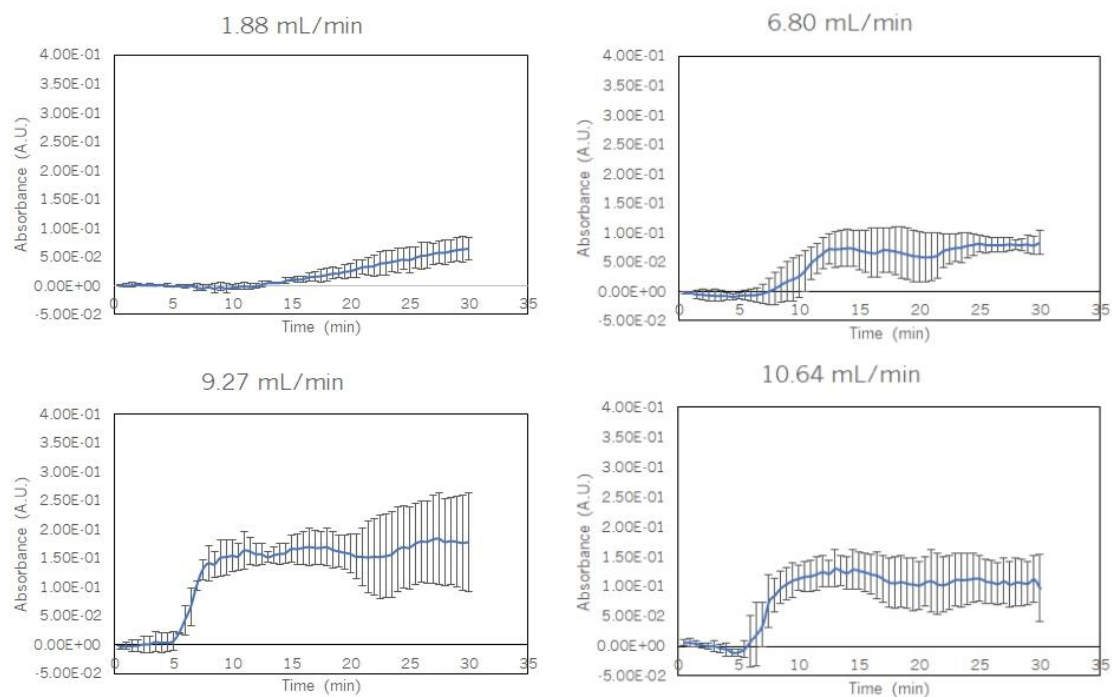


**Figure 14** – Response of the stomach to a tracer injection at different volumetric flow rates.

It is possible to observe from Figure 14 that the geometry of the stomach itself promotes high variability in the dispersion and transportation of the tracer particles (i.e., high standard deviation of the curves). Except for the 1.88 mL/min flow rate, all other experiments showed a similar curve shape and as expected, particles at higher flow rates reach the fibre optics' sensor faster. Furthermore, the oscillations in the curve plateau may be indicative of the existence of dead zones



since the tracer is being gradually and heterogeneously released over time which promotes a sinusoidal behaviour in the plateau of the curve. In fact, this study indicates that the stomach “J” shape has a significant impact towards the tracer dispersibility, probably due to its accumulation in the stomach antrum. However, this is only speculative and more assays should be done, namely, by aping the inside of the stomach regions in terms of tracer concentration. The average particles’ residence time was also calculated, and the results are represented in Figure 15.

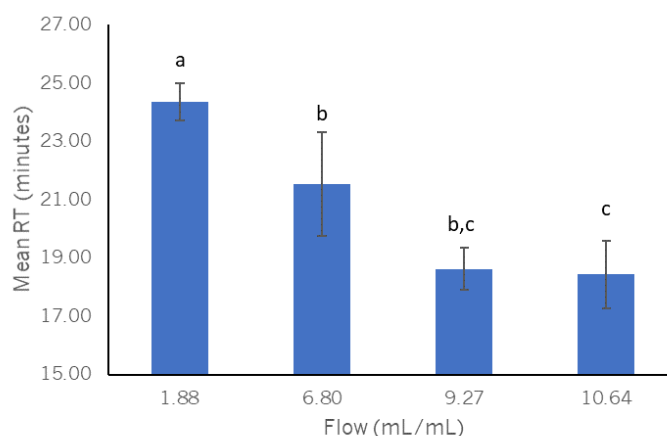


**Figure 15** – Average residence time of particles inside the stomach at different flow rates. Note: columns with the same letter are not statistically different from each other ( $p\text{-value} > 0.05$ )

It is possible to observe from Figure 15 that, despite the high variability of the dispersion assays, this variability was not translated into the average residence time of the particles and statistically significant differences ( $p\text{-value} \leq 0.05$ ) were identified. Namely, it is possible to conclude that higher flow rates resulted in lower particles’ residence time which makes sense since each particle travels at a higher velocity and thus spending less time inside the stomach. This behaviour is in fact indicative that liquid dispersion samples (i.e., faster stomach emptying) will spend less time in the stomach than solid samples which will consequently influence their interaction with enzymes and, therefore, their digestion.

### 3.4 CONCLUSIONS

The results obtained in this study represent a potential guideline towards the development of a standardized dynamic *in vitro* gastric model due to its interlaboratory reproducibility. Furthermore, the Plackett-Burman experimental design shows that the RA of PBs with higher N are more prone

to the effect of the LT of the inflation chambers. The RA of PB1 and PB2 is mainly affected by the LT of the inflation chambers while the RA of PB3 is affected by the LT, and S. These parameters were subsequently used in the DCCR experimental design. The equations obtained from the CCRD were further applied to determine each design parameter of the respective PB, depending on its location in the stomach. This way, an LT of 3.61, 3.29 and 0.86 mm was determined so that the PB1, PB2 and PB3 have an RA of 30, 40 and 80%, respectively. Furthermore, the RGM model showed to adapt and control the pH through the digestion process using a stability threshold of 0.7. However, some variability was observed probably due to the mixing properties of the RGM. In fact, the hydrodynamic characterization of the RGM also gave important insights regarding the model variability, showing that the anatomical geometry of the stomach itself is a probable cause of the RGM variability. This characterization also showed that higher stomach emptying flow rates will lower the residence time of the food samples and consequently their contact with enzymes which will change its digestion kinetics. Despite the developments of this study, much work needs to be done towards the RGM characterization and performance assessment. It is of utmost importance assessing the RGM performance in digesting food products, i.e., either liquid, semi-solid or solid foods which will be the focus of the next chapter.

### 3.5 REFERENCES

- Brodkorb, A., Egger, L., Alminger, M., Alvito, P., Assunção, R., Ballance, S., Bohn, T., Bourlieu-Lacanal, C., Boutrou, R., Carrière, F., Clemente, A., Corredig, M., Dupont, D., Dufour, C., Edwards, C., Golding, M., Karakaya, S., Kirkhus, B., Le Feunteun, S., ... Recio, I. (2019). INFOGEST static *in vitro* simulation of gastrointestinal food digestion. *Nature Protocols*, 14(4), 991–1014. <https://doi.org/10.1038/s41596-018-0119-1>
- Dang, Y., Liu, Y., Hashem, R., Bhattacharya, D., Allen, J., Stommel, M., Cheng, L. K., & Xu, W. (2020). SoGut: A Soft Robotic Gastric Simulator. *Soft Robotics*. <https://doi.org/10.1089/soro.2019.0136>
- Ferrua, M. J., & Singh, R. P. (2012). Understanding the fluid dynamics of gastric digestion using computational modeling. *Procedia Food Science*, 1, 1465–1472. <https://doi.org/10.1016/j.profoo.2011.09.217>
- Guo, Z., Cao, X., DeLoid, G. M., Sampathkumar, K., Ng, K. W., Loo, S. C. J., & Demokritou, P. (2020). Physicochemical and Morphological Transformations of Chitosan Nanoparticles across the Gastrointestinal Tract and Cellular Toxicity in an *In vitro* Model of the Small Intestinal Epithelium. *Journal of Agricultural and Food Chemistry*, 68(1), 358–368. <https://doi.org/10.1021/acs.jafc.9b05506>

Li, Y., Fortner, L., & Kong, F. (2019). Development of a Gastric Simulation Model (GSM) incorporating gastric geometry and peristalsis for food digestion study. *Food Research International*, 125(March), 108598. <https://doi.org/10.1016/j.foodres.2019.108598>

Liu, W., Fu, D., Zhang, X., Chai, J., Tian, S., & Han, J. (2019). Development and validation of a new artificial gastric digestive system. *Food Research International*, 122. <https://doi.org/10.1016/j.foodres.2019.04.015>

Madalena, D. A., Pereira, R. N., Vicente, A. A., & Ramos, Ó. L. (2019). New Insights on Bio-Based Micro- and Nanosystems in Food. In *Encyclopedia of Food Chemistry* (pp. 708–714). Elsevier. <https://doi.org/10.1016/B978-0-08-100596-5.21859-3>

Minekus, M., Alminger, M., Alvito, P., Ballance, S., Bohn, T., Bourlieu, C., Carrière, F., Boutrou, R., Corredig, M., Dupont, D., Dufour, C., Egger, L., Golding, M., Karakaya, S., Kirkhus, B., Le Feunteun, S., Lesmes, U., Macierzanka, A., Mackie, A., ... Brodkorb, A. (2014). A standardised static *in vitro* digestion method suitable for food – an international consensus. *Food Funct.*, 5(6), 1113–1124. <https://doi.org/10.1039/C3FO60702J>

Minekus, Mans, Marteau, P., Havenaar, R., & Veld, J. H. J. H. in't. (1995). A Multicompartmental Dynamic Computer-controlled Model Simulating the Stomach and Small Intestine. *Alternatives to Laboratory Animals*, 23(2), 197–209. <https://doi.org/10.1177/026119299502300205>

Mosadegh, B., Polygerinos, P., Keplinger, C., Wennstedt, S., Shepherd, R. F., Gupta, U., Shim, J., Bertoldi, K., Walsh, C. J., & Whitesides, G. M. (2013). Pneumatic Networks for Soft Robotics that Actuate Rapidly. *Advanced Functional Materials*. <http://onlinelibrary.wiley.com/doi/10.1002/adfm.201303288/full>

Mulet-Cabero, A.-I., Egger, L., Portmann, R., Ménard, O., Marze, S., Minekus, M., Le Feunteun, S., Sarkar, A., Grundy, M. M.-L., Carrière, F., Golding, M., Dupont, D., Recio, I., Brodkorb, A., & Mackie, A. (2020). A standardised semi-dynamic *in vitro* digestion method suitable for food – an international consensus. *Food Funct.* <https://doi.org/10.1039/C9FO01293A>

Pinheiro, A. C., Gonçalves, R. F., Madalena, D. A., & Vicente, A. A. (2017). Towards the understanding of the behavior of bio-based nanostructures during *in vitro* digestion. *Current Opinion in Food Science*, 15, 79–86. <https://doi.org/10.1016/J.COFS.2017.06.005>

Rahimi, A., & Mashak, A. (2013). Review on rubbers in medicine: natural, silicone and polyurethane rubbers. *Plastics, Rubber and Composites*, 42(6), 223–230. <https://doi.org/10.1179/1743289811y.0000000063>

Sadati Behbahani, E., Ghaedi, M., Abbaspour, M., Rostamizadeh, K., & Dashtian, K. (2019). Curcumin loaded nanostructured lipid carriers: *In vitro* digestion and release studies. *Polyhedron*, 164, 113–122. <https://doi.org/10.1016/j.poly.2019.02.002>

Simões, L., Abrunhosa, L., Vicente, A. A., & Ramos, Ó. L. (2020). Suitability of  $\beta$ -lactoglobulin micro- and nanostructures for loading and release of bioactive compounds. *Food Hydrocolloids*, 101, 105492. <https://doi.org/https://doi.org/10.1016/j.foodhyd.2019.105492>

Tawk, C., & Alici, G. (2020). Finite Element Modeling in the Design Process of 3D Printed Pneumatic Soft Actuators and Sensors. *Robotics*, 9(3), 52. <https://doi.org/10.3390/robotics9030052>

Wang, J., Wu, P., Liu, M., Liao, Z., Wang, Y., Dong, Z., & Chen, X. D. (2019). An advanced near real dynamic *in vitro* human stomach system to study gastric digestion and emptying of beef stew and cooked rice. *Food & Function*, 10(5), 2914–2925. <https://doi.org/10.1039/C8FO02586J>

Xavier, M. S., Fleming, A. J., & Yong, Y. K. (2020). Finite Element Modeling of Soft Fluidic Actuators: Overview and Recent Developments. *Advanced Intelligent Systems*, n/a(n/a), 2000187. <https://doi.org/https://doi.org/10.1002/aisy.202000187>

CHAPTER 4.

REAL-TIME ASSESSMENT OF FOOD *IN VITRO* DIGESTION USING UV-VIS-SWNIR  
SPECTROSCOPY IN AN RGM

4.1	INTRODUCTION .....	81
4.2	MATERIALS AND METHODS.....	81
4.3	RESULTS AND DISCUSSION .....	87
4.4	CONCLUSIONS .....	97
4.5	REFERENCES .....	98

## **4.1 INTRODUCTION**

The use of *in vitro* digestion models is very well established by the scientific community study the digestion process of food. The use of *in vivo* models can then be avoided, or at least reduced, since these are expensive, labour-intensive models that present some ethical issues (Bellmann et al., 2016; Madalena et al., 2019; Simões et al., 2020). Consequently, many *in vitro* digestion models have been developed to address the increasing interest on this topic. In fact, the COST INFOGEST group is responsible for developing static (Brodkorb et al., 2019; Minekus et al., 2014) and semi-dynamic (Mulet-Cabero et al., 2020) digestion models that can be used for inter-laboratory comparisons. However, the development of a fully dynamic standardized *in vitro* digestion model is still a challenge, and the previous chapter addresses this issue by proposing the development of a reproducible RGM that has the potential to be used as a standardized dynamic *in vitro* gastric model. The current assay aims at assessing the performance of the RGM in the digestion of food. For this purpose, commercially available semi-skimmed milk was used since it is a very complete and nutritious food product that contain several proteins, fats, and carbohydrates. As such, the standardized semi-dynamic *in vitro* digestion protocol was used, and protein hydrolysis and fat digestion were assessed. Protein digestion was evaluated using the OPA method (i.e., to quantify the release of amino-acids) and SDS-PAGE while milk fat globules digestion was analyzed using GC to quantify the release of FFA. CLSM was also used to visually assess both protein and fat digestion throughout the *in vitro* digestion process. In addition to these conventional analytical techniques, UV-VIS-SWNIR spectroscopy was also used to assess, in real-time the digestion of proteins.

## **4.2 MATERIALS AND METHODS**

### **4.2.1 Materials**

The potassium chloride (KCl), potassium di-hydrogen phosphate (KH<sub>2</sub>PO<sub>4</sub>), sodium bicarbonate (NaHCO<sub>3</sub>), sodium chloride (NaCl), magnesium chloride hexahydrate (MgCl<sub>2</sub>(H<sub>2</sub>O)<sub>6</sub>), ammonium carbonate ((NH<sub>4</sub>)<sub>2</sub>CO<sub>3</sub>), TEMED, Tris, APS, Coomassie Blue R-250 solution, ethanol, absolute, (with purity >=99,8% HPLC grade), acetic acid glacial, Nile red, FITC,  $\alpha$ -amylase 10 mg.mL<sup>-1</sup> (1154 U.mg<sup>-1</sup>), pepsin from porcine gastric mucosa (1264 U.mg<sup>-1</sup>) and lipase from porcine pancreas (15.7 U.mg<sup>-1</sup>) were purchased from Merck (Darmstadt, Germany). All enzyme activities were determined using the protocol described by Mulet-Cabero et al., (2020). The SDS was purchased

form Panreac Química SLU (Castellar del Vallès, Barce-lona). The commercially available semi-skimmed milk was purchased in the local supermarket containing 3.4 g/100mL of proteins, 1.6 g/ 100mL of lipids and 4.9 g/100 mL of carbohydrates (mainly sugars) which represent ca. 10% of solids in milk.

#### **4.2.2 *In vitro* digestion protocol**

The INFOGEST 2.0 *in vitro* digestion protocol (Mulet-Cabero et al., 2020) was used to assess the gastric digestion of milk that is being used as a food model to evaluate the performance of the RGM. Briefly, the simulated electrolyte fluids were prepared using stock salt solutions of KCl (15.1 mmol.L<sup>-1</sup>), KH<sub>2</sub>PO<sub>4</sub> (3.7 mmol.L<sup>-1</sup>), NaHCO<sub>3</sub> (13.6 mmol.L<sup>-1</sup>), MgCl<sub>2</sub>(H<sub>2</sub>O)<sub>6</sub> (0.15 mmol.L<sup>-1</sup>), (NH<sub>4</sub>)<sub>2</sub>CO<sub>3</sub> (0.06 mmol.L<sup>-1</sup>) for the simulated salivary fluid (SSF) and KCl (6.9 mmol.L<sup>-1</sup>), KH<sub>2</sub>PO<sub>4</sub> (0.9 mmol.L<sup>-1</sup>), NaHCO<sub>3</sub> (25 mmol.L<sup>-1</sup>), NaCl (47.2 mmol.L<sup>-1</sup>), MgCl<sub>2</sub>(H<sub>2</sub>O)<sub>6</sub> (0.12 mmol.L<sup>-1</sup>) and (NH<sub>4</sub>)<sub>2</sub>CO<sub>3</sub> (0.5 mmol.L<sup>-1</sup>) for the simulated gastric fluid (SGF) – values within parentheses correspond to the final salt concentration in the respective simulated fluid. The *in vitro* digestion conditions were calculated according to the samples' nutritional composition which are detailed in Table 8. Subsequently, 250 g of milk were mixed with SSF, 0.3M CaCl<sub>2</sub> and water. Salivary amylase was added and the oral phase started with a duration of 2 minutes. The contents were transferred into the RGM which contained a basal volume of 21.01 mL of SGF and 0.3M CaCl<sub>2</sub>. Both SGF and enzymes were gradually pumped at a flow rate of 3.99 and 0.17 mL/min, respectively.

**Table 8** – Summary of the main *in vitro* digestion conditions.

	<b>Oral phase</b>	<b>Gastric phase</b>	<b>SGF flow (mL/min)</b>	<b>Enzymes flow (mL/min)</b>	<b>SE rate (mL/min)</b>	<b>Number of SE</b>
Electrolyte solution (mL)	20.0 (SSF)	210.0 (SGF)				
0.3M CaCl <sub>2</sub> (μL)	125.0	137.50	3.99	0.17	9.24	12
Water (mL)	3.87	54.86				

#### **4.2.3 Offline milk *in vitro* digestion assessment**

Some offline techniques were used to assess the *in vitro* digestion of milk namely the OPA method to quantify the release of amino acids during protein gastric digestion, an SDS-PAGE under reducing conditions to assess protein aggregates during digestion, a FFA quantification (i.e., C18:1, C18,

C16, C14, C12, C10) using GC and, finally, microscopy images were taken using confocal scanning laser microscope (CSLM) to assess the protein particles and lipid droplets' integrity throughout the *in vitro* gastric digestion.

#### 4.2.3.1. OPA Method

The OPA method was used to quantify the amino acids released during the *in vitro* gastric digestion, using serine as a reference. For this purpose, all samples were previously centrifuged at 14000 rpm for 15 min to separate the protein aggregates from the free amino acids. Subsequently, 20  $\mu$ L of centrifuged samples were transferred to a 96 well microplate and 200  $\mu$ L of OPA reagent was added. The micro plate was then incubated at 50 °C for 60 min and a fluorescence read was made with an excitation and emission wavelengths of 340 and 455 nm, respectively, with a gain of 50.

#### 4.2.3.2. SDS-PAGE

An SDS-PAGE under reducing conditions was performed in order to evaluate the behaviour of milk proteins under gastrointestinal conditions throughout the digestion time, based on previous works (Ferreira et al., 2021; Pereira et al., 2021). All samples were diluted with sample buffer to a final protein concentration of 0.15% aiming at eliminating the effect of sample dilution during GI digestion caused by the presence of the simulated gastric secretion. The sample buffer used was 2 $\times$  Laemmli Solution (Bio-Rad Laboratories, Inc., Hercules, CA, USA). All samples were added to the sample buffer to achieve the desired final protein concentration, heated at 80 °C for 10 min and then loaded into the gel well. A molecular weight marker (PageRuler™ Unstained Broad Range Protein Ladder 5–250 kDa, where 100, 50, and 20 kDa bands were used as reference, Thermo Scientific) was used to identify the respective molecular weight of the bands and consequently the respective protein/ protein aggregate. A Mini Protean Tetra-cell (Bio-Rad Laboratories, Hercules, CA, USA) was used to perform the electrophoresis analysis along with acrylamide/bisacrylamide gels. Resolving and stacking gels of acrylamide/bisacrylamide (37.5:1, 30%) were prepared at a concentration of 12% and 4%, respectively. A solution of Tris-HCl 1.5 mol/L at pH 8.8, %, APS at 10%, SDS at 10% and TEMED was used to prepare the resolving gel. The stacking gel was prepared similarly with the slight difference of replacing tris-HCl 1.5 mol/L at pH 8.8 with tris-HCl 0.5 mol/L at pH 6.8. A stock solution of running buffer was prepared with Tris (0.250 mol.L<sup>-1</sup>), glycine (1.920 mol.L<sup>-1</sup>) and SDS (36  $\times$  10<sup>-3</sup> mol.L<sup>-1</sup>) and diluted 10 times before use. The running conditions used



were 300 V and 60 mA for, approximately, 40 min. The staining of gels was performed with a Coomassie Blue R-250 solution (0.1%) prepared with ethanol and acetic acid at 40% and 10%, respectively. The staining of gels was followed by the destaining with a solution of ethanol and acetic acid at 40% and 10%.

#### 4.2.3.3. Free fatty acid analysis using GC

A GC analysis was applied to assess lipid digestion of milk in the *in vitro* RGM by quantifying FFA, namely the C18:1 (oleic acid), C18 (stearic acid), C16 (palmitic acid), C14 (myristic acid), C12 (lauric acid) and C10 (capric acid). For this purpose, the assay developed by Neves et al., (2009) was applied. The analysis was carried out in a GC system (VARIAN 3800) equipped with an FID. LCFA are separated using a Stabilwax-MS column (30 m × 0.25 mm × 0.25 µm), with He as the carrier gas at 1.0 mL/min. The air flow is set at 250 mL/min, nitrogen and hydrogen flow of 30 mL/min. Temperatures of the injection port and detector were 220 and 250 °C, respectively. Initial oven temperature was 50 °C for 2 minutes, with a 10 °C/ min ramp to 225 °C, and a final isothermal for 10 minutes. Briefly, 2 mL of the digestion samples were transferred to glass tubes and mixed with 1.5 mL of IS solution (1000 mg/mL), 1.5 mL of 25 % (v/v) HCl (37%):1-propanol and 2 mL of DCM. The solution is then vortex mixed and digested at 100 °C for 3.5 hours. The tubes are let to cool down at room temperature, vortexed and the content is transferred with 2 mL of ultra-pure water into a 10 mL vial that is subsequently closed with a rubber stopper and aluminium crimp cap. The vials are inverted for about 30 minutes so that the organic phase of the solution is in contact with the rubber stopper. A plastic syringe is used to transfer 2 mL of the organic phase to a 2 mL vial containing a small amount of Na<sub>2</sub>SO<sub>3</sub> to remove any residual water in the samples. The supernatant (i.e., samples without Na<sub>2</sub>SO<sub>3</sub>) is carefully transferred to another 2 mL vial that is tightly closed with a screw cap containing a silicone/PTFE septum. Finally, the samples are put in the GC sample holder and 1 µL is transferred to the GC. The chromatogram peaks were identified by comparing the digestion results with the calibration chromatogram using C6:0, C8:0, C10:0, C12:0, C14:0, C16:0, C16:1, C18:0, C18:1, and C18:2. However, only the most abundant FFA were analysed in the digestion proteins, i.e., C18:1, C18:0, C16:0, C14:0, C12:0 and C10:0 (Clulow et al., 2018). The respective digestion chromatogram peaks were integrated and compared with the ones in the calibration.

#### 4.2.3.4. CSLM

Microscopy images were taken using CSLM (Olympus BX61, Model FluoView 1000) to assess the integrity of protein and lipid structures in the milk samples, using a 60x oil immersed objective lens. The samples from times 0, 30 and 59.5 min were stained according to Liang et al., (2017). Briefly, 5  $\mu$ L of fluorescein isothiocyanate (FITC, 10 mg/mL in dimethyl sulfoxide) and 10  $\mu$ L of Nile red (1mg/mL in methanol) were added to 200  $\mu$ L of sample for protein and lipid staining, respectively. The stained samples were then vortexed for 5 minutes and 7  $\mu$ L were transferred to the microscope slide. The samples were then analysed using a green (laser488 BA:505-540) and red (laser559 BA:575-675) laser since the emission and excitation wavelengths form FITC and Nile red are 488-545 nm and 515-605, respectively. All images were acquired and processed with the software FV10-Ver4.1.1.5 (Olympus).

### **4.2.4 UV-VIS-SWNIR Spectroscopy**

#### 4.2.4.1. Description

The *in vitro* milk digestion was also assessed via UV-VIS-SWNIR spectroscopy using a fibre optics (T300-RT-VIS/NIR, Oceanoptics, Orlando, USA) multichannel spectrophotometer (AvaSpec-2048-DT-4, 2048-pixel, 200-1100 nm). A halogen light source (AvaLight-Hal LS-0308016, 360-2500nm, Avantes, Apeldoorn, the Netherlands) was used since it covers the region of interest of the spectrum (360-1100 nm). The spectra were subsequently acquired using AvaSoft 7.5.3 by averaging 30 spectra on each acquisition. A multivariate calibration was made using serine as a reference amino acid, similar to the OPA method. For this purpose, 200 mL of distilled water was put in the RGM. Subsequently, 1 mL of serine solution (1 mg/mL, w/v) was sequentially added and mixed. Furthermore, 50 spectra were acquired at each serine concentration. During the digestion process, the spectra were obtained at each stomach emptying, using time 0 as a blank. The free NH<sub>2</sub> was predicted using the previous calibration.

#### 4.2.4.2. Signal processing software

The software responsible for the NIR spectra pre-processing was developed using python version 3.9.12. The *sci-kit learn* library was used for spectra smoothing, wavelength selection, peak identification, and regression. The library *pyDOE2* was used to obtain the DOE matrix. The numpy and pandas libraries were used for matrix calculations.

#### 4.2.4.3. Sample separation

The serine calibration dataset consisted in a collection of 500 spectra containing 10 serine concentrations. As such, the dataset was randomly split into two groups: a calibration and evaluation set in a 3:1 ratio, respectively. This technique is often applied to ensure that overfitting does not happen.

#### 4.2.4.4. Spectrum smoothing

All obtained spectra were smoothed using the Savitzky-Golay filter. This way, the window size and polynomial order were determined using an FCD. The  $r^2$  of the serine concentration prediction was used to optimize the smoothing parameters.

#### 4.2.4.5. Baseline correction and resolution enhancement

Two strategies were tested to correct the baseline and enhance the resolution of the spectra: the SNV and MSC. The spectra transformations were manually calculated and the code snippet can be consulted below.

```
def snv(self, interval=[0, None]):
    snv_data = []
    num_spectra = len(self.spectra_abs)
    for i in range(num_spectra):
        print(f"\rApplying SNV correction to spectrum {i+1}/{num_spectra}", end="")
        spectrum = self.spectra_abs[i][interval[0]:interval[1]]
        snv_data.append((spectrum - np.average(spectrum)) / np.std(spectrum))
    return snv_data

# Code adapted from https://towardsdatascience.com/scatter-correction-and-outlier-detection-in-nir-
# spectroscopy-7ec924af668

def msc(self, window=10):
    print("Applying MSC correction...")
    input_data = np.array(self.spectra_abs, dtype=np.float64)
    ref = []
    sampleCount = int(len(input_data))
    for i in range(input_data.shape[0]):
        input_data[i, :] -= input_data[i, :].mean()
    data_msc = np.zeros_like(input_data)
    for i in range(input_data.shape[0]):
        for j in range(0, sampleCount, window):
```

```
ref.append(np.mean(input_data[j:j+window], axis=0))
fit = np.polyfit(ref[i], input_data[i,:], 1, full=True)
data_msc[i,:] = (input_data[i,:] - fit[0][1]) / fit[0][0]
return (data_msc)
```

#### 4.2.4.6. Wavelength selection

To identify and select the wavelengths that contribute the most to explain the serine variance in the dataset, VIP values of PLS were used with a threshold of -0.8 and 0.8. The selected wavelengths were subsequently used in regression.

#### 4.2.4.7. Regression

Several regression models were compared, namely, the MLR, RR, LR, ENR, BRR, SVMR and RFR. The models were fitted with the calibration subset and the  $r^2$  was calculated using the evaluation subset.

### 4.2.5 Statistical Analysis

All statistical analyses applied to experimental data were performed using Origin (2018, OriginLab Corporation, Massachusetts, USA), unless it indicated in the text otherwise. The statistical significance (at  $p \leq 0.05$ ) was determined using one-way ANOVA followed by post hoc. Tukey's tests with at least triplicate samples, unless it is mentioned on the respective section otherwise. The FCD matrix was obtained by the pyDoE library and the optimization curves were further obtained in Protimiza Experiment Design Software (<http://experimental-design.protimiza.com.br>).

## 4.3 RESULTS AND DISCUSSION

### 4.3.1 *Ex situ* assessment of milk digestion.

#### 4.3.1.1. Protein hydrolysis

Milk products are very well known for their nutritious value due to its content of proteins, lipids and carbohydrates. This way, milk was used as a food model to assess the performance of the *in vitro* RGM. To evaluate protein hydrolysis, the OPA method and an SDS-PAGE were made to quantify the free  $\text{NH}_2$  and assess the protein fractions. It is possible to observe from the analysis of Figure

16 that, despite the differences observed between the three independent digestion assays, all assays have the same curve shape, i.e., an exponential increase in the release of  $\text{NH}_2$  with an initial lag phase. In fact, several factors may have contributed to the late release of  $\text{NH}_2$  groups during the digestion. For instance, the gradual acidification of the digestion fluids may have significantly contributed to a gradual release of free  $\text{NH}_2$  groups. In fact, for all experiments, a high correlation was observed when the pH kinetics and protein hydrolysis were compared with an  $r^2$  of 0.961, 0.837 and 0.934 for the experiment 1, 2 and 3, which are depicted in Figure 16B, C and D, respectively. Since some variability was observed in the pH profile across experiments, the variability of  $\text{NH}_2$  groups release could be explained by the different pH kinetics of the experiments. The gradual input of enzymes, namely the pepsin, may also have contributed to the gradual release of  $\text{NH}_2$  and explaining the lag phase in the curves. The combination of pepsin gradual input and pH kinetics gave shape to the release kinetics' curves of the  $\text{NH}_2$  groups since pepsin activity is optimal between pH 1.6 and 4.0 (Mackie et al., 2020; Shani-Levi et al., 2017). This way, lower pH values correspond to a higher protein hydrolysis. This behaviour was observed elsewhere (Hodgkinson et al., 2018) where the authors obtained higher protein hydrolysis at pH 3.0 when compared to pH 5.0. Other studies also observed similar exponential protein hydrolysis. For instance, Dong et al., (2021) used an AGDS to assess the digestion of milk and other dairy products (i.e., yoghurt and cheese). The authors observed an exponential release of free  $\text{NH}_2$  during the gastric *in vitro* digestion process with a concentration ca. 0.9 mg/mL of free  $\text{NH}_2$  at the 60 minutes of digestion.

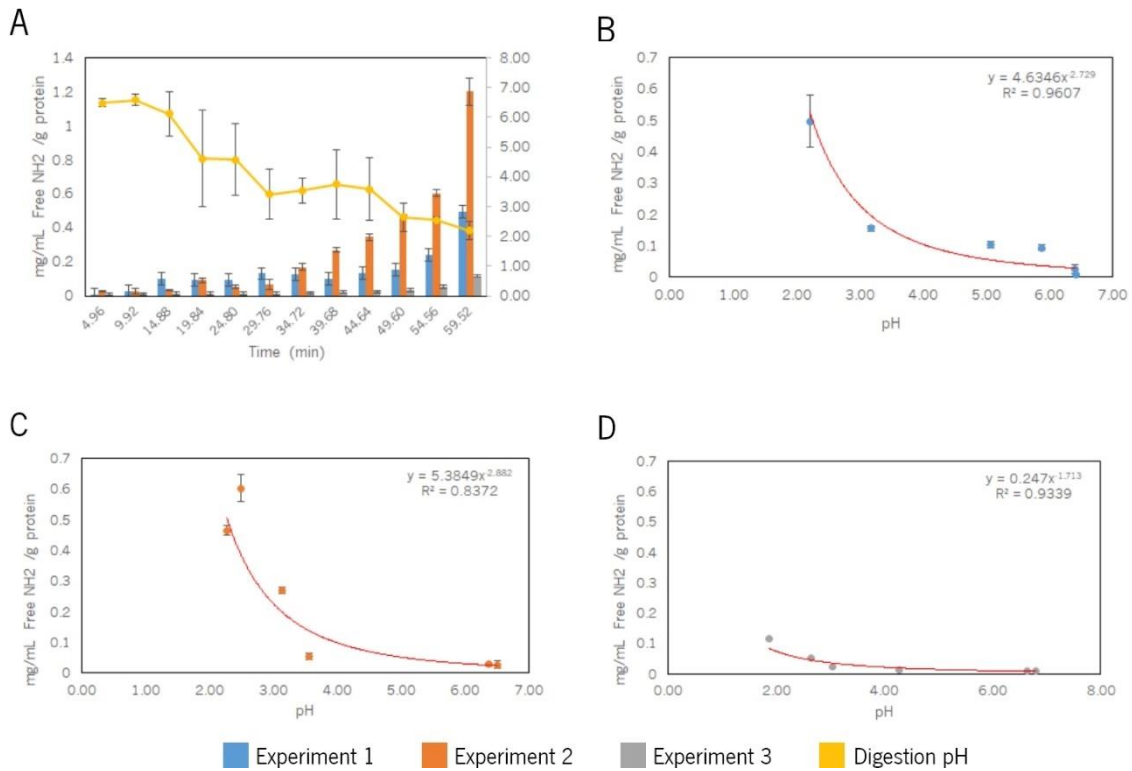


**Figure 16** – Protein hydrolysis during the *in vitro* RGM digestion where: A – quantification of free NH<sub>2</sub> per gram of protein; B, C and D correspond to the correlation between the experiment 1, 2 and 3 pH profile and the free NH<sub>2</sub> per gram of protein, respectively.

With the *pI* of casein, the main protein of milk, being at 4.6 (Tagliazucchi et al., 2016), protein destabilization may occur which can in turn promote protein aggregation. To further assess this process an SDS-PAGE was made, and the results are depicted in Figure 17. It is possible to observe that all bands suffered a decrease in intensity, except for SE10 and SE12 where protein aggregation may have occurred. Furthermore, a band at ca 15 kDa (para *k*-CN) appeared at the early stages of digestion (i.e., from SE1) and its intensity remain constant (despite the dilution of samples) until SE8 where its intensity starts to decline. This indicated that some fractions of *k*-CN were hydrolysed into para *k*-CN. Similar results were observed by Ye et al., (2019) and the authors attributed the cause of protein aggregation to the appearance of para *k*-CN. Roy et al., (2022) also observed *in vivo* the appearance of para *k*-CN as a result of *k*-casein hydrolysis. Whey proteins like  $\beta$ -Lg and  $\alpha$ -La were observed throughout the digestion process. This indicates that they resist the *in vitro* digestion process, as expected. This is in accordance with previous studies (Dong et al., 2021; Li et al., 2021; Madalena et al., 2016) where whey proteins were able to resist pepsin digestion. For instance, the resistance to proteolysis from  $\beta$ -Lg is often attributed to its low pH stability (Ye et al., 2019) since its *pI* is around 5.2 which is further from the highly acidic conditions of the stomach

(Madalena et al., 2016). On the other hand, despite its appearance,  $\alpha$ -La bands decreased in intensity, specially from SE8 which indicates that some extent of protein hydrolysis occurs.

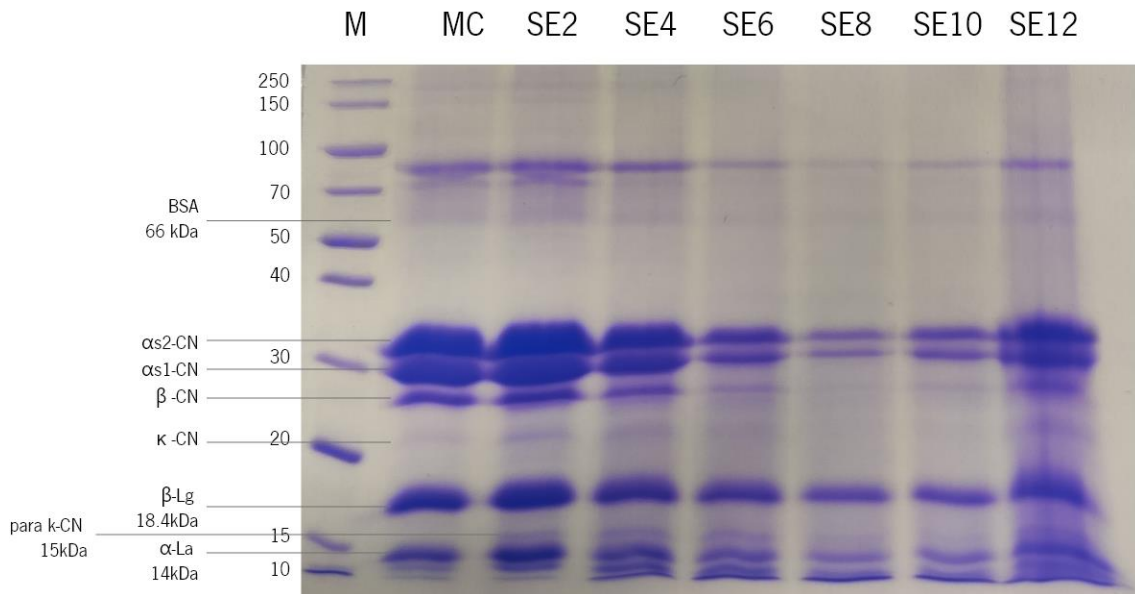


**Figure 17** – Protein digestion assessment using SDS-PAGE where: Molecular weight marker; MC – undigested milk samples; the lanes identified with the numbers 2, 4, 6, 8, 10 and 12 correspond to the respective stomach emptying.

#### 4.3.1.2.FFA assessment through GC

Lipids in milk are mainly expressed as triglycerides which comprise ca. 98% of the fat content of milk (Clulow et al., 2018). Despite of the main digestion site being the small intestine (i.e., by interacting with pancreatic lipase) some extent of lipid digestion still occurs in the stomach (De Oliveira et al., 2016) and the results of this process are described in this topic. This way, the lipolysis of milk was assessed through GC to identify and quantify the release of FFA in milk and the results are depicted in Figure 18. Despite the high variability of the samples, some trends can be identified in the digestion data. It is possible to observe the same kinetic curve shape for all FFA, i.e., an exponential increase with a lag phase. C16:0 was the most released FFA followed by C18:1, C14, C18, C12 and C10 with a release of ca.  $61.98 \pm 31.72$ ,  $33.48 \pm 16.54$ ,  $21.24 \pm 12.12$ ,  $16.39 \pm 7.99$ ,  $7.69 \pm 2.17$  and  $5.47 \pm 3.42$  mg/mL FAA/ g lipid, respectively. It is also possible to observe that the FFA release kinetics «present a similar shape when compared with the

free NH<sub>2</sub> groups release. To further explore this observation, CSLM was made in conjunction with a multivariate analysis through PCA.

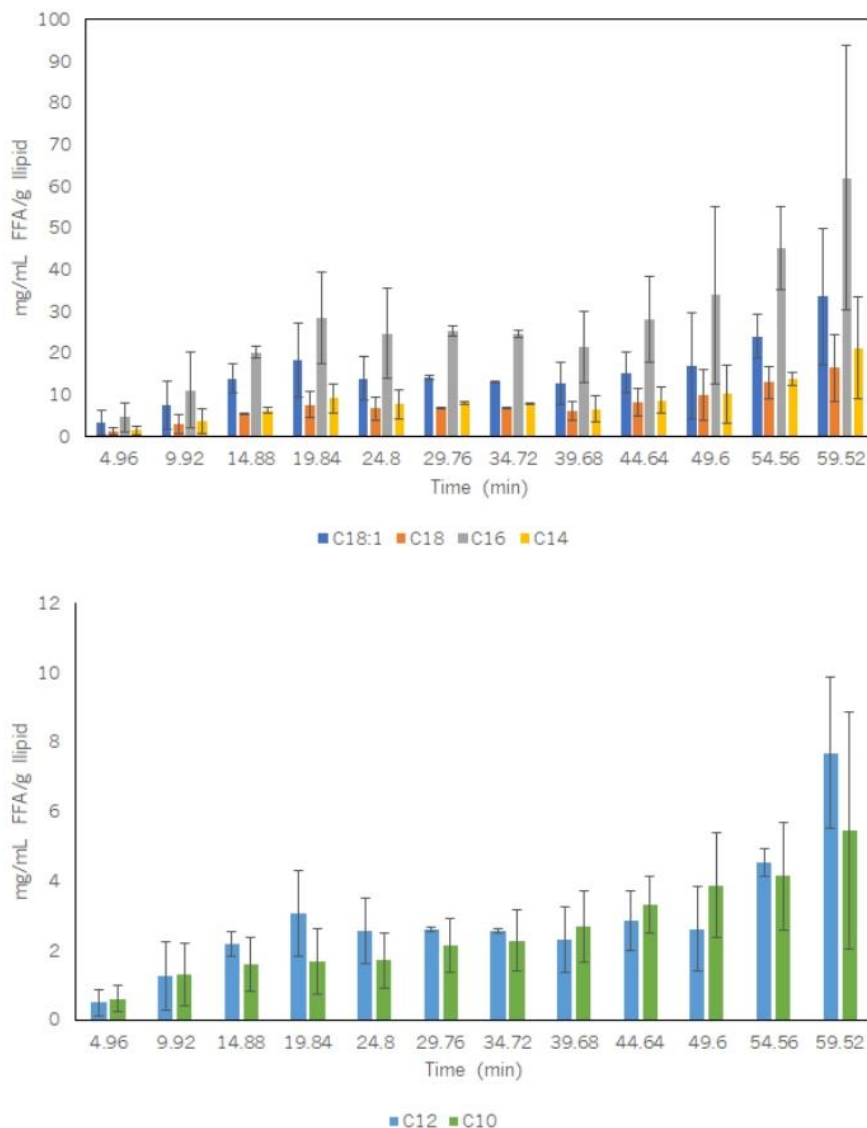


**Figure 18** – FFA release profiles during the RGM *in vitro* digestion.

#### 4.3.1.3. Assessing milk protein and lipid digestion – A multivariate analysis.

Protein and milk digestion is highly dependent on milk composition and structure. As such, it is known that fat globules may interact with casein and significantly influence its coagulation under gastric conditions (Ye, 2021). This way, CSLM was used to assess the *in vitro* digestion of both milk proteins and fat and the images are represented in Figure 19. It is possible to observe that the initial milk samples (i.e., undigested milk samples) are composed by small protein particles with ca. 5-10  $\mu\text{m}$  (represented by green particles) and fat globules (represented by red particles). It is also possible to observe that lipid and protein particles seem to interact with each other since



fat globules inside protein particles were observed. Some variability regarding the different experiments were observed but some conclusions can be drawn. For instance, all experiments exhibit protein aggregation in SE6 and SE12 which can be explained by casein coagulation during gastric digestion due to its instability at low pH and its interaction with  $\text{Ca}^{2+}$  ions (Ye, 2021; Ye et al., 2019). It is also possible to observe that fat globules were tendentially near protein agglomerates. This tendency was also found elsewhere (Dong et al., 2021) with different dairy products, including milk. However, the SE6 of experiment 2 appears to have some degree of lipid coalescence. With the exception of samples SE12 from experiment 3, where protein particles aggregated and formed a network structure, it is possible to observe the appearance of smaller particles that can be small polypeptides that are being released due to proteolysis. Further investigation made to unravel the correlations and interactions between all factors during the digestion and, as such, a multivariate analysis was made, i.e., a PCA.

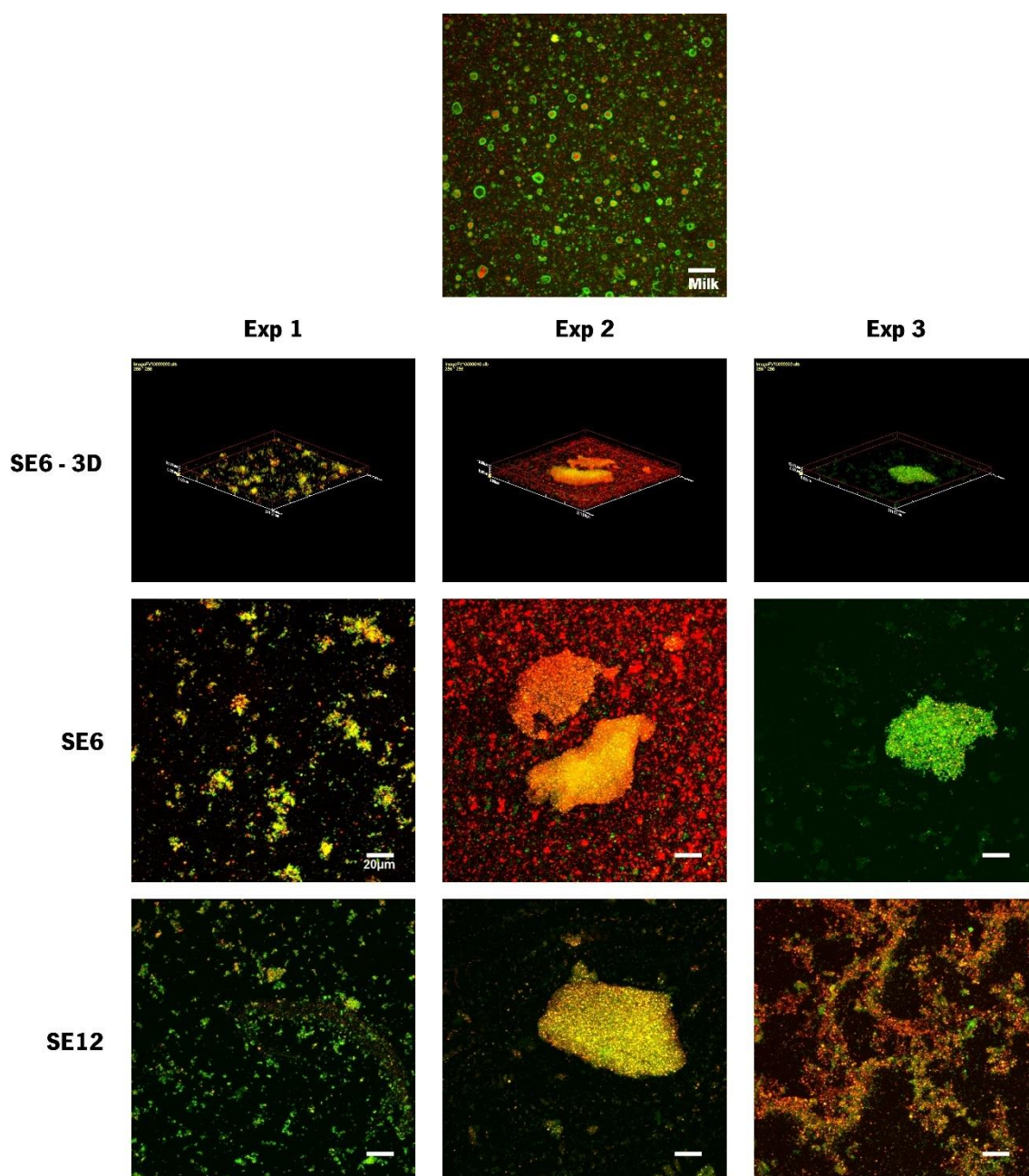


**Figure 19** – CLSM images obtained through the digestion process of three distinct experiments (i.e., Exp1, Exp 2, and Exp 3) at times 0 (milk sample), 29.76 (SE6) and 59.50 (SE12) minutes as well as the 3D projection at time 29.76 minutes. The white bar represents 20  $\mu\text{m}$ .

It is possible to observe from the analysis of the PCA (Figure 20) that the extraction of two PCs explains 99.71% of the data variability which means that two PC account for a major part of data variability and are good representations of the data, with PC1 itself explaining 91.59% of data variability and PC2 8.12%. This means that the horizontal distance between points is significantly more important than their distance along the  $y$ -axis, which means that the release of  $\text{NH}_2$  groups during the digestion is correlated with the C10:0, C12:0, pH (despite its vertical distance), C14:0

and C18:0, while C18:1 and C16:0 appear to be on separate groups. This indicates that in fact, the digestion of proteins and lipids in milk can be correlated and the digestion pH takes an important role towards protein and lipid digestion.

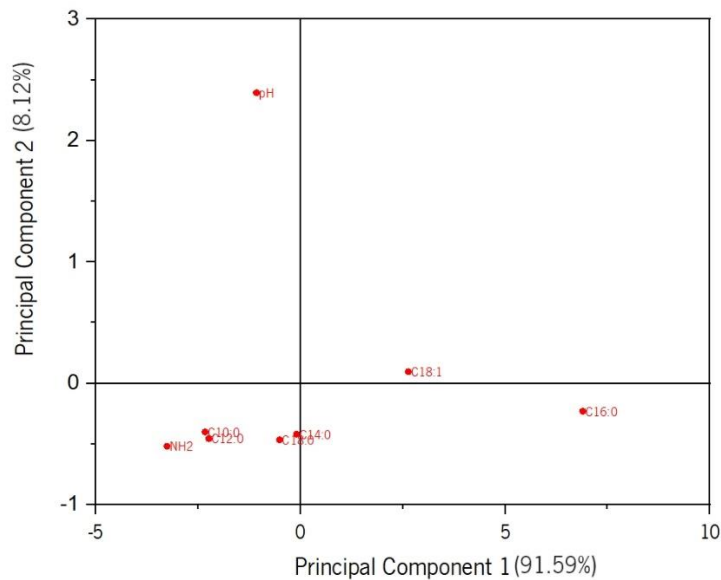


**Figure 20** - PCA of milk *in vitro* digestion in the RGM. Values within parenthesis account for the variability explained by the respective principal component.

### 4.3.2 Real-time monitoring of milk protein digestion

To assess milk digestion in real-time, a fibre optics UV-VIS-SWNIR spectroscope was used. This technique allows a rapid, non-destructive way to measure the release of amino acids during the *in vitro* digestion process without sample manipulation (i.e., centrifuging, extraction, ice bathing, etc). This way, serine was used to calibrate the equipment using the NIR region of the spectra by smoothing the data, correcting the baseline of the spectra, selecting the most important wavelengths and estimating the concentration of serine by fitting several regression models, namely, MLR, RR, LR, ENR, BRR, SVMR, and RFR. Primarily, the optimum window and polynomial order were determined for the Savitzky-Golay filter using an FCD. The results are depicted in Figure 21. It was possible to determine a  $w$  of 73. Note that the coefficients of the polynomial were removed since they were not statistically significant ( $p$ -value > 0.05).

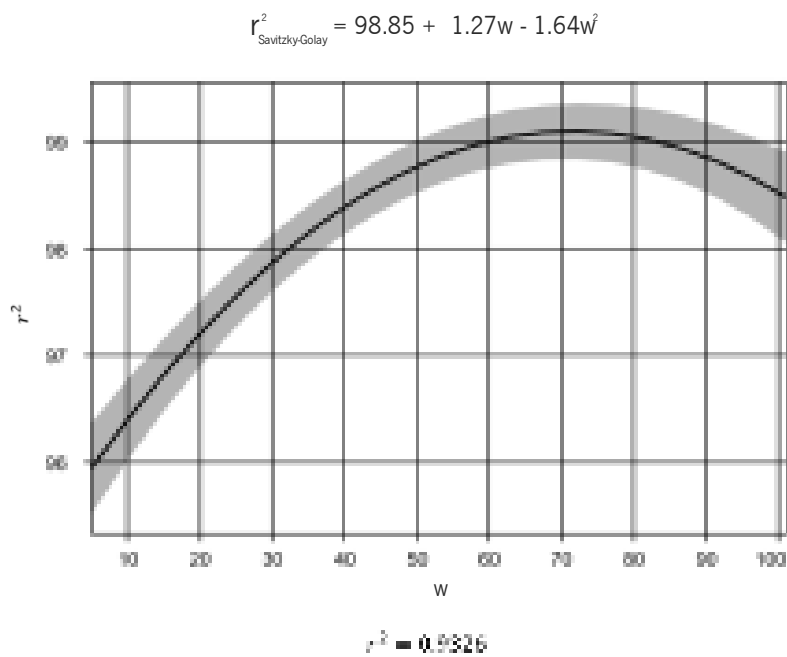


**Figure 21** – Savitzky-Golay optimization using an FCD.

An SNV was made to correct the baseline of the spectra to remove the effects of light scattering. The effect of smoothing and SNV can be seen in Figure 22.

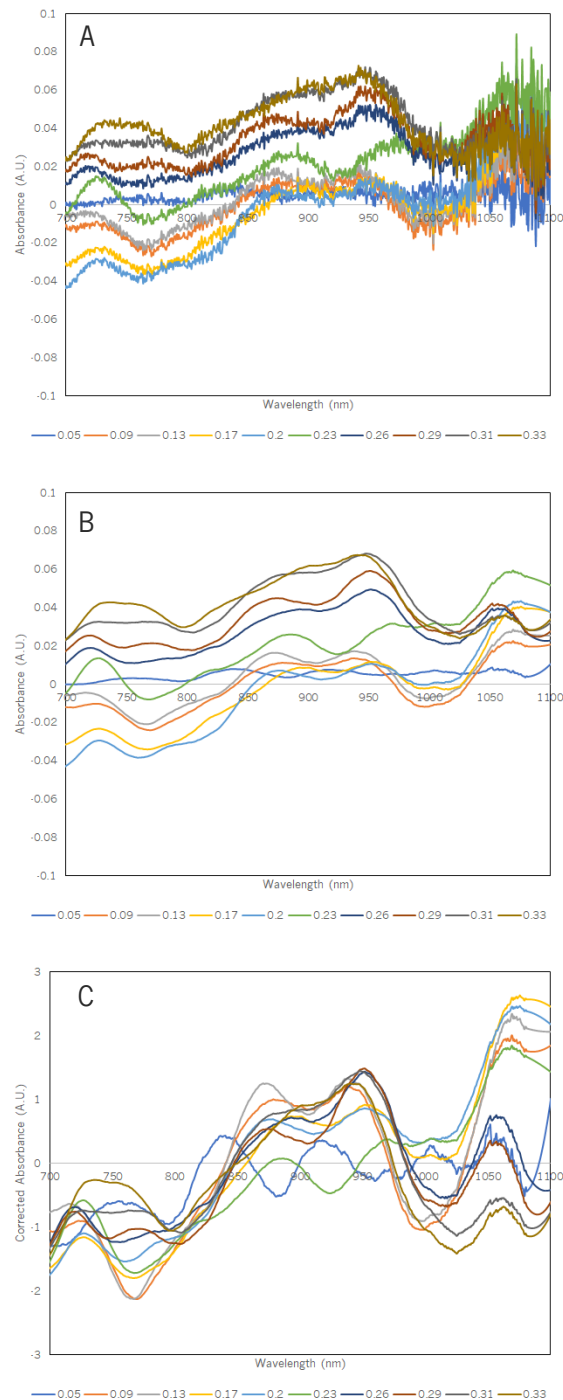


**Figure 22** – Effect of smoothing and SNV transformation of the serine spectra at different concentrations where: A – raw spectra; B – smoothed spectra; C – SNV. Note that each spectrum is represented as the average of 50 acquired spectra.

Subsequently, PLS was used to select the wavelengths that contributed the most for the serine concentration variance. This way, the wavelengths 721.21, 776.53, 858.72, 869.83, 967.36,

987.02, and 1080.11 nm. The wavelengths were further used to fit the regression models and the results are represented in Table 9.

**Table 9** – Regression results.

MLR	RR	LR	ENR	BRR	SVMR	RFR
0.8901	0.9488	0.9607	0.9635	0.9527	0.9838	<b>0.9873</b>

It is possible to observe that the RFR algorithm has shown to be more precise in predicting the serine concentration using the selected wavelengths. Furthermore, it is also possible to conclude that machine learning algorithms (SVMR, RFR) had better performance when compared with the linear models (MLR, RR, LR, ENR, and BRR). This way, the calibration of the NIR spectroscope was further used in the digestion data to predict the digestion of proteins in the *in vitro* RGM and the results are depicted in Figure 23.

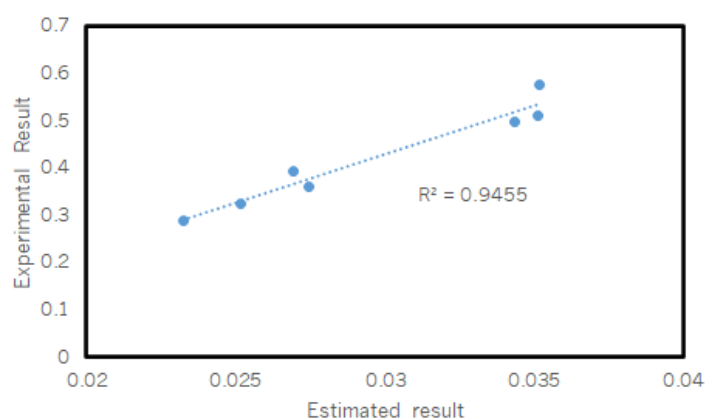


**Figure 23** – Comparison between protein hydrolysis obtained experimentally and estimated.

It is possible to observe that the estimated and experimental values present a high correlation coefficient of ca. 0.9455. This indicates that in fact UV-VIS-SWNIR spectroscopy can be used to predict the release kinetics of amino acids during protein hydrolysis.

#### 4.4 CONCLUSIONS

An *in vitro* RGM was used to assess milk digestion in terms of its protein and lipid hydrolysis. This way, conventional assessment techniques were used to assess protein (OPA, SDS-PAGE), lipid (GC) and the combination of both (CLSM). Very interesting results were observed in this study, namely,

the high dependence of protein hydrolysis with pH due to enzyme activation and protein clumping; the exponential hydrolysis kinetics with a lag phase was observed for both protein and lipid digestion; the appearance of para  $\kappa$ -CN due to the hydrolysis of  $\kappa$ -casein as it has been seen on previous studies (Roy et al., 2022; Ye et al., 2019); The morphology of protein particles drastically changed during the *in vitro* digestion process. In fact, protein aggregation was seen in SE6 and SE 12 when compared with the undigested milk samples. Furthermore, it was also possible to observe a tendency of fat globules to associate with milk proteins as well as the formation of smaller particles, despite the existence of protein aggregation, which may be attributed to the appearance of small polypeptides. In fact, the PCA results reinforced the connection between proteins and lipids. Protein hydrolysis was also measured in real-time using fibre optics UV-VIS-SWNIR spectroscopy. For this purpose, the spectra were pre-processed and a Savitzky-Golay window of 73 was determined for all spectra smoothing. The SNV transformation was applied and the most important wavelengths were identified using PLS VIP being 721.21, 776.53, 858.72, 869.83, 967.36, 987.02, and 1080.11 nm. Subsequently several regression models (i.e., both linear and machine learning models) were used to estimate protein hydrolysis and RFR obtained the best results with a correlation of 0.9873. The RFR model was further used in the digestion spectra and a correlation of 0.9455 was obtained between the estimated and experimental data which shows that UV-VIS-SWNIR spectroscopy is in fact a suitable technique to assess protein *in vitro* digestion in real-time. The results in this study suggests that the RGM is a suitable *in vitro* digestion model that can potentially be used as a standard *in vitro* gastric model.

#### **4.5 REFERENCES**

- Bellmann, S., Lelieveld, J., Gorissen, T., Minekus, M., & Havenaar, R. (2016). Development of an advanced *in vitro* model of the stomach and its evaluation versus human gastric physiology. *Food Research International*, 88. <https://doi.org/10.1016/j.foodres.2016.01.030>
- Brodkorb, A., Egger, L., Alming, M., Alvito, P., Assunção, R., Ballance, S., Bohn, T., Bourlieu-Lacanal, C., Boutrou, R., Carrière, F., Clemente, A., Corredig, M., Dupont, D., Dufour, C., Edwards, C., Golding, M., Karakaya, S., Kirkhus, B., Le Feunteun, S., ... Recio, I. (2019). INFOGEST static *in vitro* simulation of gastrointestinal food digestion. *Nature Protocols*, 14(4), 991–1014. <https://doi.org/10.1038/s41596-018-0119-1>
- Clulow, A. J., Salim, M., Hawley, A., & Boyd, B. J. (2018). A closer look at the behaviour of milk lipids during digestion. *Chemistry and Physics of Lipids*, 211, 107–116.

<https://doi.org/10.1016/J.CHEMPHYSLIP.2017.10.009>

- De Oliveira, S. C., Bourlieu, C., Ménard, O., Bellanger, A., Henry, G., Rousseau, F., Dirson, E., Carrière, F., Dupont, D., & Deglaire, A. (2016). Impact of pasteurization of human milk on preterm newborn *in vitro* digestion: Gastrointestinal disintegration, lipolysis and proteolysis. *Food Chemistry*, 211, 171–179. <https://doi.org/10.1016/J.FOODCHEM.2016.05.028>
- Dong, L., Wu, K., Cui, W., Fu, D., Han, J., & Liu, W. (2021). Tracking the digestive performance of different forms of dairy products using a dynamic artificial gastric digestive system. *Food Structure*, 29, 100194. <https://doi.org/10.1016/J.FOOSTR.2021.100194>
- Ferreira, S., Machado, L., Pereira, R. N., Vicente, A. A., & Rodrigues, R. M. (2021). Unraveling the nature of ohmic heating effects in structural aspects of whey proteins – The impact of electrical and electrochemical effects. *Innovative Food Science & Emerging Technologies*, 74, 102831. <https://doi.org/10.1016/J.IFSET.2021.102831>
- Hodgkinson, A. J., Wallace, O. A. M., Boggs, I., Broadhurst, M., & Prosser, C. G. (2018). Gastric digestion of cow and goat milk: Impact of infant and young child *in vitro* digestion conditions. *Food Chemistry*, 245, 275–281. <https://doi.org/10.1016/J.FOODCHEM.2017.10.028>
- Li, S., Ye, A., Pan, Z., Cui, J., Dave, A., & Singh, H. (2021). Dynamic *in vitro* gastric digestion behavior of goat milk: Effects of homogenization and heat treatments. *Journal of Dairy Science*. <https://doi.org/10.3168/JDS.2021-20980>
- Mackie, A., Mulet-Cabero, A.-I., & Torcello-Gómez, A. (2020). Simulating human digestion: developing our knowledge to create healthier and more sustainable foods. *Food & Function*, 11(11), 9397–9431. <https://doi.org/10.1039/D0FO01981J>
- Madalena, D. A., Pereira, R. N., Vicente, A. A., & Ramos, Ó. L. (2019). New Insights on Bio-Based Micro- and Nanosystems in Food. In *Encyclopedia of Food Chemistry* (pp. 708–714). Elsevier. <https://doi.org/10.1016/B978-0-08-100596-5.21859-3>
- Madalena, D. A., Ramos, Ó. L., Pereira, R. N., Bourbon, A., Pinheiro, A. C., Malcata, F., Teixeira, J. A., & Vicente, A. A. (2016). *In vitro* digestion and stability assessment of  $\beta$ -lactoglobulin/riboflavin nanostructures. *Food Hydrocolloids*, 58, 89–97. <https://doi.org/10.1016/j.foodhyd.2016.02.015>
- Minekus, M., Alminger, M., Alvito, P., Ballance, S., Bohn, T., Bourlieu, C., Carrière, F., Boutrou, R., Corredig, M., Dupont, D., Dufour, C., Egger, L., Golding, M., Karakaya, S., Kirkhus, B., Le Feunteun, S., Lesmes, U., Macierzanka, A., Mackie, A., ... Brodkorb, A. (2014). A standardised static *in vitro* digestion method suitable for food – an international consensus. *Food Funct.*, 5(6), 1113–1124. <https://doi.org/10.1039/C3FO60702J>
- Mulet-Cabero, A.-I., Egger, L., Portmann, R., Ménard, O., Marze, S., Minekus, M., Le Feunteun, S., Sarkar, A., Grundy, M. M.-L., Carrière, F., Golding, M., Dupont, D., Recio, I., Brodkorb, A., & Mackie, A. (2020). A standardised semi-dynamic *in vitro* digestion method suitable for food – an international consensus. *Food Funct.* <https://doi.org/10.1039/C9FO01293A>
- Neves, L., Pereira, M. A., Mota, M., & Alves, M. M. (2009). Detection and quantification of long chain fatty acids in liquid and solid samples and its relevance to understand anaerobic



- digestion of lipids. *Bioresource Technology*, 100(1), 91–96. <https://doi.org/10.1016/J.BIORTECH.2008.06.018>
- Pereira, R. N., Rodrigues, R. M., Machado, L., Ferreira, S., Costa, J., Villa, C., Barreiros, M. P., Mafra, I., Teixeira, J. A., & Vicente, A. A. (2021). Influence of ohmic heating on the structural and immunoreactive properties of soybean proteins. *LWT*, 148, 111710. <https://doi.org/10.1016/J.LWT.2021.111710>
- Roy, D., Moughan, P. J., Ye, A., Hodgkinson, S. M., Stroebinger, N., Li, S., Dave, A. C., Montoya, C. A., & Singh, H. (2022). Structural changes during gastric digestion in piglets of milk from different species. *Journal of Dairy Science*. <https://doi.org/10.3168/JDS.2021-21388>
- Shani-Levi, C., Alvito, P., Andrés, A., Assunção, R., Barberá, R., Blanquet-Diot, S., Bourlieu, C., Brodkorb, A., Cilla, A., Deglaire, A., Denis, S., Dupont, D., Heredia, A., Karakaya, S., Giosafatto, C. V. L., Mariniello, L., Martins, C., Ménard, O., El, S. N., ... Lesmes, U. (2017). Extending *in vitro* digestion models to specific human populations: Perspectives, practical tools and bio-relevant information. In *Trends in Food Science and Technology* (Vol. 60). <https://doi.org/10.1016/j.tifs.2016.10.017>
- Simões, L., Martins, J. T., Pinheiro, A. C., Vicente, A. A., & Ramos, Ó. L. (2020).  $\beta$ -lactoglobulin micro- and nanostructures as bioactive compounds vehicle : *In vitro* studies. *Food Research International*. <https://doi.org/10.1016/j.foodres.2020.108979>
- Tagliacruzchi, D., Helal, A., Verzelloni, E., & Conte, A. (2016). Bovine milk antioxidant properties: effect of *in vitro* digestion and identification of antioxidant compounds. *Dairy Science & Technology* 2016 96:5, 96(5), 657–676. <https://doi.org/10.1007/S13594-016-0294-1>
- Ye, A. (2021). Gastric colloidal behaviour of milk protein as a tool for manipulating nutrient digestion in dairy products and protein emulsions. *Food Hydrocolloids*, 115, 106599. <https://doi.org/10.1016/J.FOODHYD.2021.106599>
- Ye, A., Cui, J., Carpenter, E., Prosser, C., & Singh, H. (2019). Dynamic *in vitro* gastric digestion of infant formulae made with goat milk and cow milk: Influence of protein composition. *International Dairy Journal*, 97, 76–85. <https://doi.org/10.1016/j.idairyj.2019.06.002>

CHAPTER 5.

GENERAL CONCLUSIONS AND FUTURE WORK

5.1	GENERAL CONCLUSIONS .....	102
5.2	FUTURE PERSPECTIVES .....	103

## 5.1 GENERAL CONCLUSIONS

The application of *in vitro* digestion models to study food digestion has been well established by the scientific community. As such, the work presented in this dissertation aims at developing a more realistic *in vitro* gastric digestion model that encompasses the anatomical geometry of the human stomach. The *in vitro* RGM has the potential to be used as a novel standard dynamic *in vitro* gastric model due to its interlaboratory reproducibility. This way, several conclusions can be taken from this work. For instance, the optimization of the PB enabled the mathematical modulation of the PB's behaviour and, consequently, the determination of the design specification so that the PB would rotate at a specific, pre-determined angle, namely, an LT of 3.61, 3.29 and 0.86 mm could be used so that PB1, PB2 and PB3 would rotate 30, 40 and 80%, respectively. It was also possible to observe that the RGM presented some intrinsic variability due to its geometry, more specifically and probably, due to the geometry of the antrum which hypothetically promoted a potential dead zone and gradual mixing of the tracer. Furthermore, higher flow rates resulted in lower residence times, as expected, which indicates that in fact, liquid food products have a lower residence time than solid food products which in turn indicates a lower contact and interaction with gastric enzymes.

Milk was used to assess the performance of the RGM since it is a very complete food product containing proteins, lipids and carbohydrates. It was possible to observe that both lipids and proteins had an exponential hydrolysis with an initial lag phase which could be indicative of the slow mixing and storage in the stomach antrum, along with the gradual input of gastric enzymes. It was also possible to observe the high dependence of protein hydrolysis with pH due to enzyme activation and protein clothing. Furthermore, both the morphological assessment and multivariate analysis indicated that proteins and lipids' digestion were interconnected since it was observed the association of fat globules to protein aggregates during the *in vitro* digestion process. In addition, a real-time analysis was also made to assess *in situ* the digestion of proteins. For this purpose, UV-VIS-SWNIR spectroscopy using fibre optic was applied. Some spectra pre-processing techniques were applied to extract important information from the spectra and correlate it with the release of free NH<sub>2</sub> groups using serine as a reference amino acid, similar to the OPA method. This way, the optimization of the Savitzky-Golay filter resulted in the determination of an operation window of 73 with a third order polynomial order. Subsequently, the spectra were baseline corrected and the most important wavelengths were identified using PLS VIP being 721.21, 776.53, 858.72, 869.83,

967.36, 987.02, and 1080.11 nm. The selected spectra were further used for NH<sub>2</sub> groups estimation. The RFR showed to be the most precise regression model by showing a higher correlation coefficient of 0.9873. This model was subsequently applied to predict free NH<sub>2</sub> groups during the *in vitro* digestion process and a correlation of 0.9455 was obtained between the estimated and experimental data which shows that UV-VIS-SWNIR spectroscopy is in fact a suitable technique to assess protein *in vitro* digestion in real-time.

This way, the development and application of dynamic *in vitro* digestion models is of utmost importance since they try to recreate as close as possible the physiological conditions of the human GI tract by mimicking its chemical environment and motility. However, much work needs to be done towards the development, standardization and validation of novel *in vitro* digestion models since both the food and pharmaceutical industries could benefit from such developments which would consequently lead to tailoring innovative food products and bioactive compounds' delivery systems.

## 5.2 FUTURE PERSPECTIVES

Despite the developments of this thesis, many work still needs to be done and many questions need to be answered. This way, this work can lead to the development of, for instance, novel *in vitro* digestion models. Consequently, the approach here applied can be easily transferred to develop an *in vitro* small intestine model that could also incorporate nutrient absorption through the application electroporated membranes as well as a real-time analytical system using UV-VIS-SWNIR spectroscopy. A standard dynamic *in vitro* oral digestive system with mastication is still inexistent and should also be a focus of new developments in the field. Furthermore, despite the development of many *in vitro* digestion models, their validation is still a major challenge. As such, the development of guidelines and standards for this purpose should also be a priority. For this purpose, an international open access database should be created, specially regarding the *in vivo* assessment of food so that the factors responsible for inter-individual, or even intra-individual variability could be identified and recreated *in vitro*, if possible.